NASA TECHNICAL NOTE

NASA TN D-6577

C. 1

NASA TN D-6577

TECH LIBRARY KAFB, NM

0133292

LOAN COPY: RETURN T
AFWL (DOUL)
KIRTLAND AFB, N. M.

AERODYNAMIC CHARACTERISTICS OF AN ALL-BODY HYPERSONIC AIRCRAFT CONFIGURATION AT MACH NUMBERS FROM 0.65 TO 10.6

by Walter P. Nelms, Jr., and Charles L. Thomas

Ames Research Center
Moffett Field, Calif. 94035

NATIONAL AERONAUTICS AND SPACE ADMINISTRATION • WASHINGTON, D. C. • NOVEMBER 1971

TECH LIBRARY KAFB, NM
0133392

1. Report No.	2. Government Accession No.	3. Recipie.
NASA TN D-6577		

4. Title and Subtitle
AERODYNAMIC CHARACTERISTICS OF AN ALL-BODY HYPERSONIC AIRCRAFT CONFIGURATION AT MACH NUMBERS FROM 0.65 TO 10.6

5. Report Date
November 1971

6. Performing Organization Code

7. Author(s)
Walter P. Nelms, Jr., and Charles L. Thomas

8. Performing Organization Report No.
A-4017

10. Work Unit No.
722-01-10-02-00-21

9. Performing Organization Name and Address
NASA Ames Research Center
Moffett Field, California 94035

11. Contract or Grant No.

13. Type of Report and Period Covered
Technical Note

12. Sponsoring Agency Name and Address
National Aeronautics and Space Administration
Washington, D. C. 20546

14. Sponsoring Agency Code

15. Supplementary Notes

16. Abstract

Aerodynamic characteristics of a model designed to represent an all-body, hypersonic cruise aircraft are presented for Mach numbers from 0.65 to 10.6. The configuration had a delta planform with an elliptic cone forebody and an afterbody of elliptic cross section. Detailed effects of varying angle of attack (-2° to +15°), angle of sideslip (-2° to +8°), Mach number, and configuration buildup were considered. In addition, the effectiveness of horizontal tail, vertical tail, and canard stabilizing and control surfaces was investigated. The results indicate that all configurations were longitudinally stable near maximum lift-drag ratio and the configurations with the vertical tails were directionally stable at all angles of attack. Trim penalties were small at the hypersonic speeds for a center-of-gravity location representative of the airplane, but because of the large rearward travel of the aerodynamic center, trim penalties were severe at transonic Mach numbers.

17. Key Words (Suggested by Author(s))
Hypersonic aircraft
Hypersonic flight
Lift-drag ratio
Aircraft stability
Aerodynamic characteristics
Wind tunnel models

18. Distribution Statement
Unclassified – Unlimited

19. Security Classif. (of this report)	20. Security Classif. (of this page)	21. No. of Pages	22. Price*
Unclassified	Unclassified	100	$3.00

*For sale by the National Technical Information Service, Springfield, Virginia 22151

NOTATION

The longitudinal force and moment coefficients are referred to the stability-axis system and the lateral-directional coefficients are referred to the body-axis system. Unless otherwise noted, the moment reference center is located on the body center line at 32.5 percent of the mean aerodynamic chord, which corresponds to the 55.0 percent point of the body length.

a.c.	longitudinal aerodynamic center defined at $(L/D)_{max}$, percent $\bar{c}$
a_π	semimajor axis of maximum cross section
A_b	model balance cavity area
b	span (measured between body tips)
b_π	semiminor axis of maximum cross section
c	local chord length of airfoil section
$\bar{c}$	mean aerodynamic chord $\left(\frac{2}{3}l\right)$
C_A	axial-force coefficient, $C_{A_{total}} - C_{A_b}$
C_{A_b}	balance cavity axial-force coefficient, $\frac{(p_\infty - p_b)A_b}{qS}$
$C_{A_{total}}$	total measured axial-force coefficient
C_D	drag coefficient, $\frac{drag}{qS}$
C_{D_0}	drag coefficient at zero lift
C_L	lift coefficient, $\frac{lift}{qS}$
C_{L_0}	lift coefficient at zero angle of attack
C_{L_α}	lift-curve slope at zero lift, $\frac{\partial C_L}{\partial \alpha}$, per deg
C_l	rolling-moment coefficient, $\frac{\text{rolling moment}}{qSb}$
C_{l_β}	lateral-stability parameter, $\frac{\partial C_l}{\partial \beta}$, per deg
C_m	pitching-moment coefficient, $\frac{\text{pitching moment}}{qS\bar{c}}$

C_{m_0}	pitching-moment coefficient at zero lift
C_N	normal-force coefficient, $\frac{\text{normal force}}{qS}$
C_n	yawing-moment coefficient, $\frac{\text{yawing moment}}{qSb}$
C_{n_β}	directional-stability parameter, $\frac{\partial C_n}{\partial \beta}$, per deg
C_Y	side-force coefficient, $\frac{\text{side force}}{qS}$
C_{Y_β}	side-force parameter, $\frac{\partial C_Y}{\partial \beta}$, per deg
K	boundary-layer trip (grit) size, cm
$\frac{L}{D}$	lift-drag ratio
$\left(\frac{L}{D}\right)_{max}$	maximum lift-drag ratio
l	body length
l_π	forebody length (measured from nose to maximum cross section)
M	free-stream Mach number
p_b	model balance cavity pressure
p_∞	free-stream static pressure
q_∞	free-stream dynamic pressure
Re	unit Reynolds number, per m
S	reference area (body planform area defined as $\frac{lb}{2}$)
S_π	maximum cross-sectional area
t	maximum thickness of airfoil section
$\frac{t}{c}$	airfoil thickness-to-chord ratio
x	longitudinal coordinate, measured rearward from model nose
y	spanwise coordinate, measured from body center line

z	vertical coordinate, measured from body center line
α	angle of attack (referred to body center line), deg
β	angle of sideslip (referred to body center line), deg

The following code is used to designate the various components of the model:

B	body
C	canard (trailing edge down for positive deflection)
H	horizontal tail (trailing edge down for positive deflection)
R	rudder
V	vertical tail

Subscripts

R	right (looking upstream)
L	left (looking upstream)

Number subscripts (either plus or minus) indicate deflection angles of the control surface in degrees.

AERODYNAMIC CHARACTERISTICS OF AN ALL–BODY HYPERSONIC AIRCRAFT CONFIGURATION AT MACH NUMBERS FROM 0.65 TO 10.6

Walter P. Nelms, Jr., and Charles L. Thomas

Ames Research Center

SUMMARY

An experimental investigation was conducted at Mach numbers from 0.65 to 10.6 of the aerodynamic characteristics of a model designed to represent an all-body, hypersonic cruise aircraft. The configuration had a delta planform with an elliptic cone forebody and an afterbody of elliptic cross section. Detailed effects of varying angle of attack (-2° to +15°), angle sideslip (-2° to +8°), Mach number, and configuration buildup were considered. In addition, the effectiveness of horizontal tail, vertical tail, and canard stabilizing and control surfaces was investigated.

The results indicate that for the Mach number range of the test, all configurations were longitudinally stable near maximum lift-drag ratio, $(L/D)_{max}$, and the configurations with the vertical tails were directionally stable at all angles of attack. At Mach numbers below 2, the lift and pitching-moment curves were essentially linear up to $(L/D)_{max}$ for the complete configurations. For these same configurations, the lateral-directional characteristics were nearly linear for the angle-of-sideslip and Mach number ranges of the tests. Trim penalties were small at the hypersonic speeds for a center-of-gravity location representative of the airplane, but because of the large rearward travel of the aerodynamic center, trim penalties were severe at transonic Mach numbers.

INTRODUCTION

Results of a number of performance studies typified by those presented in references 1 through 4 have shown that hydrogen-fueled, hypersonic aircraft configurations with airbreathing propulsion systems are potentially suitable for both cruise and boost missions. These studies were based largely on estimated aerodynamic characteristics because of the lack of experimental data on configurations having large fuselage volumes necessitated by the storage requirements of low-density hydrogen fuel. Therefore, a program was undertaken at Ames Research Center to provide this needed data over a broad Mach number range, as well as to assess the adequacy of various theoretical procedures for use on these types of configurations. To date, experimental and theoretical results have been obtained for two wing-body designs and a blended wing-body concept. References 5 through 7 present a portion of the results from these studies. The next phase of the program was to investigate the aerodynamic characteristics of an all-body concept. An all-body shape represents the obvious limit in wing-fuselage blending to obtain the large volumes required for fuel storage. This report includes results from wind-tunnel tests of an all-body hypersonic aircraft configuration.

The experimental investigation was conducted in the Ames 6– by 6–Foot Supersonic and the 3.5 Foot Hypersonic Wind Tunnels at Mach numbers from 0.65 to 10.6. The Reynolds number was held constant at 8.2×10^6/m for most of the tests; at Mach numbers 2.00 and 10.6, the Reynolds number was limited to 4.9×10^6/m. Angles of attack ranged from -2° to +15° and angles-of-sideslip ranged from -2° to +8°.

MODEL

A drawing of the complete model with pertinent dimensions is shown in figure 1(a), and details of the stabilizing and control surfaces are presented in figure 1(b). Figure 2 presents photographs of the model.

The model is representative of a hypersonic cruise vehicle derived from the analytical studies of references 8 through 11. These studies considered an all-body design, featuring an air-breathing propulsion system with liquid hydrogen as a fuel. This particular all-body configuration was selected for wind-tunnel testing both because of its geometrical simplicity, which simplifies theoretical estimates, and because of the mission studies that had been accomplished on this shape (refs. 8–11). The model was designed to allow a complete buildup of the various configuration components during the wind-tunnel tests. Effects of the propulsion system on the aerodynamic characteristics were not investigated experimentally.

The body had a delta planform with leading edges swept back 75°. The forebody was an elliptic cone, and the afterbody had elliptical cross sections (fig. 1(a)). The maximum cross-sectional area of the body was located at the break point between the forebody and afterbody at 2/3 of the body length from the nose ($l_\pi/l = 0.6667$). The ratio of the maximum cross-sectional area to the body planform area (S_π/S) was 0.0935, and the major-to-minor axis ratio of the maximum cross section (a_π/b_π) was 4. Since the forebody was an elliptic cone, it had a major-to-minor axis ratio of 4 at all stations. The ellipticity continuously increased with increasing body station for the elliptic cross sections of the afterbody which terminated in a straight-line trailing edge. Removable outboard tips were provided so that the body could be tested alone as well as with aft stabilizing surfaces. The model span (b) was defined with these tips in place (body alone), as indicated in figure 1(a).

Horizontal tails, twin vertical tails, and a canard surface were provided for the wind-tunnel model (fig. 1(b)). The horizontal tails, mounted on the body center line, had 55° of leading-edge sweep and symmetrical wedge-slab airfoil sections with the ridge lines at 50-percent chord locations. The maximum thickness-to-chord ratio (t/c) was 4 percent, and the total exposed area of both the right and left horizontal-tail surfaces was 12.5 percent of the body planform area. For control, the right and left horizontal tails could be rotated either symmetrically or differentially about a point corresponding to the longitudinal location of the centroid of the tail areas (fig. 1(b)).

The outboard-mounted vertical tails had 60° swept-back leading edges with an unsymmetrical wedge-slab airfoil section (the inboard sides were flat). Ridge lines were located at 50-percent chord on the outboard sides, and the thickness-to-chord ratio was 4 percent. The combined plan area of the two vertical tails was approximately 16.9 percent of the body planform area. The major portion of the vertical tail surfaces was above the horizontal tail and a small portion was below. Screw-on

wedges were added to the aft 50 percent of the vertical tails (upper portion only) to simulate deflected rudders either in an outboard or inboard direction. The rudder hinge line was along the 50-percent chord line at a 50.4° sweepback angle (fig. 1(b)). This deflection could be either symmetrical (rudder flare) or differential.

A canard, with 50° swept-back leading edges, could be mounted on the fuselage center line as shown in figure 1(a). The combined exposed plan area of the right and left canard surfaces was 4 percent of the body planform area. The canard airfoil was a symmetrical wedge slab section with ridge lines at 50-percent chord and with a maximum thickness-to-chord ratio of 6 percent. For longitudinal control, the canard could be rotated (symmetrical deflection only) about a point corresponding to the longitudinal location of the centroid of the canard area (fig. 1(b)).

TESTS

Data were obtained in air in two Ames wind tunnels at Mach numbers from 0.65 to 10.6. The 6– by 6–foot supersonic tunnel is a closed-circuit, continuous-flow facility with a sliding block nozzle and a slotted wall test section; in this tunnel, the Mach number was varied from 0.65 to 2.00. Mach numbers of 5.37, 7.38, and 10.6 were obtained in the 3.5-foot hypersonic tunnel, which uses interchangeable nozzles; this tunnel is a blowdown facility in which incoming air is preheated by a pebble-bed heater to prevent liquification of air in the test section. The stagnation temperature was maintained at about 720° K for Mach numbers of 5.37 and 7.38 and at about 1050° K for Mach number 10.6. Data were obtained at a constant Reynolds number of 8.2×10^6/m at all Mach numbers except 2.00 and 10.6 where the Reynolds number was limited to 4.9×10^6/m because of wind-tunnel limitations.

The model was sting-mounted through the aft upper surface of the body; this method of support was used so as to maintain a smooth lower body surface for testing at hypersonic speeds. Force and moment measurements were made with an internally mounted, six-component strain-gage balance. Test angles of attack ranged nominally from -2° to +15°, and angles of sideslip ranged nominally from -2° to +8° at about 5° angle of attack. Additional tests were conducted for the model in pitch at a constant angle of sideslip. The angles of attack and sideslip were corrected for wind-tunnel-flow misalinement and for balance and sting deflections caused by the aerodynamic loads. Balance cavity pressure was measured and the drag data were adjusted to a condition corresponding to free-stream static pressure in the cavity.

Generally, boundary-layer transition was not fixed on the model, but grit was used in some studies at several of the lower Mach numbers to provide an all-turbulent boundary layer as a basis for data evaluation. At the hypersonic speeds, no effective method was found for fixing transition near the leading edges of the model components to achieve fully turbulent flow. Studies utilizing sublimation techniques and Reynolds number variation indicated the hypersonic boundary layers to be nearly all laminar with possible small areas of transitional flow. The results of the grit and Reynolds number variation studies are presented in a later section of the report.

Based on repeatability of the data and known precision of the measuring equipment the test Mach numbers 0.65–2.00 and 5.37–10.6 are considered accurate within ± 0.01 and ± 0.05,

respectively; the corresponding dimensionless aerodynamic coefficients are considered accurate within ±2 and ±3 percent, respectively. The angles of attack and sideslip are considered to be accurate within ±0.2°.

RESULTS AND DISCUSSION

The experimental results are presented in figures 3 through 20. The contents of these figures are summarized in table 1 which lists the configurations and briefly notes the purpose of each figure.

Component Buildup

Longitudinal characteristics– The longitudinal aerodynamic characteristics of the body alone and in combination with horizontal tails, vertical tails, and a canard are presented as a function of lift coefficient (fig. 3) and of Mach number (fig. 4). Table 2 is a tabulation of the data used in figure 3 for selected Mach numbers. The balance cavity axial-force coefficients subtracted from the drag measurements of the body alone configuration are listed in table 3 (similar corrections were applied to the data of the other configurations). The lift curves for the body alone configuration were nonlinear (particularly above an angle of attack of about 5°) at all Mach numbers of the test with increasing lift-curve slope for increasing lift coefficients. Also, the body alone configuration had the lowest lift-curve slope for all test Mach numbers (fig. 4). The addition of horizontal tails not only produced essentially linear lift curves through Mach number 2, but the additional lifting area substantially increased lift coefficient for a given angle of attack at all Mach numbers of the test. The vertical tails and canard generally had no significant effects on the lift characteristics of the model. However, at M = 1.10 and 1.30, the vertical tails reduced the lift coefficients, and at M = 10.6, the canard increased the lift coefficients at positive angles of attack.

The addition of model components resulted in increases in drag coefficient at zero lift (C_{D_0}) as shown in figure 4. The horizontal tails reduced the drag due to lift associated with the body alone configuration (fig. 3) at all test Mach numbers.

Adding the horizontal tails increased the maximum lift-to-drag ratio ($(L/D)_{max}$) above those of the body alone configuration, particularly for Mach numbers from about 1 to 5 as indicated in figure 4. The vertical tails caused fairly large losses in $(L/D)_{max}$ at supersonic Mach numbers. Generally, the addition of model components had only small effects on $(L/D)_{max}$ at Mach numbers above about 5. Values of untrimmed $(L/D)_{max}$ varied from about 4.1 at M = 5 to about 3.2 at M = 10.

In general, the horizontal tails tended to increase longitudinal stability, the canard tended to reduce longitudinal stability, and the vertical tails had only small effects on longitudinal stability at all Mach numbers of the test (fig. 3). For most Mach numbers below about 2, the pitching-moment curves were reasonably linear for a range of lift coefficients beyond those for $(L/D)_{max}$. At the highest test angles of attack, some indication of pitch-up was exhibited at the subsonic Mach numbers (fig. 3(a)–(c)). All configurations tested had positive stability near $(L/D)_{max}$ for the selected moment reference center of 0.325$\bar{c}$ (0.550l). From mission studies involving this

configuration (refs. 8–11), it appears that the center of gravity would be located aft of this point at approximately 0.445$\bar{c}$ (0.630l). As shown in figure 4, the aerodynamic centers moved forward with increasing supersonic Mach numbers and gradually moved rearward at the higher hypersonic speeds. The overall travel from the most aft to the most forward location was about 16 to 20 percent of the mean aerodynamic chord depending on the configuration.

As previously indicated, the sting support exited from the aft, upper surface of the model in order to provide an undisturbed lower body surface for testing at hypersonic speeds. The sting exiting in this manner tended to produce a region of higher pressure on the aft upper surface than would be obtained without the sting. This increased pressure resulted in a slightly negative C_{L_0} and a small positive C_{m_0} at the lower speeds as seen in figure 3 for the body-alone configuration. As anticipated, this effect essentially disappeared at the hypersonic Mach numbers of the test.

Lateral-directional characteristics– The effects of component buildups on the lateral-directional aerodynamic characteristics are presented as a function of β in figure 5 and summarized as a function of Mach number in figure 6. The effects of angle of attack are shown in figure 7. In general, the lateral-directional characteristics were nearly linear over the angle-of-sideslip range of the test at all Mach numbers (fig. 5). The body-alone configuration had negative directional stability at transonic speeds and essentially neutral stability at all other Mach numbers. Adding the vertical tails produced positive directional stability at all Mach numbers and angles of attack of the test. Making the vertical tails smaller would probably increase $(L/D)_{max}$. The canard had no effect on C_{n_β} except at $M = 1.3$ where adding this surface slightly increased directional stability (fig. 5(c)). There were only small effects of angle of attack on C_n (fig. 7).

Near $\alpha = 5°$, all configurations had positive effective dihedral ($-C_{l_\beta}$) at all test Mach numbers and, in general, adding model components had little effect on this parameter (fig. 6). The variation of C_l with angle of attack (fig. 7) indicates the increase in effective dihedral for angles of attack beyond that in figure 5.

Except for the body-alone results near $M = 1$, all configurations had negative values of C_{Y_β}. Also, there were only small effects of angles of attack on C_Y (fig. 7).

Horizontal-Tail Deflection

Symmetrical deflection– The effects of negative horizontal-tail deflections on the longitudinal aerodynamic characteristics for the configuration with the canard off are presented as a function of lift coefficient (fig. 8) and Mach number (fig. 9). Deflecting the horizontal tails negatively had no effect on C_{L_α} in the test Mach number range (fig. 9), but at a given angle of attack, C_L was reduced, as expected. At all speeds, C_{D_0} increased, but at Mach numbers of 2 or less, deflecting the horizontal tails reduced the drag due to lift. Except for the -6.5° deflection at Mach numbers of 0.6 through about 2.5, deflecting the horizontal tails reduced $(L/D)_{max}$.

At supersonic Mach numbers, deflecting the horizontal tails had little or no effect on longitudinal stability, but at subsonic and hypersonic speeds the aerodynamic center moved forward (fig. 9). For the selected moment reference center, about -6° of horizontal tail deflection was

required to trim near $(L/D)_{max}$ at the higher Mach numbers, causing a loss of about 0.5 in L/D. A more aft center-of-gravity location (representative of the airplane used in the mission studies of refs. 8–11) would result in small trim penalties at the hypersonic Mach numbers. On a more refined configuration, a small amount of negative camber could be provided in the forward part of the fuselage which should essentially eliminate longitudinal trim penalties at the hypersonic speeds. Because of the large aft movement of the aerodynamic center at transonic Mach numbers (fig. 9), there was insufficient control power available to trim near $(L/D)_{max}$ for the selected moment reference location. A more aft center-of-gravity location or greater control deflections or both would provide trim nearer $(L/D)_{max}$, but the deflections would result in severe trim penalties. Thus it appears that a program of fuel management or a fuel transfer system would be necessary in order to reduce the large trim penalties at transonic speeds.

The effects of deflecting the horizontal tails on the longitudinal aerodynamic characteristics for the complete configuration with the canard are presented in figures 10 and 11. These results are similar to those for the canard-off results, but the trim penalties would be slightly less since adding the canard moved the aerodynamic center approximately 5 percent farther forward.

Differential deflection– The effects of differential deflection of the horizontal tails on the hypersonic lateral-directional aerodynamic characteristics as a function of angle of attack are presented in figure 12 for Mach numbers 7.38 and 10.6. Positive deflections of the left horizontal tail produced positive rolling moments, but also caused large values of adverse yaw, which worsened with increasing angle of attack. Equal but opposite deflections (plus left and negative right) of the horizontal tails produced positive rolling moments and improved yawing moments, which however, became adverse at angles of attack above 3°. These results indicate that an upward deflection of the right horizontal tail would probably provide positive roll with acceptable yaw. The effectiveness in producing rolling moments by differential deflection of the horizontal tails indicates that elevators on the horizontal tails might suffice for roll control; however, for these tests, the model was not provided with this type of control.

Canard Deflection

The effects of deflecting the canard on the longitudinal aerodynamic characteristics are presented in figures 13 and 14 as functions of lift coefficient and of Mach number, respectively. Deflecting the canard had only minor effects on C_{L_α} (fig. 14) and, except at the highest Mach numbers, the lift curves were essentially linear. As expected, the canard when deflected increased C_{D_0} and decreased $(L/D)_{max}$ at all Mach numbers. In contrast to deflecting the horizontal tail, the canard had little or no effect on the drag due to lift at Mach numbers below 2. Deflecting the canard had essentially no effect on the aerodynamic center location at any of the test Mach numbers. Like the horizontal tail, the canard was capable of trimming the vehicle near $(L/D)_{max}$ at the hypersonic Mach numbers for the selected moment reference point. However, at the lower Mach numbers, the canard was even less effective than the horizontal tail in trimming the configuration.

Rudder Deflection

Rudder flare– The effects of rudder flare on the hypersonic longitudinal aerodynamic characteristics at Mach numbers 7.38 and 10.6 are presented in figure 15. Both outboard and inboard deflections are considered. Except for the 30° deflections, flaring the rudders had only minor effects on the lift curves. Rudder flare increased the C_{D_0} and reduced the $(L/D)_{max}$ as expected. Flaring the rudder produced positive values of C_{m_0}, and for the highest deflection, a slight increase in stability was obtained. These effects may be attributed primarily to the 50.4° of sweepback of the simulated rudder hinge line (fig. 1(b)), where a downward component results from the rudder loading. With exception of C_{D_0} at Mach 10.6, there was little difference between the effects of outboard and inboard rudder flare on the longitudinal aerodynamic characteristics.

The effects of outboard and inboard rudder flare on the lateral-directional characteristics are presented in figure 16 for Mach numbers of 7.38 and 10.6. Outboard rudder flare increased directional stability, but flaring the rudders inboard had very little effect. The 15° rudder flares (both outboard and inboard) had only small effects on C_{l_β}; the 30° outboard flare reduced C_{l_β} to zero. Rudder flare had only minor effects on C_{Y_β}, which increased slightly with outboard deflections.

Individual rudder deflection– The effects of outboard or inboard deflection of individual rudders on the lateral-directional aerodynamic characteristics in sideslip are presented in figure 17. The rudder was effective in changing the yawing moments at nearly all Mach numbers, with C_n becoming more negative with increasing left rudder. The inboard deflections were generally not as effective in varying C_n as were the outboard deflections, and inboard deflections produced adverse rolling moments. Rudder deflections changed C_l, and the direction of this change (in a positive or negative sense) depended first on whether the inboard or outboard surface was deflected and second on the downward component of the rudder load caused by the 50.4° sweptback hinge line.

Figure 18 presents the effects of individual rudder deflections on the lateral-directional aerodynamic characteristics in pitch. At the lower Mach numbers, the effects of rudder deflections were relatively constant with angle of attack up to about 8°. At Mach number 7.38, the effectiveness of individual deflections of the rudder decreased significantly with increasing angle of attack.

Boundary-Layer Studies

Studies were conducted to determine the nature of the boundary layer on the wind-tunnel model. Some of the results of these investigations are presented in this section.

Grit studies– Grit-type boundary-layer trips were used to establish the drag level at Mach numbers 0.90, 1.30, and 1.99 for the wind-tunnel model with an all turbulent boundary layer. The model configuration used for these tests was the body with horizontal and vertical tails. Grit was applied around the model nose, along the top and bottom of the body near the leading edges (similar to the procedure used on delta wings), and near the leading edges of the tail surfaces. A drag

polar was then obtained for six different grit sizes at each Mach number, and the drag level for an all-turbulent boundary layer was determined by the procedures described in reference 12. These results are presented in figure 19.

For the subsonic Mach number of 0.90, the drag coefficient versus grit size is plotted in figure 19(a) for various lift coefficients. The plateau on the curve defines the grit-free drag level (ref. 12) for an all-turbulent boundary layer for particular lift coefficients. The drag coefficients defined in this manner are plotted in the lower part of figure 19(a) in the form of a grit-free drag polar for an all-turbulent boundary layer. Figures 19(b) and (c) present the results obtained for the supersonic Mach numbers of 1.30 and 1.99. Here the drag coefficient is plotted versus the square of the grit dimension for various lift coefficients. A linear extrapolation of the data to zero-grit size (ordinate) defines the drag levels for an all-turbulent boundary layer for each lift coefficient (ref. 12). The grit-free drag polars for an all-turbulent boundary layer are plotted at the bottom of the two figures. The results obtained from these grit studies are summarized in figure 19(d) in the form of C_{D_0} and $(L/D)_{max}$ as a function of Mach number. For comparison, the data for the body with horizontal and vertical tails and with untripped boundary layer (from fig. 4) are also presented in figure 19(d). As can be seen, extrapolating to all-turbulent boundary-layer conditions on the model resulted in a small decrease in $(L/D)_{max}$.

Reynolds number variation– There was no effective method of fixing transition near the leading edge of the model components at the hypersonic Mach numbers. On the basis of sublimation studies on similar models in the 3.5 foot hypersonic facility (ref. 5), it was concluded that the boundary layer on the present model would be mostly laminar with possible small areas of transitional flow at the hypersonic Mach numbers of the tests. To support this conclusion, Reynolds number variation studies were conducted similar to those of reference 5. The configuration consisting of the body with horizontal and vertical tails was used for these tests. Three unit Reynolds numbers were investigated at $M = 5.37$ and 7.38; the resulting drag polars are plotted at the top of figures 20(a) and (b). Since it was suspected that the boundary layer on the model was laminar, the values of C_{D_0} and drag coefficient at $(L/D)_{max}$ from the polars at different Reynolds numbers were plotted versus the parameter $1/\sqrt{Re}$, which is representative of a drag-coefficient variation associated with a laminar boundary layer. These results are shown at the bottom of figures 20(a) and (b). An extrapolation of the resulting straight lines back to the ordinate (infinite Re), as represented by the dashed lines, indicates the pressure drag of the configuration, which agrees well with the calculated pressure drag for the model. These theoretical estimates were based on tangent-wedge theory for all windward surfaces of the model using the method described in reference 13. A Prandtl-Meyer expansion was employed on the leeward or expansion surfaces. Thus, this analysis and the previous sublimation studies indicate that the boundary layer on the model was mostly laminar at the hypersonic Mach numbers of this investigation.

CONCLUSIONS

An experimental investigation of the aerodynamic characteristics of a model representative of an all-body, hypersonic cruise aircraft was conducted at Mach numbers from 0.65 to 10.70. The configuration had a delta planform with an elliptic cone forebody and an elliptic cross-section afterbody. The effects of varying angles of attack and sideslip, Mach number, and configuration

buildup were considered. In addition, the effectiveness of horizontal tail, vertical tail, and canard stabilizing and control surfaces was investigated. The following conclusions are drawn from these results:

1. For Mach numbers below about 2, the complete configuration exhibited essentially linear lift and pitching-moment curves. At all Mach numbers of the test, the lateral-directional characteristics of the complete configuration were nearly linear over the angle-of-sideslip range.

2. Values of untrimmed maximum lift-drag ratio, $(L/D)_{max}$, at hypersonic speeds varied from about 4.1 at Mach number 5 to about 3.2 at Mach number 10.

3. For the selected moment reference center, all configurations tested were longitudinally stable near $(L/D)_{max}$ at all Mach numbers of the test.

4. The configurations with the vertical tails had positive directional stability for the Mach number and angle-of-attack ranges of the test.

5. The aerodynamic centers moved forward with increasing supersonic Mach numbers and gradually moved rearward at the higher hypersonic speeds. The overall travel from the most aft to the most forward location was about 16 to 20 percent of the mean aerodynamic chord, depending on the configuration.

6. Trim penalties were small at the hypersonic speeds for a center-of-gravity location representative of the airplane; but because of the large rearward movement of the aerodynamic center, trim penalties were severe at transonic Mach numbers.

7. The horizontal tails provided marginal longitudinal trim capability except at the hypersonic Mach numbers. The canard was even less effective in providing longitudinal trim.

Ames Research Center
National Aeronautics and Space Administration
Moffett Field, Calif., 94035, August 30, 1971

REFERENCES

1. Gregory, Thomas J.; Petersen, Richard H.; and Wyss, John A.: Performance Tradeoffs and Research Problems for Hypersonic Transports. J. Aircraft, vol. 2, no. 4, July-Aug. 1965, pp. 266–271.

2. Petersen, Richard H.; Gregory, Thomas J.; and Smith, Cynthia L.: Some Comparisons of Turboramjet-Powered Hypersonic Aircraft for Cruise and Boost Missions. J. Aircraft, vol. 3, no. 5, Sept-Oct. 1966, pp. 398–405.

3. Jarlett, F. E.: Performance Potential of Hydrogen Fueled, Airbreathing Cruise Aircraft. General Dynamics/Convair Division Rep. GD/C–DCB–66–004, vols. 1–4 (Contract NAS2–3180), May and Sept. 1966.

4. Morris, R. E.; and Williams, N. B.: Study of Advanced Airbreathing Launch Vehicles With Cruise Capability. Lockheed-California Company Rep. LR21042, vols. 1–6 (Contract NAS2–4084), Feb. 1968.

5. Nelms, Walter P., Jr.; and Axelson, John A.: Longitudinal Aerodynamic Characteristics of Three Representative Hypersonic Cruise Configurations at Mach Numbers From 0.65 to 10.70. NASA TM X–2113, 1970.

6. Nelms, Walter P., Jr.; and Axelson, John A.: Effects of Wing Elevation, Incidence, and Camber on the Aerodynamic Characteristics of a Representative Hypersonic Cruise Configuration at Mach Numbers From 0.65 to 10.70. NASA TN D–6049, 1970.

7. Nelms, Walter P., Jr.; Carmichael, Ralph L.; and Castellano, Charles R.: An Experimental and Theoretical Investigation of a Symmetrical and a Cambered Delta Wing Configuration at Mach Numbers From 2.0 to 10.7. NASA TN D–5272, 1969.

8. Gregory, Thomas J.; Ardema, Mark D.; and Waters, Mark H.: Hypersonic Transport Preliminary Performance Estimates for an All-Body Configuration. AIAA Paper 70–1224. Presented at the AIAA 7th Annual Meeting and Technical Display, Houston, Texas, October 19–22, 1970.

9. Williams, Louis J.: Estimated Aerodynamics of All-Body Hypersonic Aircraft Configurations. NASA TM X–2091, 1971.

10. Gregory, Thomas J.; Williams, Louis J.; and Wilcox, Darrell E.: The Airbreathing Launch Vehicle for Earth Orbit Shuttle – Performance and Operation. AIAA Paper 70–270. Presented at the AIAA Advanced Space Transportation Meeting, Cocoa Beach, Florida, Feb. 4–6, 1970.

11. Gregory, Thomas J.; Wilcox, Darrell E.; and Williams, Louis J.: The Effects of Propulsion System – Airframe Interactions on the Performance of Hypersonic Aircraft. AIAA Paper 67–493. Presented at the AIAA 3rd Propulsion Joint Specialist Conference, Washington, D. C., July 17–21, 1967.

12. Braslow, Albert L.; Hicks, Raymond M.; and Harris, Roy V., Jr.: Use of Grit-Type Boundary-Layer-Transition Trips on Wind-Tunnel Models. NASA TN D–3579, 1966.

13. Gentry, Arvel E.: Hypersonic Arbitrary-Body Aerodynamic Computer Program. Douglas Rep. DAC–56080, vols. 1 and 2, 1967.

TABLE 1.– SUMMARY OF FIGURES

Figure	Model configuration	Purpose of figure
3, 4	B, BH, BHV, BHVC	Effect of component buildup on longitudinal characteristics
5, 6, 7	B, BHV, BHVC	Effect of component buildup on lateral-directional characteristics in sideslip and in pitch
8, 9, 10, 11	BHV, BHVC	Effect of horizontal-tail deflections on longitudinal characteristics
12	BHV	Effect of differential horizontal-tail deflections on lateral-directional characteristics in pitch
13, 14	BHVC	Effect of canard deflections on longitudinal characteristics
15	BHVR	Effect of rudder flare on longitudinal characteristics
16	BHVR	Effect of rudder flare on lateral-directional characteristics in sideslip
17, 18	BHVR	Effect of individual rudder deflections on lateral-directional characteristics in sideslip and in pitch
19	BHV	Boundary-layer transition results
20	BHV	Reynolds number variation results

TABLE 2.– TABULATED DATA

(a) M = 0.65; Re/m = 8.20X10^6

α	C_L	C_D	C_m	C_N	C_A	L/D	α	C_L	C_D	C_m	C_N	C_A	L/D
B							BH						
-0.38	-0.030	0.0056	0.0075	-0.030	0.0054	-5.36	-0.40	-0.038	0.0073	0.0120	-0.038	0.0070	-5.22
.68	-.002	.0054	.0044	-.002	.0054	-.33	.74	.004	.0070	.0021	.004	.0070	.58
1.81	.027	.0058	.0011	.028	.0049	4.76	1.86	.044	.0077	-.0076	.044	.0062	5.77
3.93	.080	.0091	-.0050	.081	.0035	8.86	3.86	.123	.0134	-.0271	.124	.0051	9.21
5.99	.139	.0151	-.0123	.139	.0005	9.19	6.03	.208	.0235	-.0478	.209	.0016	8.83
8.13	.204	.0259	-.0211	.206	-.0032	7.87	8.13	.295	.0397	-.0677	.298	-.0025	7.44
10.31	.296	.0492	-.0331	.300	-.0046	6.02	10.82	.438	.0782	-.0972	.445	-.0054	5.60
12.55	.399	.0846	-.0469	.408	-.0041	4.72	12.48	.518	.1095	-.1099	.530	-.0051	4.74
14.91	.507	.1293	-.0606	.524	-.0056	3.92							
15.84	.549	.1495	-.0652	.569	-.0061	3.67							
BHV							BHVC						
-0.18	-0.045	0.0111	0.0146	-0.045	0.0110	-4.07	-0.42	-0.057	0.0136	0.0151	-0.057	0.0132	-4.19
.73	-.010	.0112	.0062	-.010	.0113	-.88	.72	-.013	.0135	.0064	-.013	.0137	-.94
1.93	.036	.0118	-.0048	.036	.0106	3.03	1.82	.028	.0143	-.0007	.028	.0135	1.92
3.99	.118	.0172	-.0251	.119	.0089	6.86	4.01	.118	.0196	-.0184	.119	.0113	6.01
6.14	.205	.0280	-.0469	.207	.0059	7.33	6.17	.209	.0307	-.0359	.211	.0080	6.82
8.20	.295	.0440	-.0683	.298	.0015	6.70	8.31	.305	.0486	-.0540	.309	.0040	6.28
10.43	.401	.0719	-.0863	.407	-.0019	5.58	10.48	.395	.0726	-.0688	.402	-.0005	5.44
12.74	.509	.1090	-.1044	.521	-.0060	4.67	12.62	.493	.1079	-.0812	.504	-.0024	4.57
14.81	.598	.1494	-.1158	.616	-.0084	4.00	15.12	.594	.1554	-.0876	.614	-.0048	3.82

(b) M = 0.90; Re/m = 8.20X10^6

B							BH						
-1.75	-0.071	0.0178	0.0155	-0.072	0.0156	-4.01	-0.60	-0.059	0.0185	0.0199	-0.059	0.0179	-3.16
-.45	-.036	.0164	.0100	-.036	.0161	-2.17	.36	-.019	.0172	.0090	-.019	.0173	-1.10
.46	-.011	.0158	.0066	-.011	.0159	-.70	1.42	.023	.0172	-.0021	.023	.0166	1.33
1.54	.018	.0168	.0024	.019	.0163	1.08	2.53	.074	.0190	-.0167	.075	.0157	3.91
3.67	.077	.0197	-.0062	.078	.0148	3.88	3.61	.124	.0253	-.0307	.125	.0154	5.31
5.81	.141	.0280	-.0162	.143	.0136	5.03	6.32	.245	.0404	-.0635	.248	.0132	6.06
8.16	.225	.0423	-.0306	.229	.0098	5.33	7.93	.324	.0562	-.0851	.329	.0109	5.77
10.23	.313	.0661	-.0423	.320	.0094	4.74	9.27	.393	.0742	-.1021	.400	.0099	5.30
12.46	.415	.1004	-.0584	.427	.0085	4.13							
14.75	.523	.1451	-.0753	.543	.0072	3.61							
BHV							BHVC						
-0.58	-0.072	0.0219	0.0241	-0.72	0.0212	-3.29	-0.63	-0.075	0.0246	0.0222	-0.075	0.0238	-3.04
.57	-.024	.0220	.0111	-.024	.0222	-1.11	.61	-.023	.0244	.0105	-.022	.0247	-.92
1.49	.013	.0226	.0012	.014	.0223	.59	1.46	.011	.0248	.0033	.011	.0245	.44
3.83	.118	.0281	-.0285	.120	.0201	4.22	3.77	.118	.0320	-.0213	.120	.0241	3.69
6.01	.217	.0405	-.0558	.220	.0175	5.37	5.98	.222	.0444	-.0439	.225	.0211	4.99
8.22	.326	.0607	-.0860	.332	.0134	5.38	8.32	.337	.0675	-.0682	.343	.0181	4.99
10.38	.421	.0891	-.1032	.430	.0118	4.73	10.38	.424	.0937	-.0863	.434	.0157	4.53
12.64	.507	.1243	-.1154	.522	.0103	4.08	12.89	.513	.1326	-.0904	.530	.0148	3.87
14.93	.589	.1655	-.1222	.612	.0083	3.56	15.00	.599	.1743	-.0981	.624	.0134	3.44

TABLE 2.– TABULATED DATA – Continued.

(c) M = 1.10; Re/m = 8.20×10^6

α	C_L	C_D	C_m	C_N	C_A	L/D	α	C_L	C_D	C_m	C_N	C_A	L/D
			B							BH			
-2.72	-0.104	0.0411	0.0284	-0.105	0.0361	-2.52	-1.66	-0.096	0.0410	0.0360	-0.097	0.0382	-2.34
-1.48	-.069	.0388	.0214	-.070	.0370	-1.77	-.82	-.059	.0394	.0231	-.060	.0386	-1.50
-.70	-.046	.0373	.0160	-.046	.0368	-1.23	.38	-.006	.0385	.0051	-.006	.0385	-.15
.39	-.005	.0372	.0053	-.005	.0373	-.14	1.60	.044	.0390	-.0119	.045	.0378	1.13
1.61	.029	.0374	-.0026	.030	.0365	.76	3.56	.133	.0443	-.0395	.135	.0360	2.99
3.83	.090	.0411	-.0141	.093	.0350	2.20	5.69	.220	.0548	-.0666	.224	.0327	4.02
4.95	.116	.0441	-.0161	.119	.0339	2.63	7.18	.282	.0663	-.0860	.288	.0306	4.25
5.75	.140	.0473	-.0212	.144	.0330	2.96							
8.61	.242	.0653	-.0429	.249	.0284	3.70							
10.26	.320	.0863	-.0589	.330	.0279	3.71							
12.42	.410	.1166	-.0775	.425	.0257	3.52							
14.75	.513	.1575	-.0986	.536	.0217	3.26							
			BHV							BHVC			
-0.50	-0.064	0.0456	0.0270	-0.064	0.0451	-1.39	-1.53	-0.106	0.0494	0.0350	-0.107	0.0465	-2.14
.51	-.022	.0450	.0143	-.021	.0452	-.48	-.47	-.066	.0473	.0256	-.067	.0468	-1.40
1.48	.016	.0444	.0023	.017	.0440	.35	.52	-.020	.0461	.0130	-.020	.0463	-.44
3.75	.101	.0488	-.0238	.104	.0421	2.07	1.64	.012	.0463	.0069	.013	.0459	.25
5.96	.191	.0592	-.0520	.197	.0390	3.24	3.88	.103	.0507	-.0165	.106	.0436	2.03
8.01	.288	.0737	-.0843	.295	.0328	3.91	5.97	.191	.0608	-.0387	.197	.0405	3.15
8.78	.323	.0807	-.0957	.331	.0305	4.00	8.26	.304	.0804	-.0676	.312	.0359	3.78
							9.15	.364	.0922	-.0890	.374	.0331	3.95

(d) M = 1.30; Re/m = 8.20×10^6

α	C_L	C_D	C_m	C_N	C_A	L/D	α	C_L	C_D	C_m	C_N	C_A	L/D
			B							BH			
-2.79	-0.091	0.0358	0.0225	-0.092	0.0314	-2.53	-2.68	-0.111	0.0380	0.0366	-0.113	0.0328	-2.92
-1.61	-.058	.0334	.0155	-.059	.0318	-1.74	-1.74	-.074	.0356	.0250	-.075	.0333	-2.08
-.42	-.025	.0319	.0085	-.025	.0317	-.78	-.99	-.038	.0347	.0139	-.038	.0340	-1.09
.44	-.002	.0317	.0044	-.002	.0318	-.07	.31	.003	.0337	.0016	.003	.0337	.08
1.50	.028	.0324	-.0019	.029	.0317	.86	1.60	.050	.0346	-.0130	.051	.0332	1.43
3.75	.090	.0370	-.0140	.092	.0310	2.44	3.59	.122	.0402	-.0347	.124	.0325	3.03
5.95	.153	.0451	-.0254	.157	.0290	3.39	5.83	.207	.0515	-.0594	.211	.0302	4.01
8.02	.221	.0585	-.0375	.227	.0271	3.78	7.98	.291	.0688	-.0818	.298	.0277	4.23
10.27	.299	.0808	-.0496	.308	.0262	3.70							
12.76	.384	.1109	-.0623	.399	.0232	3.47							
14.82	.457	.1431	-.0731	.478	.0215	3.19							
			BHV							BHVC			
-2.53	-0.121	0.0443	0.0424	-0.123	0.0389	-2.74	-2.62	-0.123	0.0472	0.0358	-0.126	0.0415	-2.62
-1.58	-.087	.0418	.0317	-.088	.0394	-2.07	-1.69	-.089	.0442	.0279	-.090	.0416	-2.01
-.47	-.047	.0397	.0201	-.048	.0393	-1.19	-.62	-.053	.0424	.0195	-.053	.0418	-1.24
.65	-.006	.0391	.0082	-.006	.0391	-.16	.52	-.014	.0416	.0103	-.014	.0418	-.34
1.64	.028	.0397	-.0019	.029	.0389	.71	1.63	.024	.0420	.0012	.026	.0413	.58
3.90	.111	.0453	-.0266	.113	.0377	2.44	3.83	.108	.0468	-.0188	.111	.0395	2.30
5.93	.186	.0548	-.0494	.191	.0352	3.40	6.06	.198	.0582	-.0396	.203	.0370	3.40
8.17	.279	.0724	-.0751	.287	.0320	3.86	8.29	.289	.0769	-.0600	.297	.0344	3.76
10.30	.366	.0963	-.0961	.377	.0293	3.80	10.58	.383	.1042	-.0791	.395	.0322	3.67
							13.23	.490	.1455	-.0997	.510	.0295	3.37

TABLE 2.– TABULATED DATA – Continued.

(e) M = 2.00; Re/m = 4.90X10^6

α	C_L	C_D	C_m	C_N	C_A	L/D	α	C_L	C_D	C_m	C_N	C_A	L/D
			B							BH			
-3.27	-0.077	0.0248	0.0145	-0.078	0.0204	-3.09	-2.22	-0.063	0.0241	0.0178	-0.064	0.0217	-2.63
-2.19	-.054	.0229	.0107	-.055	.0208	-2.35	-1.52	-.036	.0233	.0111	-.037	.0223	-1.56
-1.26	-.033	.0218	.0073	-.033	.0210	-1.51	-.33	-.004	.0225	.0030	-.005	.0225	-.19
-.11	-.009	.0213	.0037	-.009	.0213	-.42	.51	.018	.0226	-.0025	.018	.0224	.80
.88	.013	.0212	.0005	.013	.0210	.61	2.91	.076	.0252	-.0173	.077	.0213	3.01
2.97	.058	.0235	-.0068	.059	.0205	2.48	5.15	.137	.0330	-.0324	.140	.0206	4.15
5.22	.108	.0298	-.0146	.110	.0198	3.63	7.11	.191	.0435	-.0442	.194	.0196	4.38
7.28	.158	.0390	-.0219	.162	.0186	4.06	9.27	.250	.0594	-.0556	.257	.0183	4.21
9.31	.206	.0511	-.0276	.212	.0170	4.04	11.39	.310	.0800	-.0658	.319	.0173	3.87
11.36	.256	.0675	-.0335	.264	.0158	3.79	13.51	.371	.1062	-.0767	.385	.0166	3.49
13.57	.311	.0905	-.0400	.324	.0150	3.44							
			BHV							BHVC			
-3.07	-0.097	0.0300	0.0278	-0.099	0.0247	-3.25	-3.19	-0.101	0.0324	0.0227	-0.103	0.0267	-3.13
-2.07	-.069	.0275	.0206	-.070	.0250	-2.51	-2.18	-.072	.0299	.0172	-.073	.0271	-2.42
-1.07	-.041	.0259	.0135	-.041	.0252	-1.58	-1.05	-.042	.0280	.0113	-.042	.0272	-1.50
.01	-.013	.0254	.0066	-.013	.0254	-.50	-.06	-.014	.0272	.0058	-.014	.0272	-.51
1.09	.016	.0254	-.0004	.016	.0251	.61	1.01	.013	.0271	.0006	.013	.0269	.47
2.96	.065	.0278	-.0130	.067	.0244	2.36	3.19	.073	.0303	-.0112	.075	.0262	2.41
5.22	.128	.0354	-.0285	.131	.0236	3.62	5.30	.133	.0378	-.0226	.136	.0253	3.53
7.37	.190	.0467	-.0426	.194	.0220	4.06	7.33	.191	.0490	-.0329	.196	.0242	3.90
9.44	.247	.0616	-.0543	.254	.0202	4.01	9.38	.252	.0650	-.0434	.260	.0230	3.88
11.35	.301	.0796	-.0647	.311	.0187	3.79	11.60	.317	.0874	-.0533	.328	.0219	3.62
13.52	.363	.1056	-.0759	.378	.0177	3.44	13.63	.375	.1129	-.0617	.391	.0214	3.32

(f) M = 5.37; Re/m = 8.20X10^6

			B							BH			
-2.16	-0.028	0.0112	0.0005	-0.028	0.0102	-2.46	-2.28	-0.035	0.0133	0.0045	-0.035	0.0120	-2.59
-1.18	-.017	.0106	.0009	-.017	.0103	-1.60	-1.18	-.020	.0123	.0027	-.020	.0119	-1.61
.10	-.001	.0105	.0004	-.001	.0105	-.07	-.24	-.006	.0119	.0012	-.006	.0119	-.54
1.00	.011	.0108	-.0002	.011	.0106	1.02	.82	.009	.0121	-.0008	.010	.0120	.78
2.18	.027	.0116	-.0010	.027	.0105	2.82	1.77	.024	.0127	-.0026	.025	.0120	1.90
3.91	.050	.0140	-.0020	.051	.0105	3.59	3.80	.057	.0158	-.0068	.058	.0120	3.58
5.83	.076	.0184	-.0031	.077	.0106	4.14	5.73	.087	.0210	-.0109	.089	.0122	4.15
7.82	.104	.0252	-.0047	.106	.0108	4.14	7.64	.119	.0286	-.0155	.122	.0126	4.16
9.81	.134	.0343	-.0067	.137	.0111	3.89	9.61	.154	.0394	-.0212	.158	.0131	3.91
11.67	.163	.0452	-.0090	.169	.0112	3.61	11.53	.191	.0529	-.0274	.198	.0136	3.61
13.42	.194	.0580	-.0117	.202	.0114	3.34	13.43	.230	.0694	-.0343	.240	.0142	3.31
			BHV							BHVC			
-2.27	-0.035	0.0150	0.0052	-0.036	0.0136	-2.36	-2.23	-0.039	0.0157	0.0040	-0.040	0.0142	-2.50
-1.21	-.021	.0139	.0035	-.022	.0135	-1.52	-1.08	-.022	.0144	.0025	-.022	.0140	-1.54
-.12	-.006	.0135	.0018	-.006	.0135	-.41	-.22	-.009	.0139	.0015	-.009	.0138	-.62
.84	.009	.0137	-.0002	.009	.0136	.67	.64	.006	.0139	.0001	.006	.0138	.45
1.99	.027	.0144	-.0025	.027	.0135	1.85	1.76	.025	.0147	-.0015	.025	.0139	1.69
3.80	.057	.0173	-.0065	.058	.0135	3.27	3.83	.060	.0178	-.0050	.061	.0138	3.38
5.85	.089	.0228	-.0111	.091	.0136	3.91	5.60	.090	.0229	-.0081	.092	.0140	3.95
7.72	.121	.0304	-.0158	.124	.0139	3.97	7.74	.130	.0326	-.0124	.133	.0148	3.98
9.57	.154	.0405	-.0212	.158	.0144	3.79	9.62	.166	.0442	-.0169	.171	.0158	3.76
11.47	.190	.0537	-.0273	.197	.0149	3.54	11.52	.206	.0591	-.0221	.214	.0167	3.49
13.39	.230	.0706	-.0343	.240	.0154	3.26	13.33	.248	.0769	-.0274	.259	.0178	3.22

TABLE 2.– TABULATED DATA – Concluded.

(g) M = 7.38; Re/m = 8.20X10^6

α	C_L	C_D	C_m	C_N	C_A	L/D	α	C_L	C_D	C_m	C_N	C_A	L/D
			B							BH			
-2.62	-0.023	0.0095	-0.0012	-0.023	0.0084	-2.44	-2.61	-0.027	0.0108	0.0008	-0.028	0.0095	-2.54
-1.52	-.014	.0087	-.0008	-.015	.0083	-1.67	-1.07	-.013	.0097	.0004	-.013	.0095	-1.34
-.54	-.006	.0085	-.0002	-.006	.0085	-.74	.50	.002	.0098	.0001	.002	.0098	.21
.62	.004	.0086	.0003	.004	.0086	.47	1.35	.011	.0103	-.0004	.011	.0100	1.08
1.29	.010	.0089	.0005	.011	.0086	1.16	3.47	.036	.0126	-.0026	.037	.0104	2.85
3.49	.033	.0110	.0003	.034	.0090	2.98	5.62	.062	.0170	-.0050	.063	.0109	3.63
5.38	.053	.0144	.0002	.054	.0094	3.68	7.32	.085	.0224	-.0073	.087	.0115	3.77
7.37	.076	.0198	-.0001	.078	.0099	3.83	9.46	.115	.0317	-.0110	.119	.0124	3.63
9.40	.101	.0275	-.0006	.104	.0107	3.66	11.26	.144	.0421	-.0149	.150	.0132	3.42
11.26	.126	.0367	-.0016	.131	.0114	3.43	13.18	.176	.0552	-.0190	.184	.0137	3.18
13.16	.152	.0476	-.0021	.159	.0117	3.20							
			BHV							BHVC			
-2.61	-0.027	0.0123	0.0019	-0.028	0.0110	-2.23	-2.54	-0.031	0.0127	0.0005	-0.032	0.0113	-2.44
-1.43	-.016	.0113	.0013	-.017	.0108	-1.46	-1.37	-.019	.0116	.0006	-.019	.0112	-1.63
-.46	-.007	.0111	.0011	-.007	.0110	-.66	-.58	-.011	.0112	.0006	-.011	.0111	-.95
.66	.005	.0111	.0004	.005	.0111	.46	.35	.001	.0110	.0005	.001	.0110	.05
1.44	.013	.0114	-.0001	.013	.0111	1.11	1.44	.014	.0118	.0003	.014	.0114	1.18
3.43	.036	.0136	-.0024	.037	.0114	2.65	3.40	.038	.0142	-.0012	.039	.0119	2.70
5.23	.059	.0171	-.0046	.060	.0117	3.43	5.27	.062	.0181	-.0026	.063	.0124	3.40
7.40	.088	.0238	-.0077	.090	.0123	3.68	7.25	.089	.0246	-.0046	.091	.0132	3.61
9.33	.115	.0321	-.0111	.119	.0130	3.59	9.20	.119	.0337	-.0071	.122	.0143	3.52
11.09	.143	.0421	-.0148	.149	.0138	3.40	11.09	.149	.0450	-.0100	.155	.0154	3.32
13.06	.176	.0556	-.0194	.184	.0143	3.17	13.04	.185	.0599	-.0136	.194	.0166	3.09

(h) M = 10.61; Re/m = 4.90X10^6

			B							BH			
-2.50	-0.015	0.0063	-0.0025	-0.015	0.0056	-2.36	-2.49	-0.019	0.0085	-0.0008	-0.019	0.0077	-2.18
-1.36	-.010	.0056	-.0012	-.010	.0053	-1.72	-.50	-.005	.0073	.0001	-.006	.0072	-.75
-.45	-.004	.0059	-.0004	-.004	.0058	-.72	.51	.002	.0076	.0003	.002	.0076	.28
.59	.002	.0062	.0004	.002	.0062	.37	1.46	.010	.0082	.0007	.010	.0080	1.17
1.46	.007	.0067	.0014	.008	.0065	1.12	3.51	.026	.0106	.0014	.027	.0090	2.46
3.67	.022	.0086	.0035	.022	.0072	2.53	5.35	.041	.0138	.0014	.042	.0099	3.00
5.56	.033	.0112	.0051	.034	.0079	2.96	7.35	.062	.0193	-.0002	.064	.0112	3.24
7.39	.050	.0157	.0058	.051	.0092	3.15	9.29	.091	.0276	-.0039	.094	.0126	3.29
9.39	.071	.0221	.0049	.074	.0103	3.21	11.25	.124	.0390	-.0085	.129	.0141	3.17
11.24	.094	.0301	.0036	.098	.0112	3.12	13.12	.159	.0529	-.0140	.167	.0154	3.01
13.11	.122	.0411	.0019	.128	.0123	2.97							
			BHV							BHVC			
-2.45	-0.021	0.0116	0.0006	-0.022	0.0106	-1.85	-2.50	-0.024	0.0118	-0.0002	-0.024	0.0108	-2.01
-.46	-.006	.0098	.0006	-.006	.0097	-.56	-1.31	-.013	.0100	-.0001	-.013	.0097	-1.31
.88	.004	.0102	.0008	.004	.0101	.41	-.59	-.007	.0099	.0001	-.008	.0098	-.75
3.61	.027	.0129	.0009	.027	.0112	2.07	1.35	.010	.0103	.0008	.011	.0100	1.01
5.68	.045	.0165	.0005	.046	.0120	2.71	1.93	.016	.0111	.0010	.016	.0106	1.42
7.62	.065	.0219	-.0015	.067	.0131	2.97	3.45	.030	.0137	.0014	.031	.0119	2.18
9.65	.095	.0306	-.0059	.099	.0143	3.10	5.49	.051	.0182	.0007	.053	.0132	2.82
11.12	.118	.0387	-.0092	.123	.0152	3.05	7.32	.073	.0235	-.0004	.075	.0141	3.10
13.24	.158	.0541	-.0154	.166	.0165	2.91	9.28	.100	.0318	-.0029	.103	.0153	3.14
							11.19	.129	.0423	-.0060	.135	.0165	3.05
							13.11	.161	.0556	-.0095	.170	.0176	2.90

TABLE 3.– BALANCE CAVITY AXIAL–FORCE COEFFICIENT (C_{A_b})

	B Configuration				
α	M = 0.65	0.80	0.90	1.10	1.30
-2.00	0.0002	0.0001	0.0008	0.0019	0.0013
-1.00	.0002	.0001	.0010	.0019	.0013
0	.0002	.0001	.0011	.0020	.0014
1.00	.0003	.0002	.0011	.0020	.0014
2.00	.0003	.0002	.0011	.0020	.0015
4.00	.0003	.0002	.0010	.0020	.0015
6.00	.0004	.0003	.0008	.0021	.0015
8.00	.0005	.0003	.0009	.0023	.0016
10.00	.0006	.0004	.0012	.0026	.0018
12.00	.0008	.0005	.0016	.0029	.0019
14.00	.0010	.0007	.0021	.0031	.0020
α	M = 1.60	2.00	5.37	7.38	10.61
-2.00	0.0008	0.0004	0.0001	0	-0.0002
-1.00	.0009	.0005	.0001	0	-.0002
0	.0009	.0005	.0001	0	-.0002
1.00	.0009	.0005	.0001	0	-.0002
2.00	.0010	.0006	.0001	0	-.0002
4.00	.0010	.0006	.0002	.0001	-.0002
6.00	.0010	.0007	.0002	.0001	-.0002
8.00	.0011	.0007	.0002	.0001	-.0002
10.00	.0012	.0008	.0002	.0001	-.0002
12.00	.0013	.0009	.0002	.0001	-.0003
14.00	.0014	.0009	.0002	.0001	-.0003

Equation for maximum cross section
(station 32.17)

$$\left(\frac{y}{a_\pi}\right)^2 + \left(\frac{z}{b_\pi}\right)^2 = 1$$

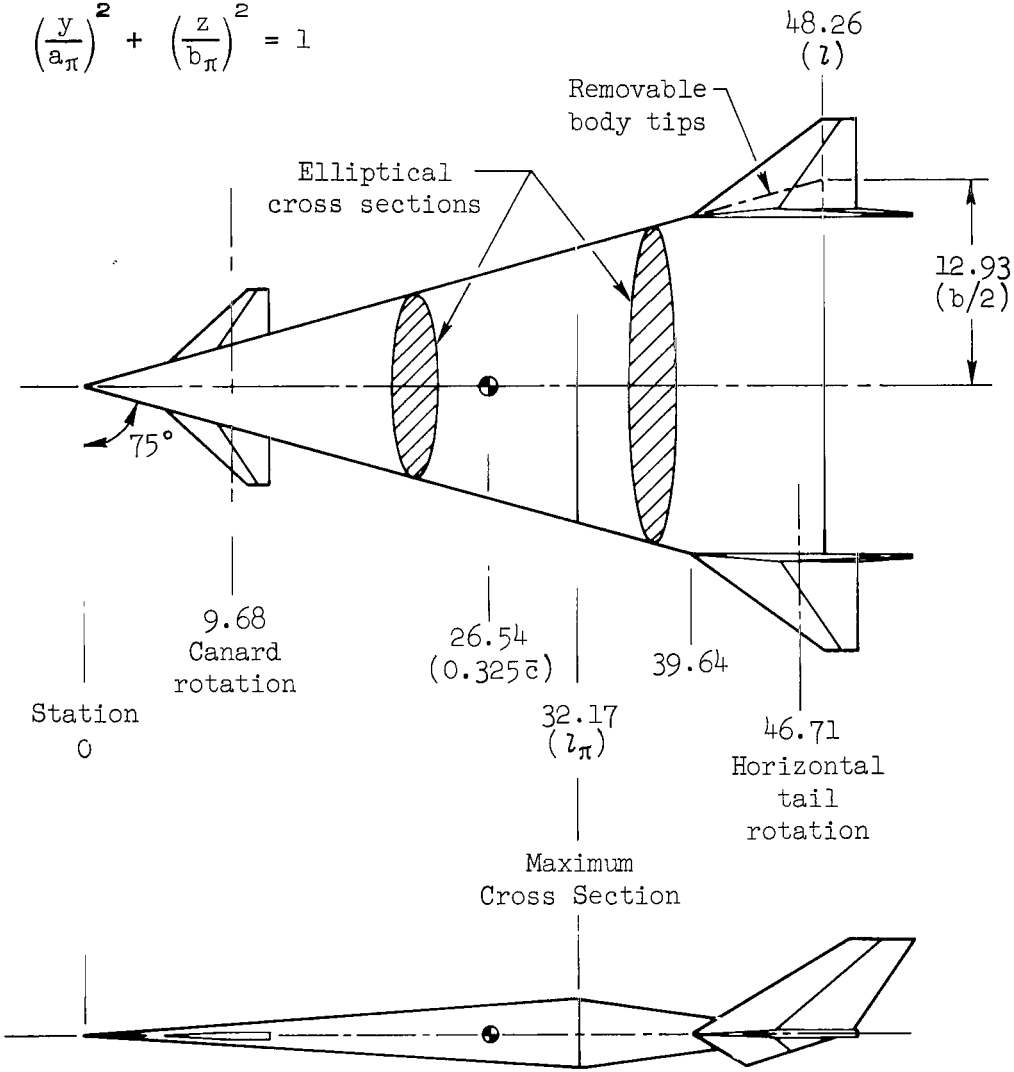

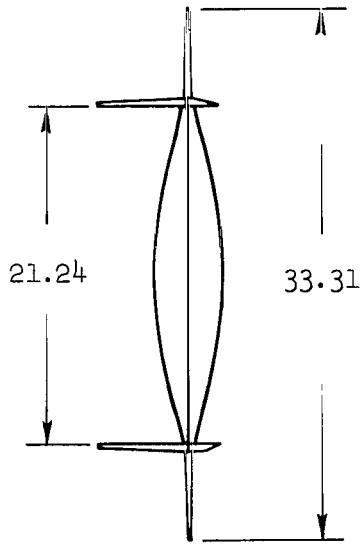

Model geometry	
S	624.06
$\bar{c}$	32.17
b	25.86
A_b	4.38
a_π	8.62
b_π	2.16
S_π	58.35
S_π/S	0.0935
l_π/l	0.6667

(a) Complete configuration

Figure 1.- Model drawings; all dimensions are in centimeters and areas in square centimeters.

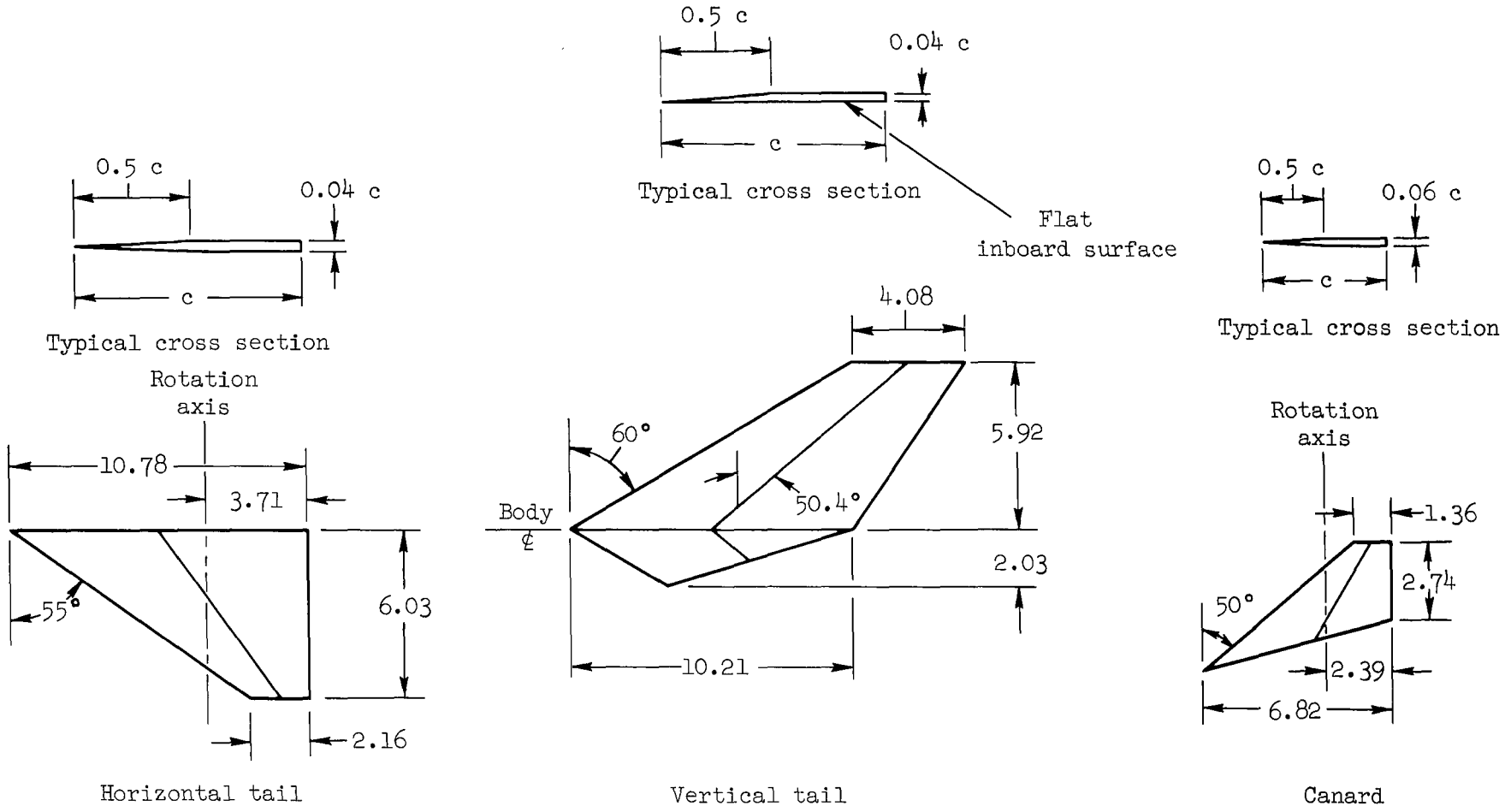

(b) Details of horizontal tail, vertical tail, and canard

Figure 1.- Concluded.

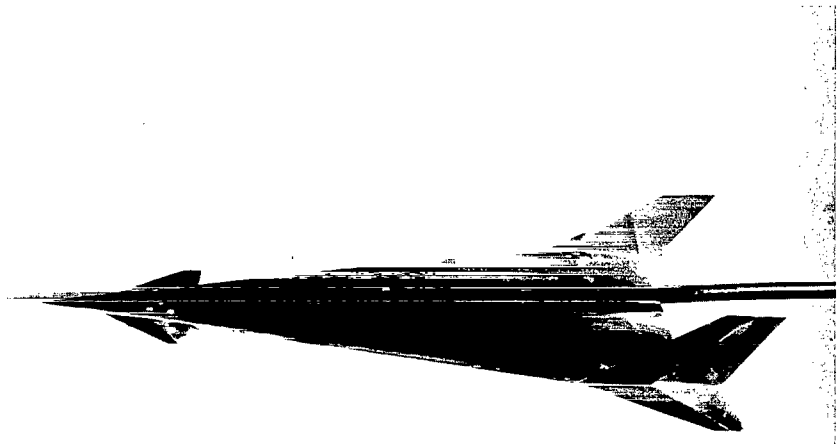

(a) BHVC configuration

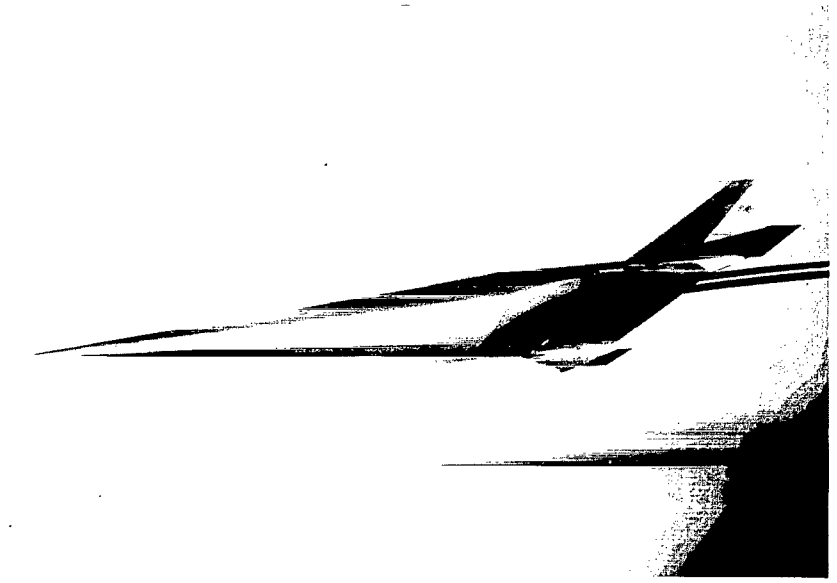

(b) BHV configuration

Figure 2.- Model photographs.

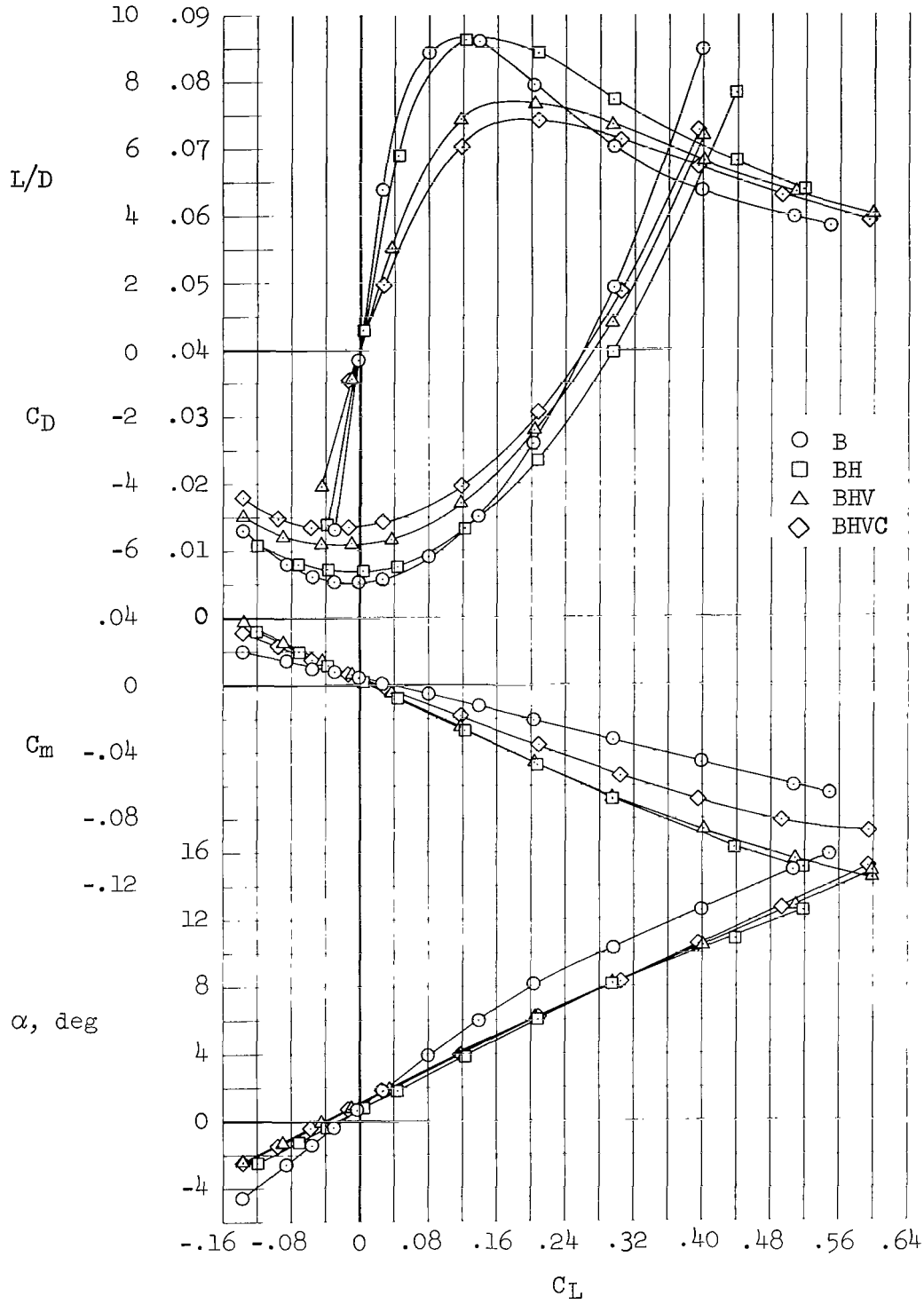

(a) M = 0.65

Figure 3.- Effect of addition of components on the longitudinal aerodynamic characteristics.

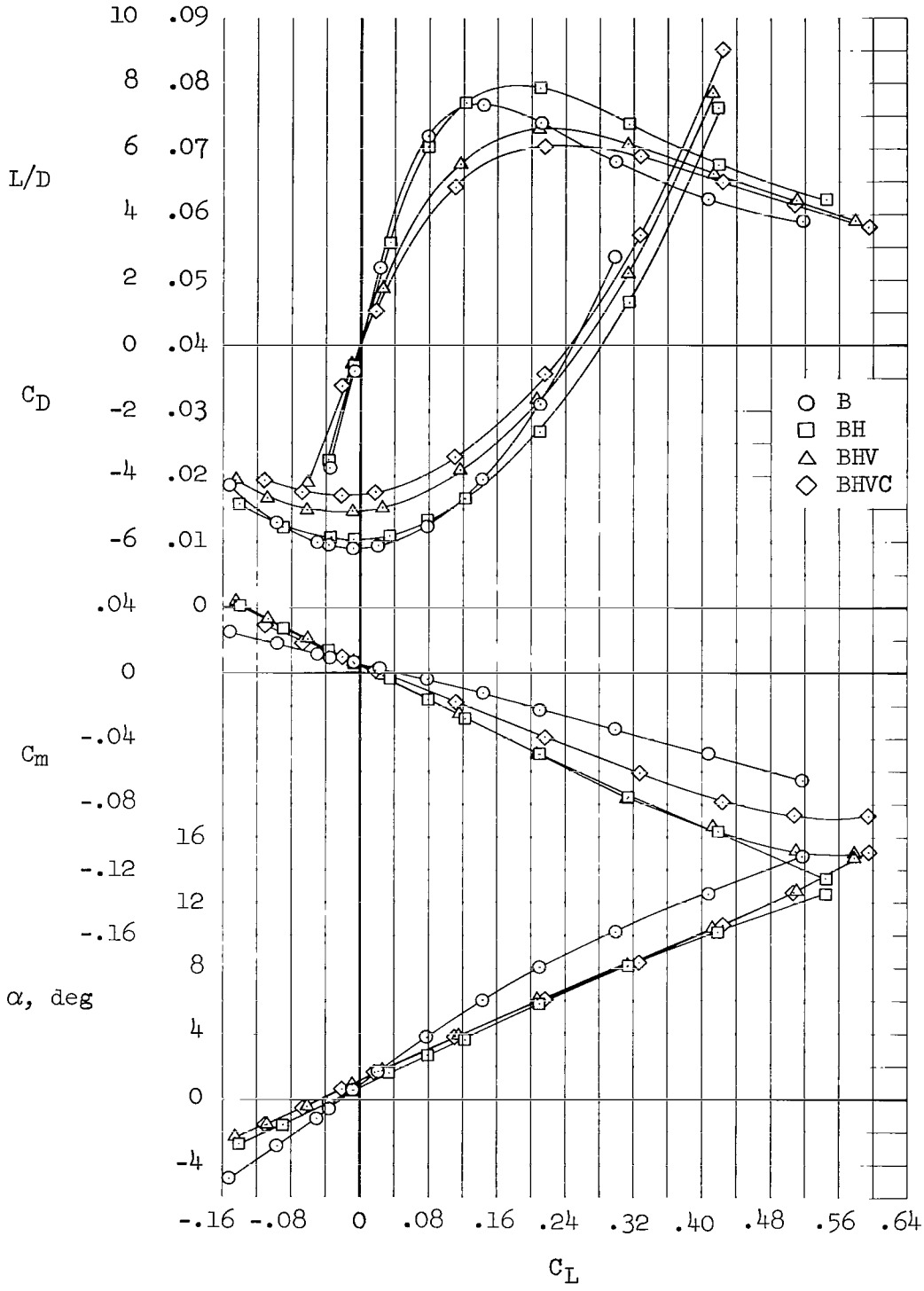

(b) M = 0.80

Figure 3.- Continued.

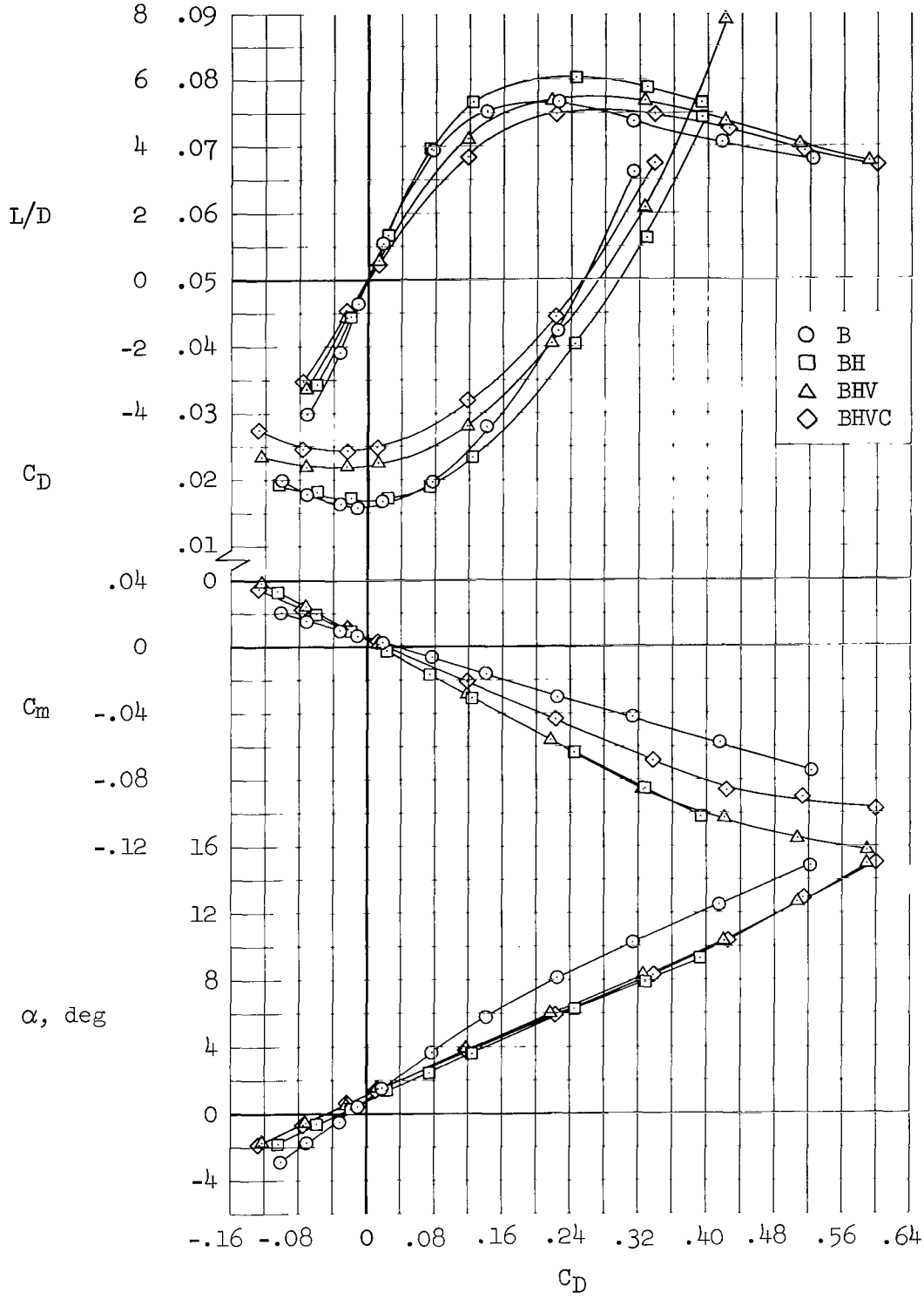

(c) M = 0.90

Figure 3.- Continued.

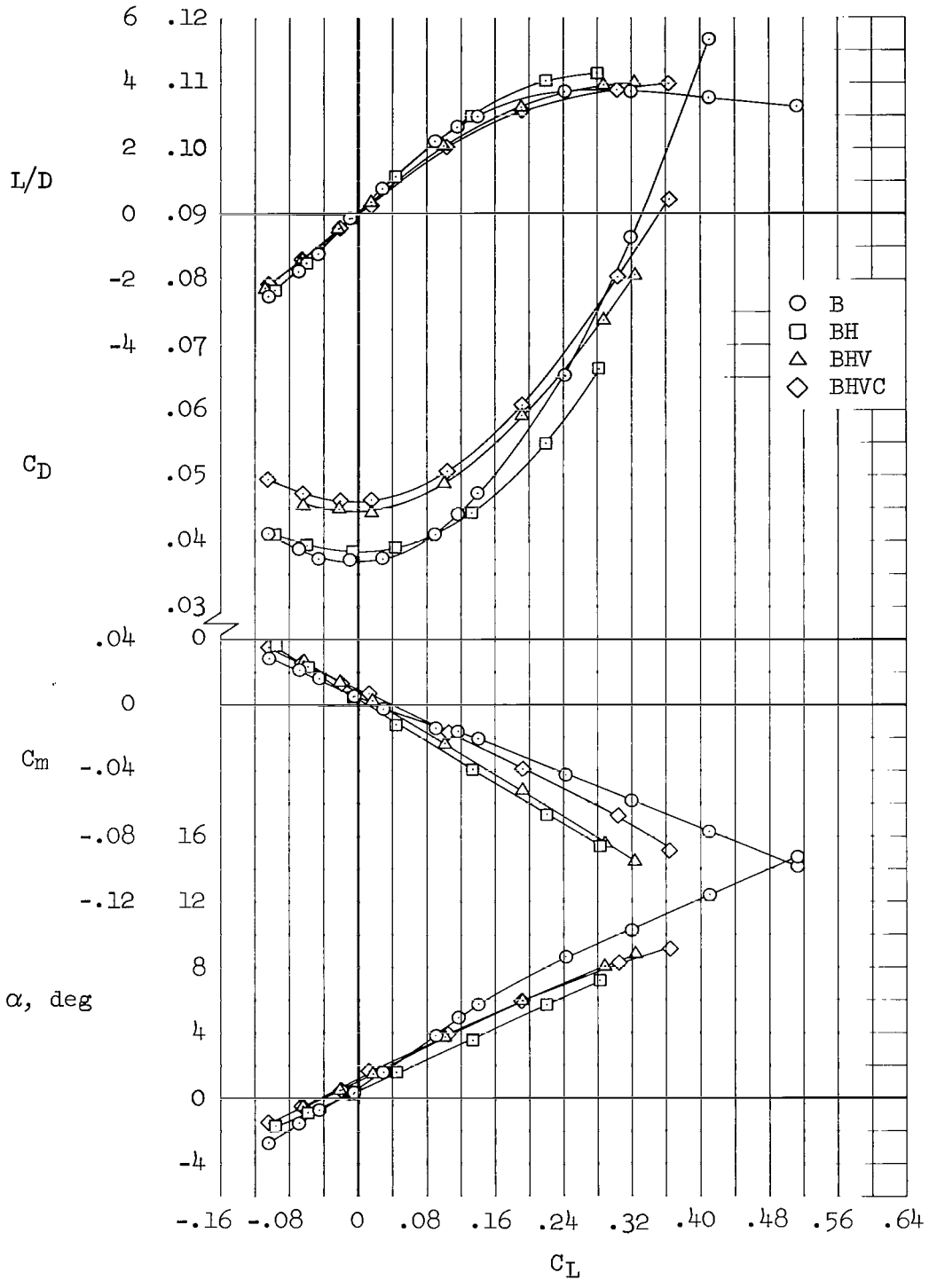

(d) M = 1.10

Figure 3.- Continued.

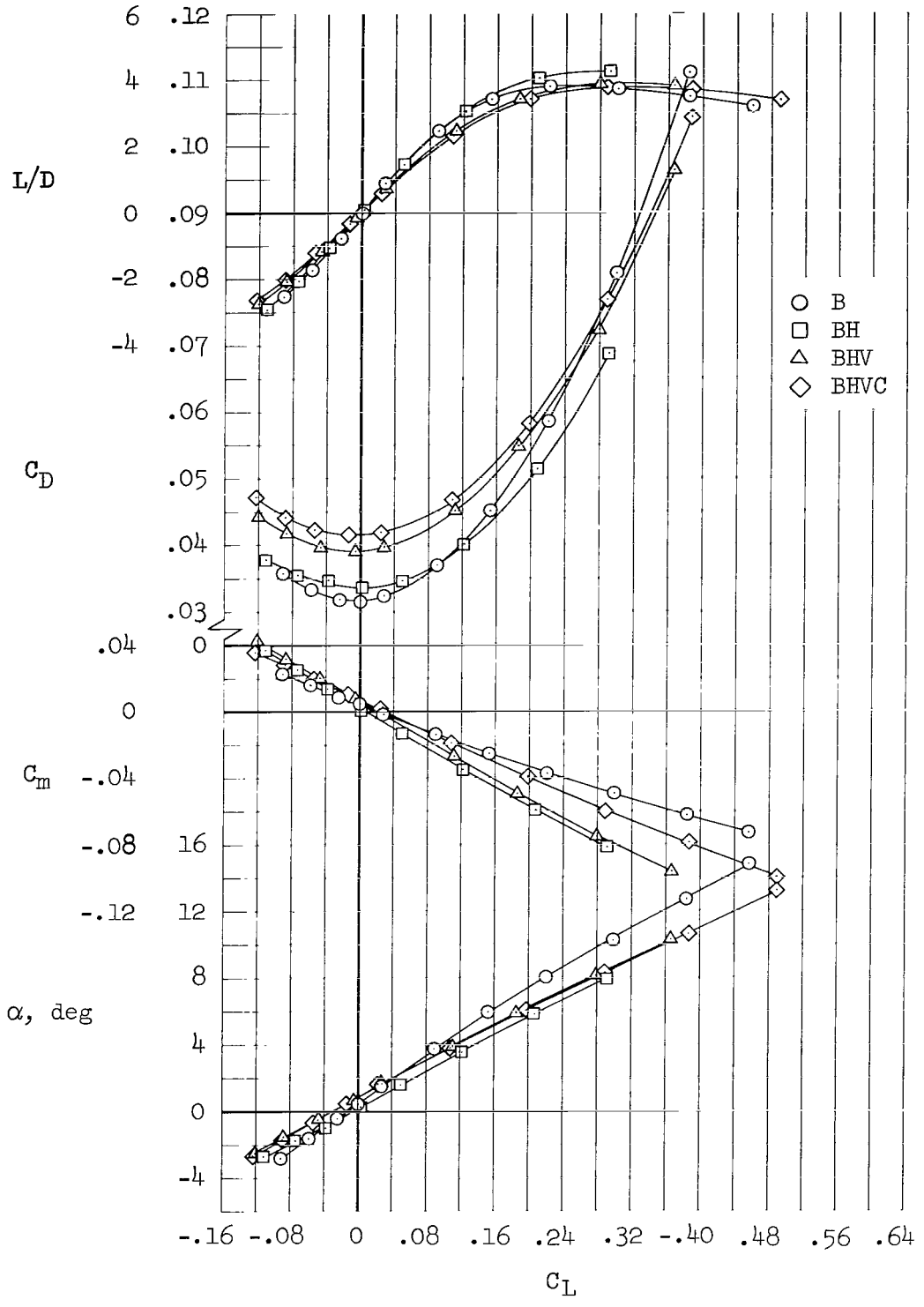

(e) M = 1.30

Figure 3.- Continued.

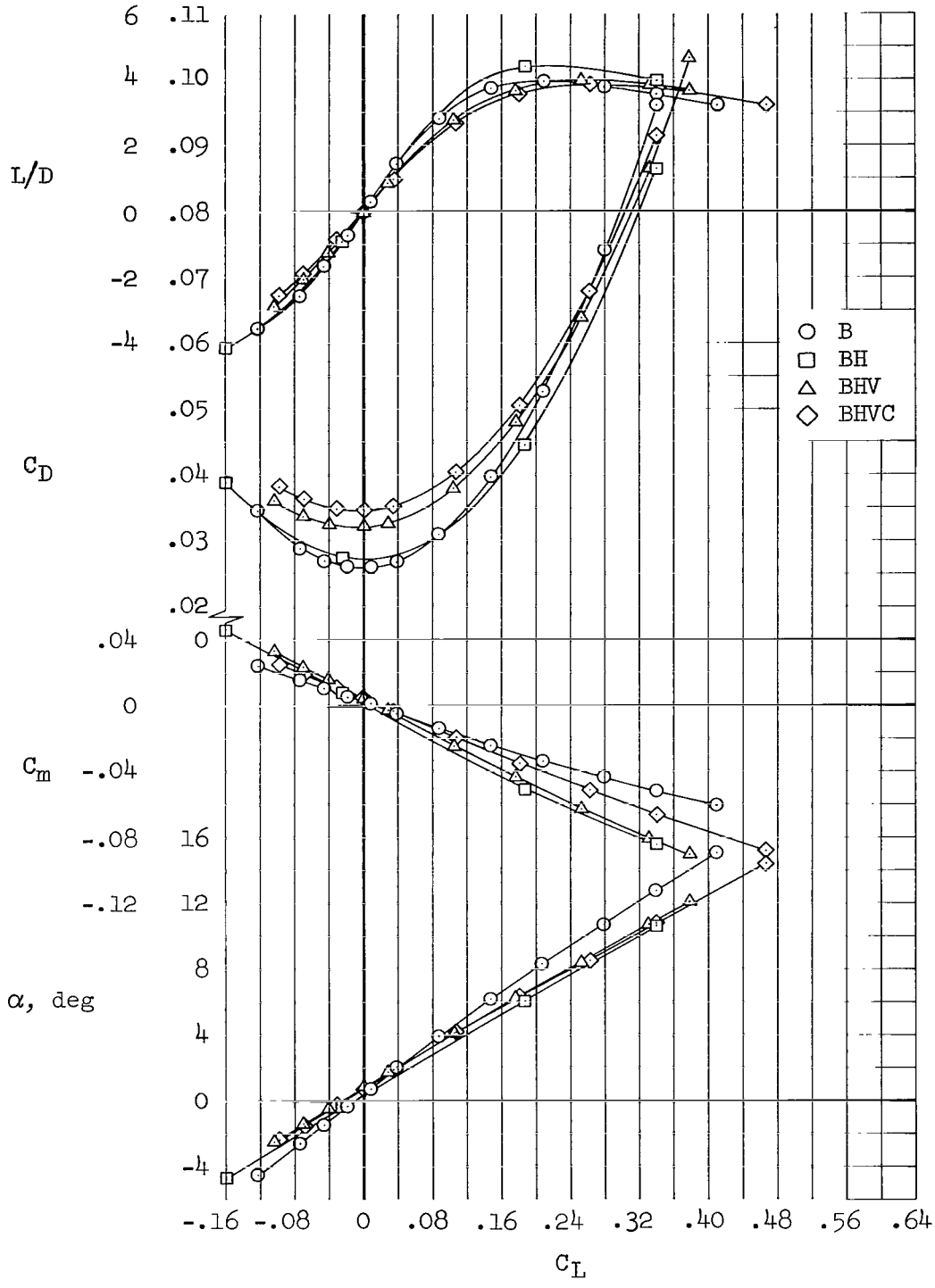

(f) M = 1.60

Figure 3.- Continued.

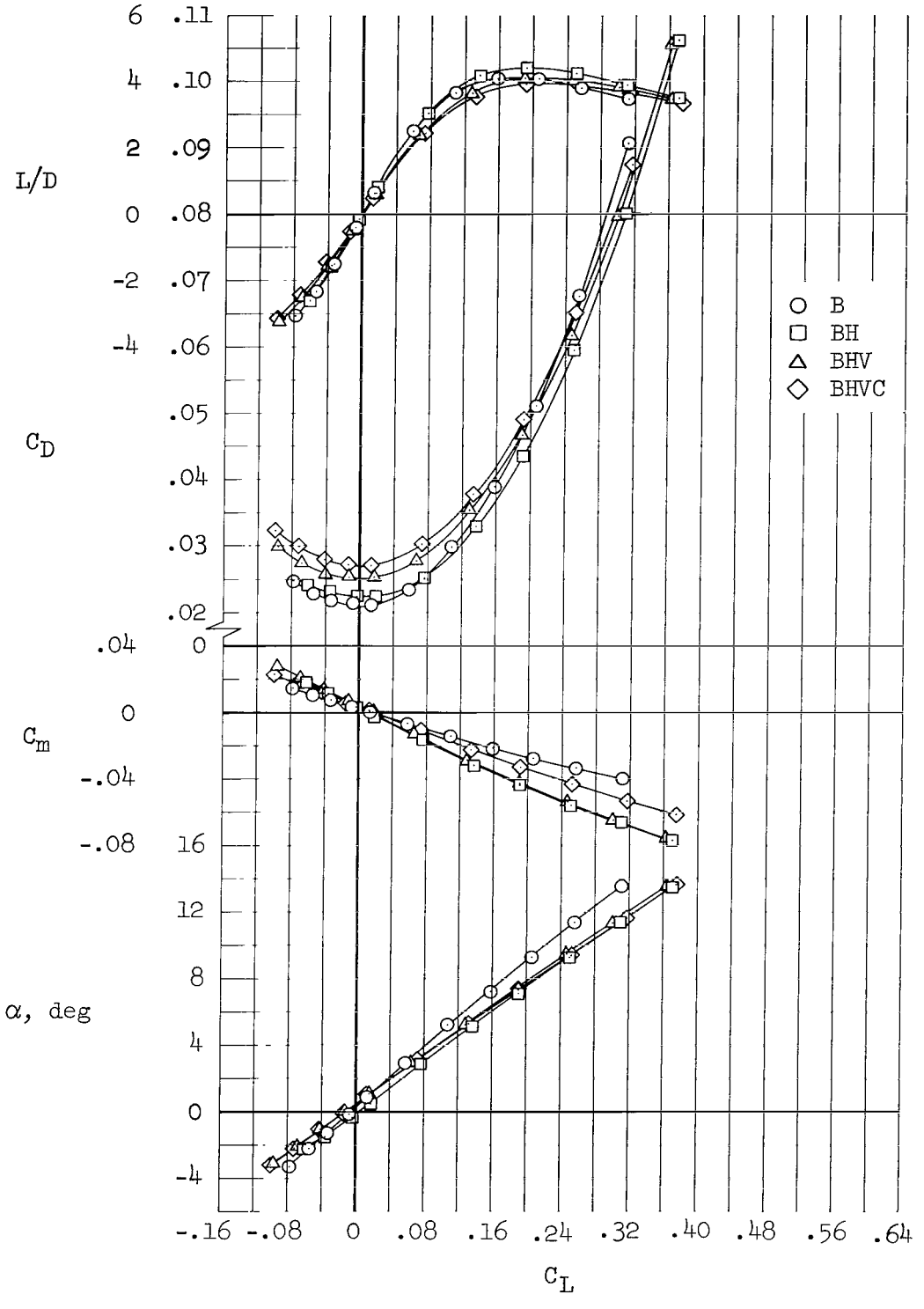

(g) M = 2.00

Figure 3.- Continued.

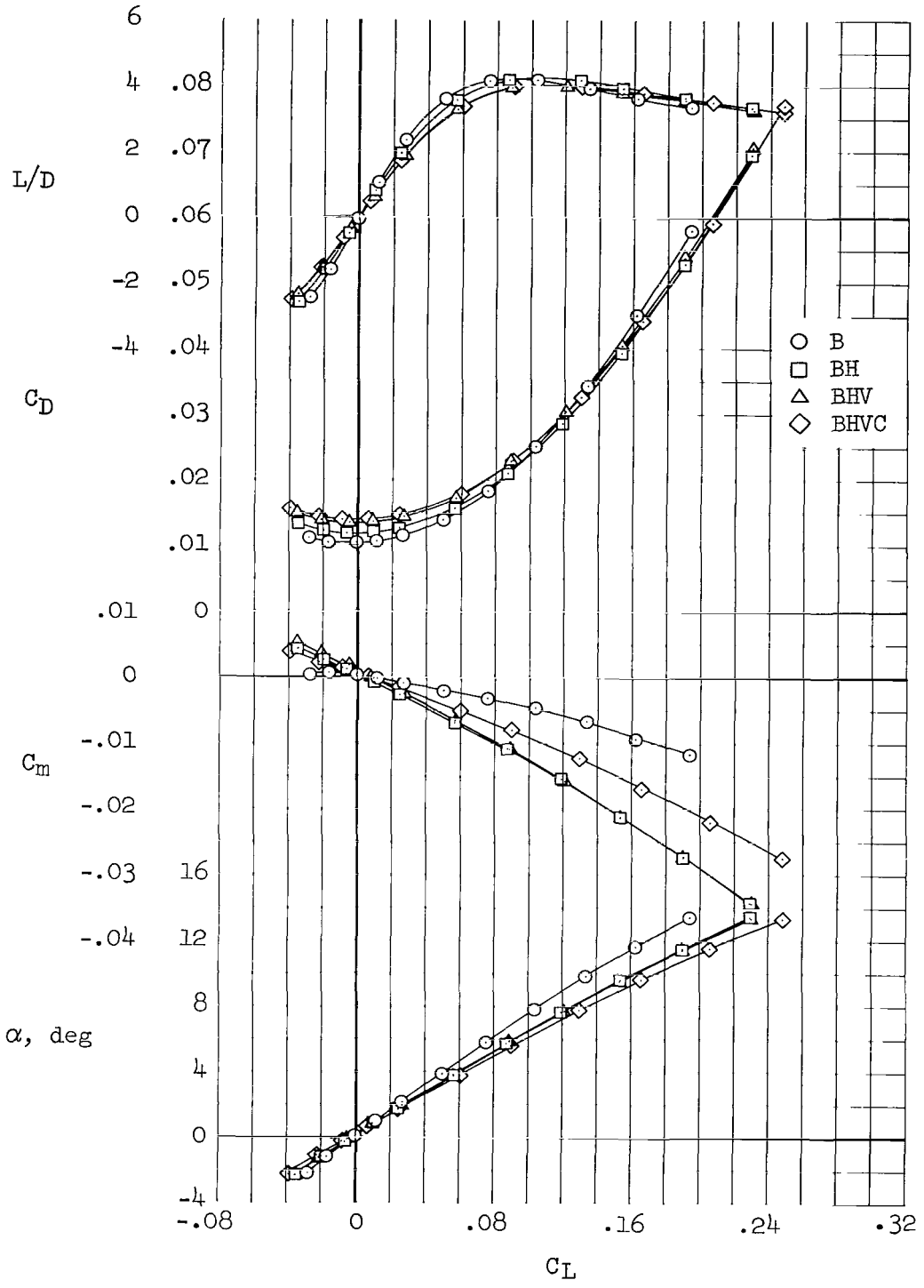

(h) M = 5.37

Figure 3.- Continued.

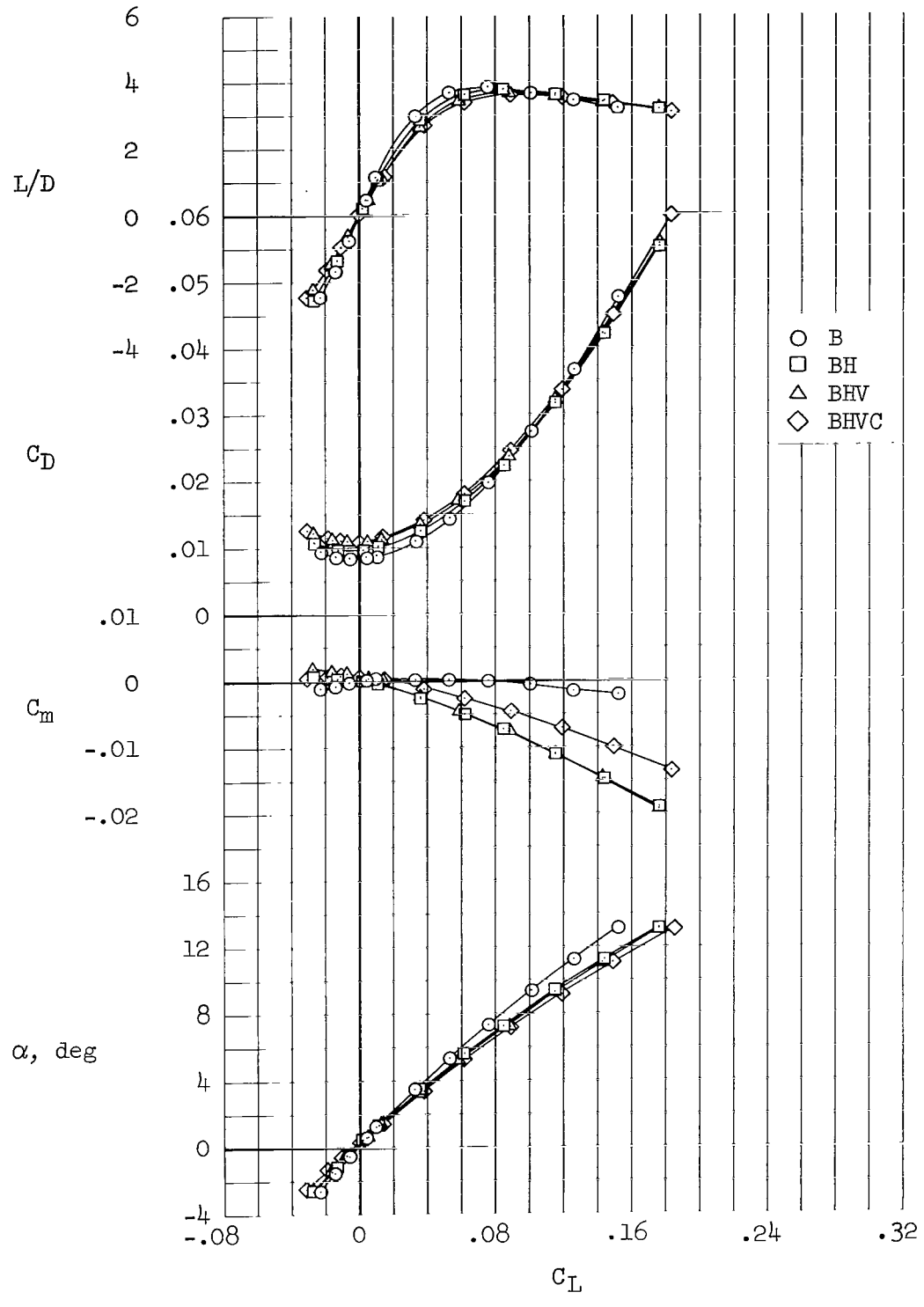

(i) M = 7.38

Figure 3.- Continued.

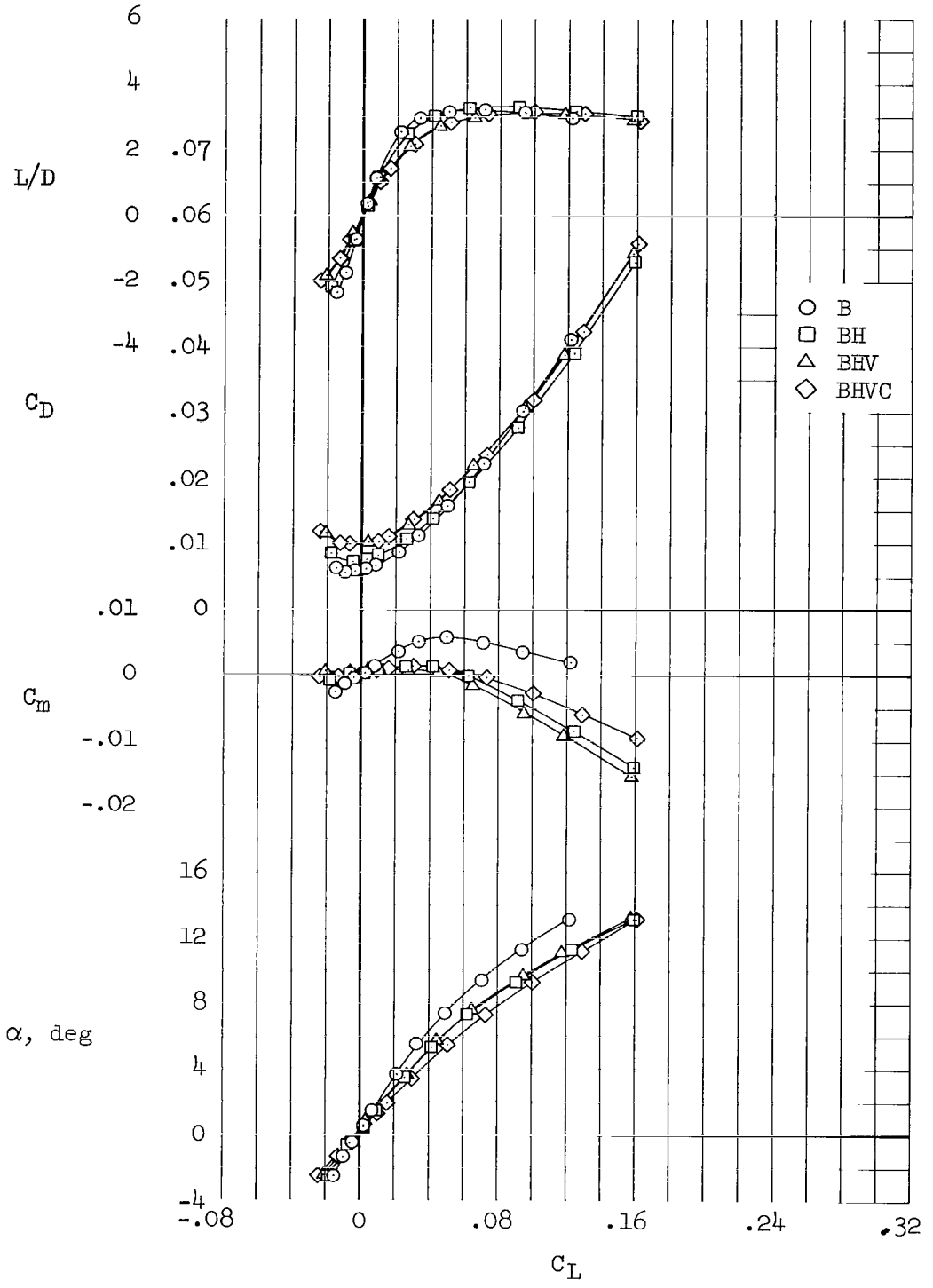

(j) M = 10.6

Figure 3.- Concluded.

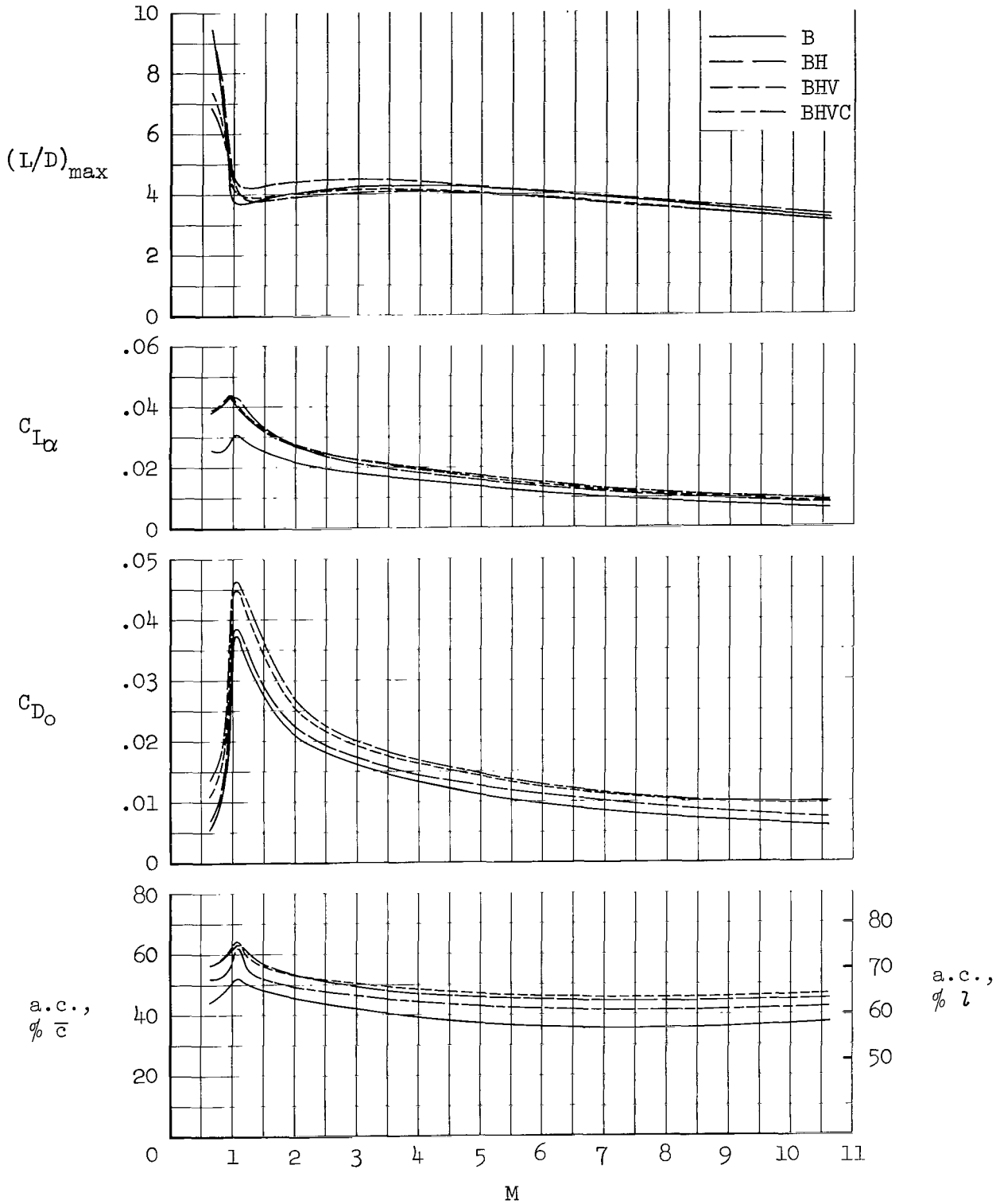

Figure 4.- Variation with Mach number of the effect of addition of components on the longitudinal aerodynamic characteristics; $\beta = 0°$.

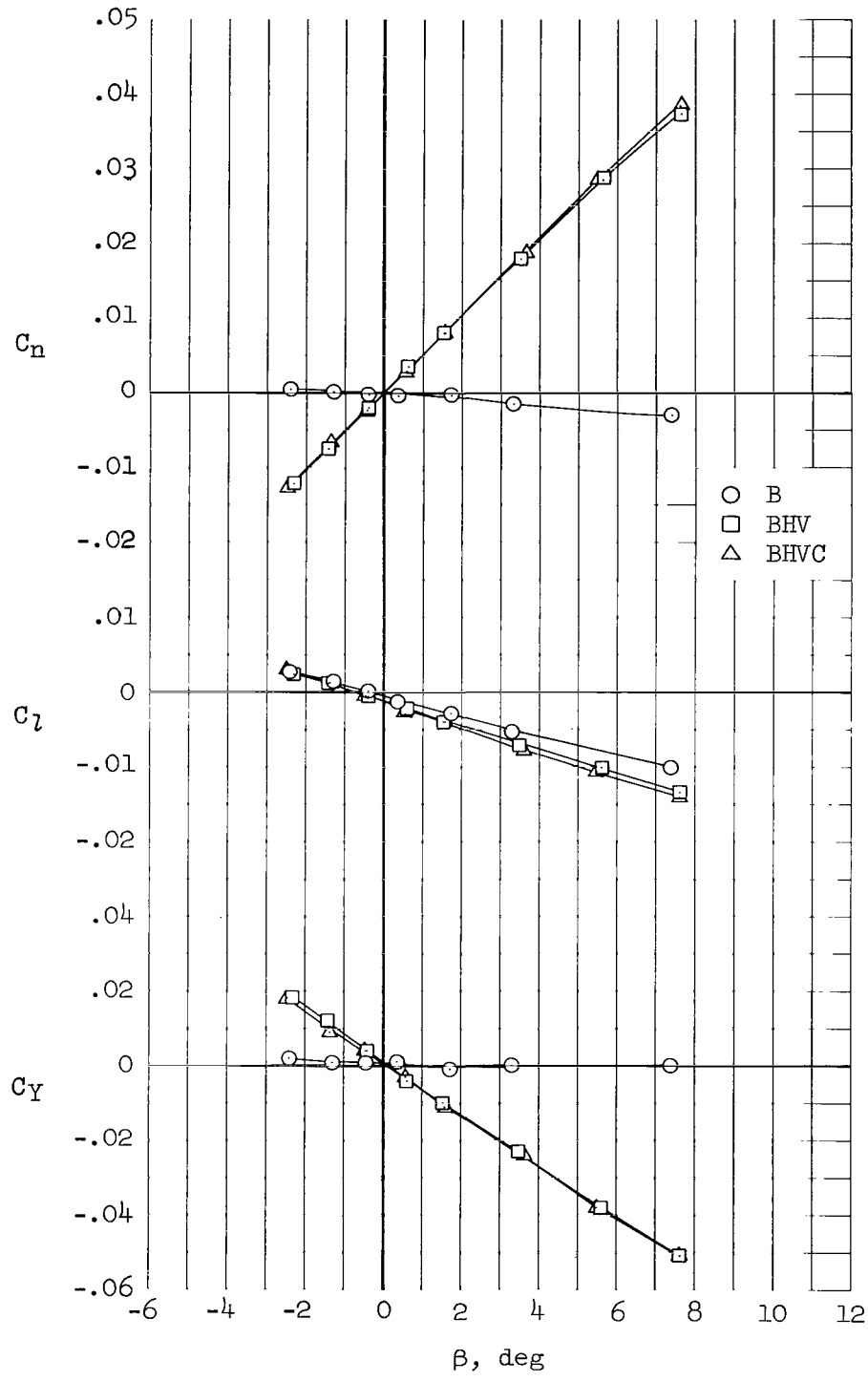

(a) M = 0.65; α = 5.3°

Figure 5.- Effect of addition of components on the lateral-directional aerodynamic characteristics in sideslip.

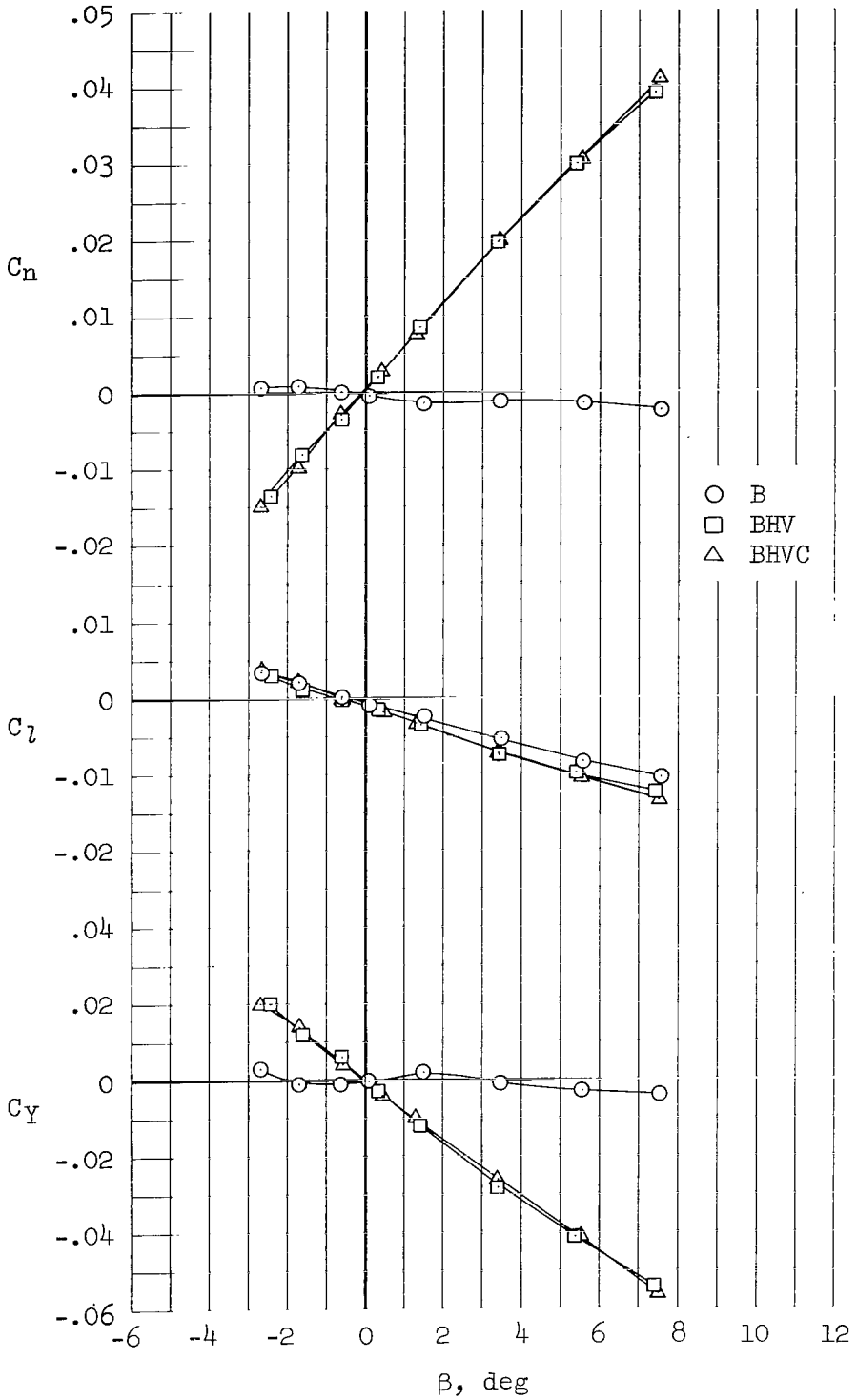

(b) M = 0.90; α = 5.3°

Figure 5.- Continued.

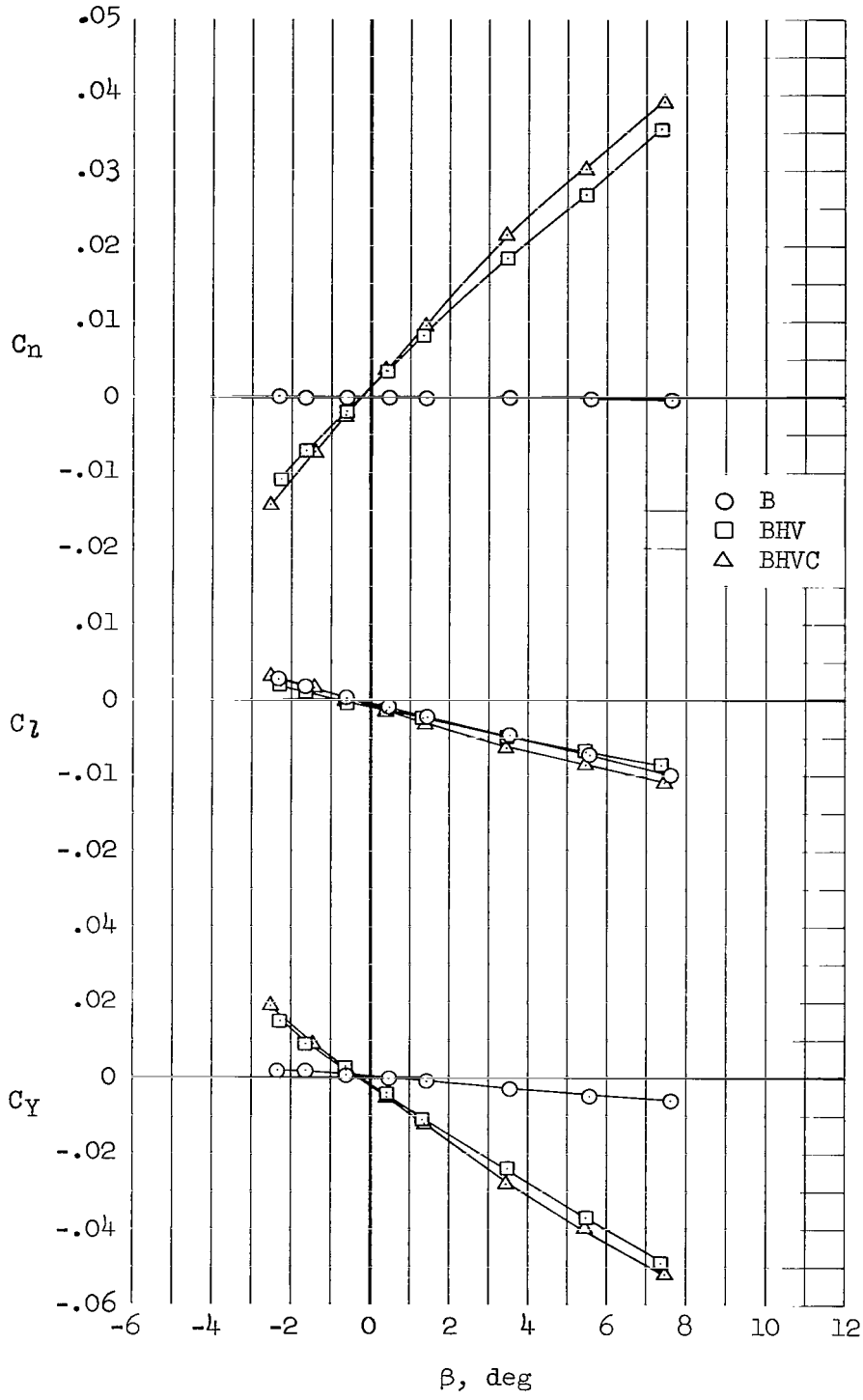

(c) M = 1.30; α = 5.4°

Figure 5.- Continued.

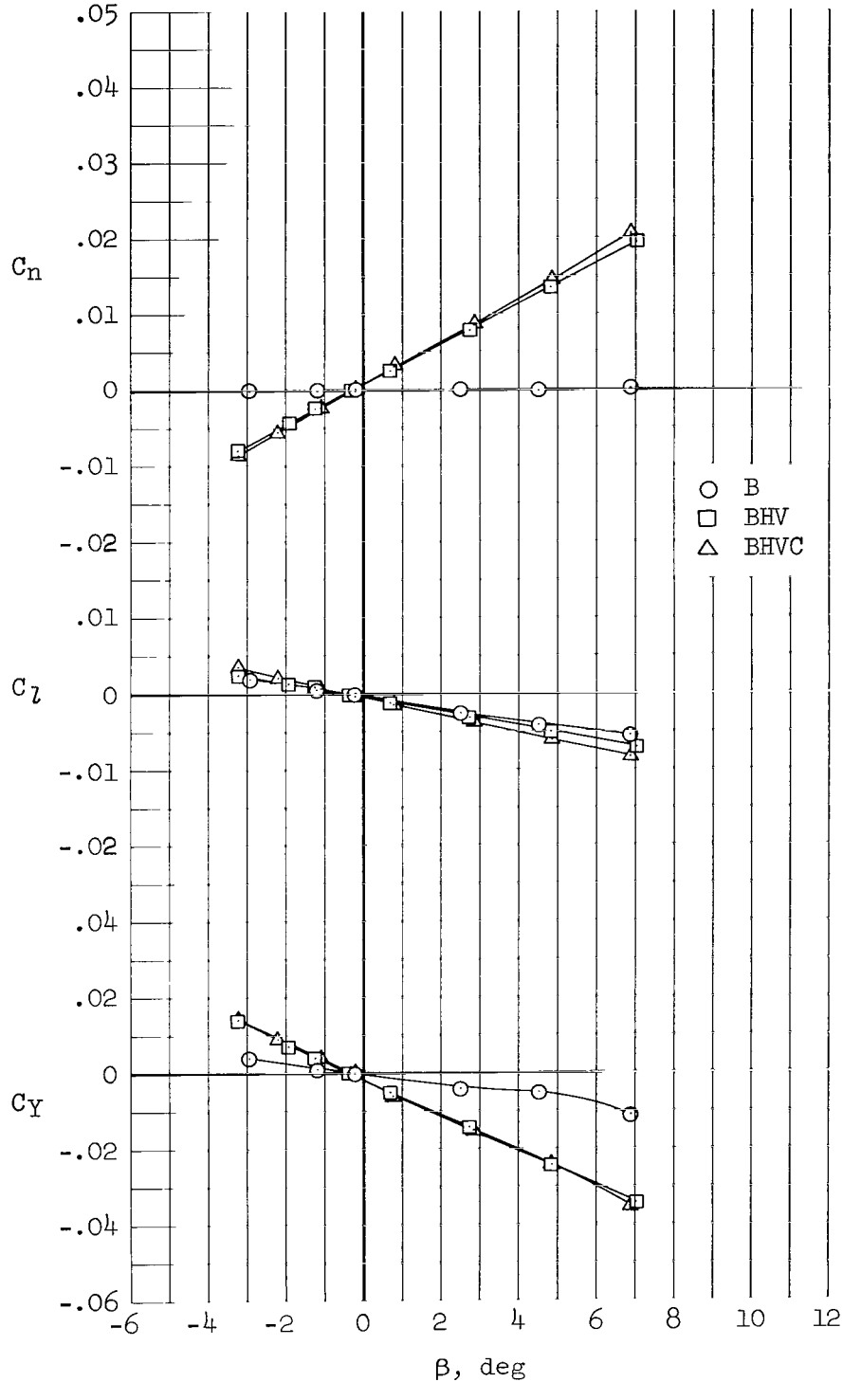

(d) M = 2.00; α = 5.2°

Figure 5.- Continued.

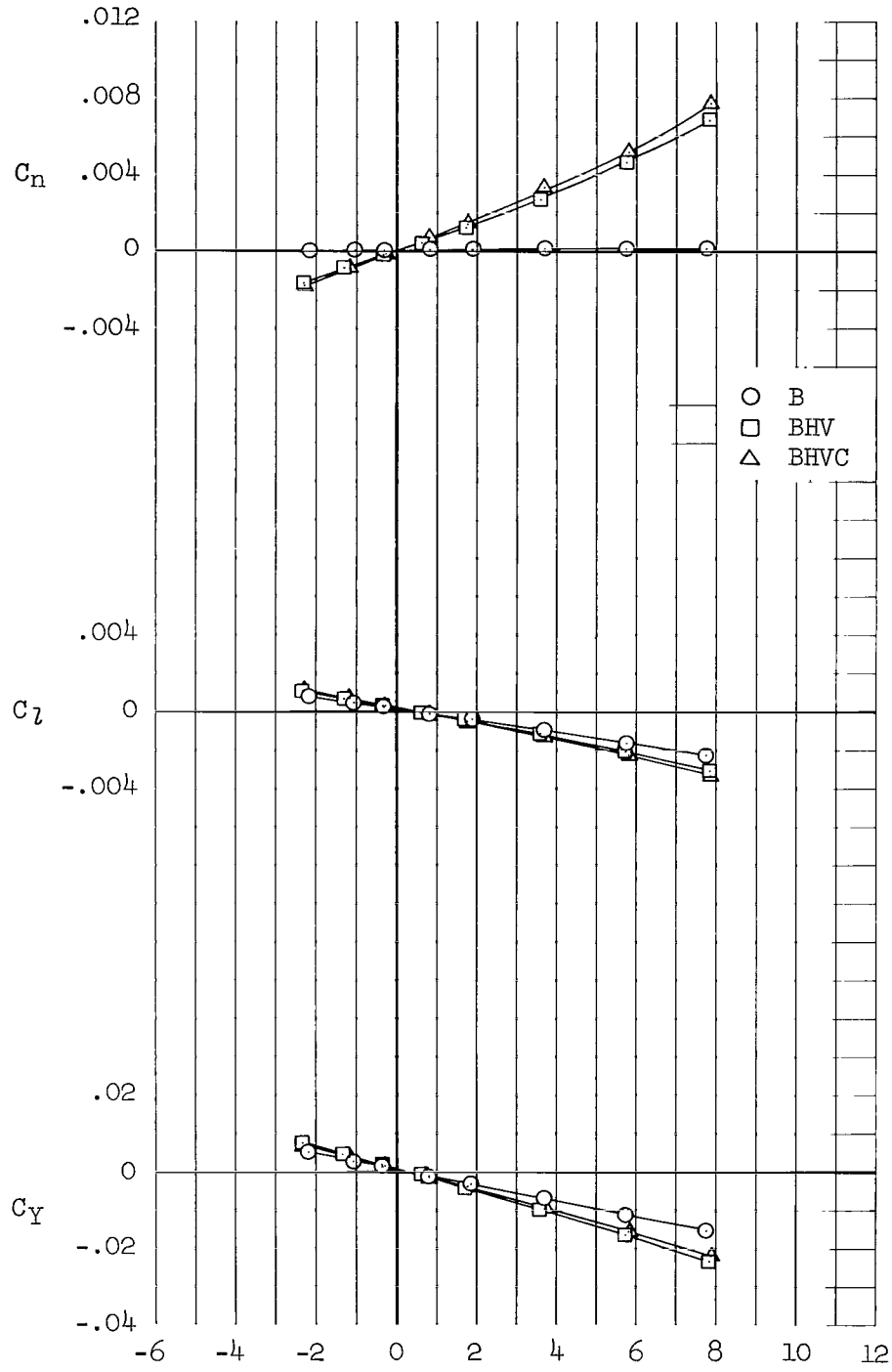

(e) M = 7.38; α = 4.8°

Figure 5.- Continued.

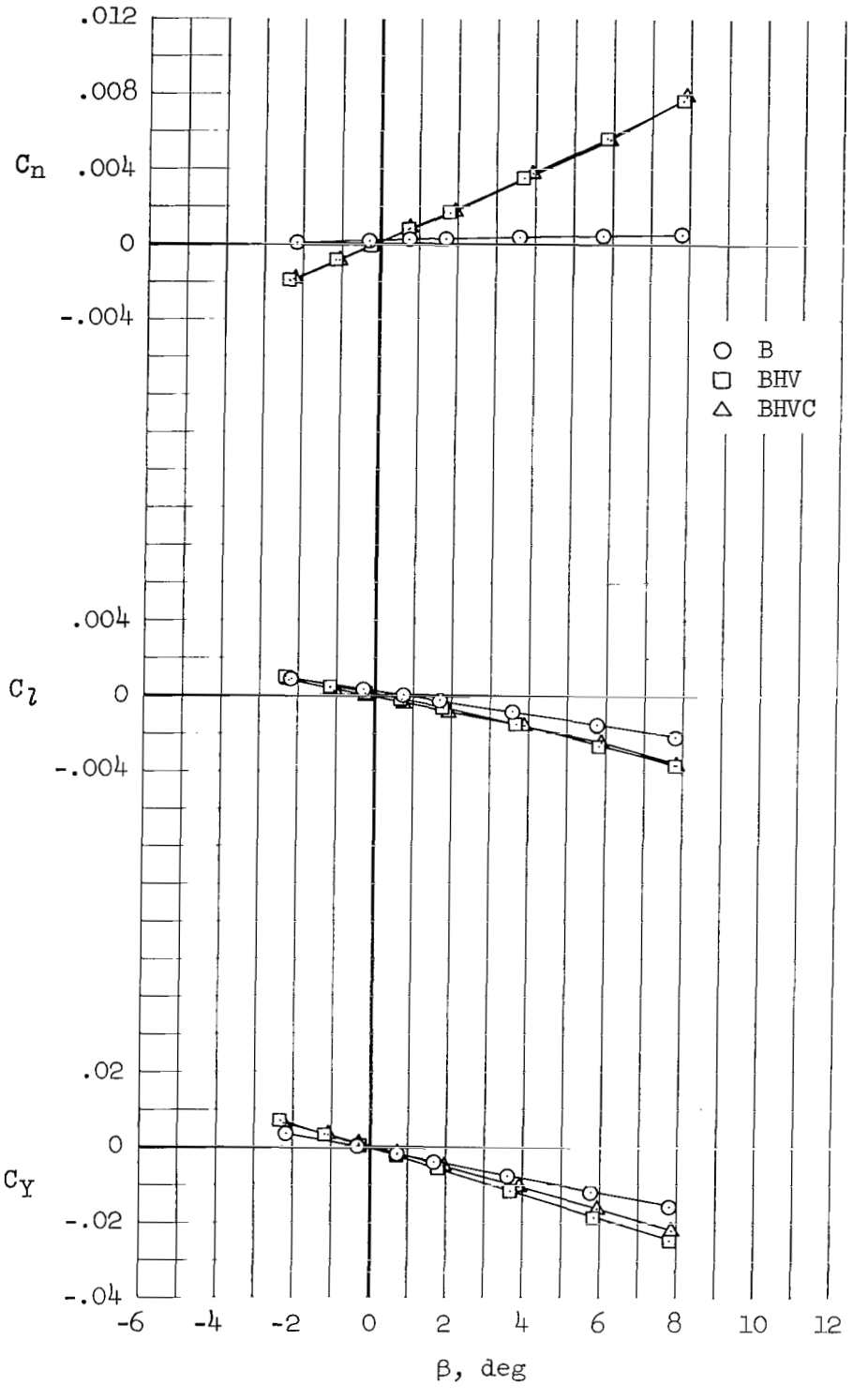

(f) M = 10.6; α = 4.7°

Figure 5.- Concluded.

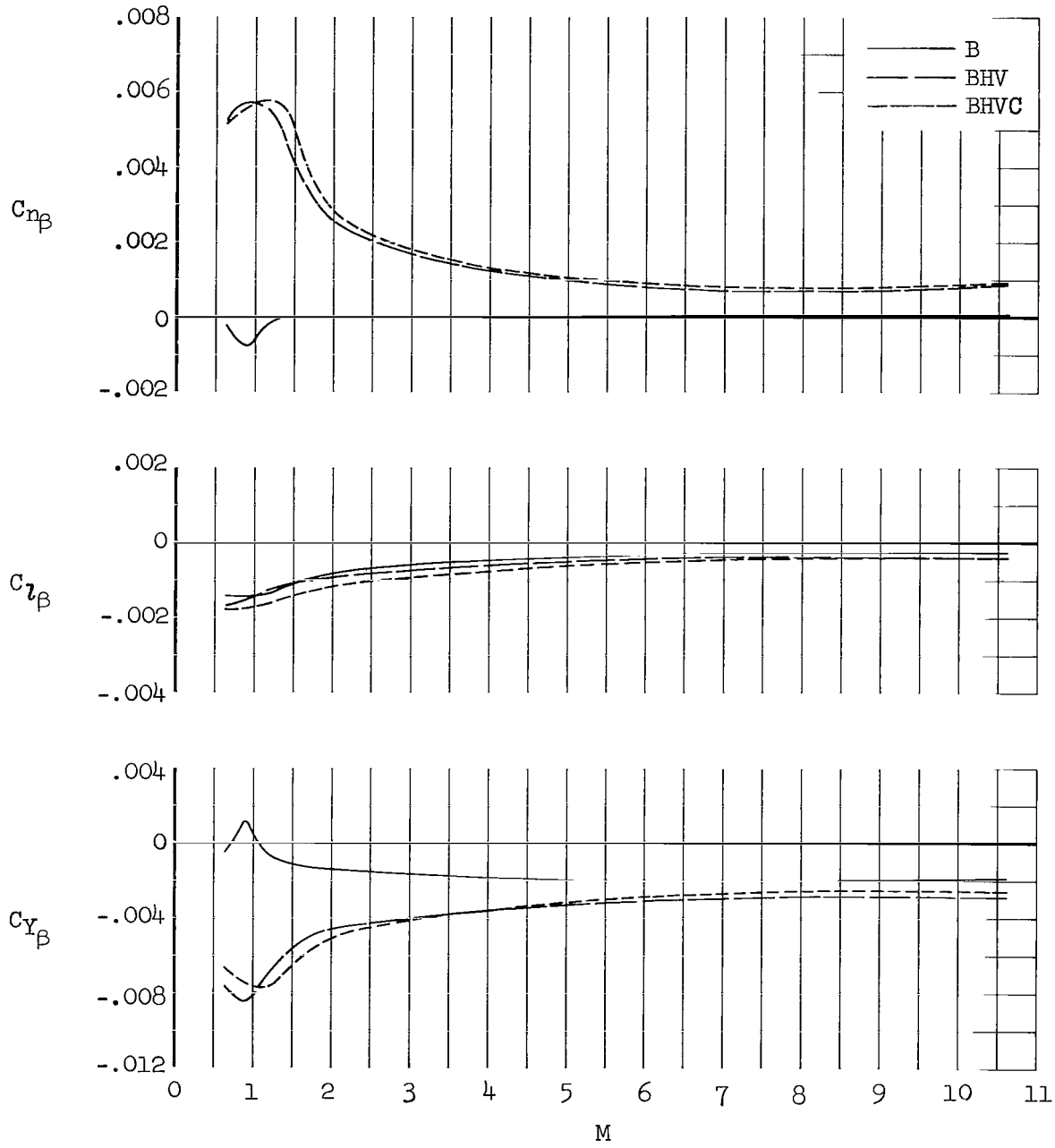

Figure 6.- Variation with Mach number of the effect of addition of components on the lateral-directional aerodynamic characteristics; α = 4.7° to 5.4°.

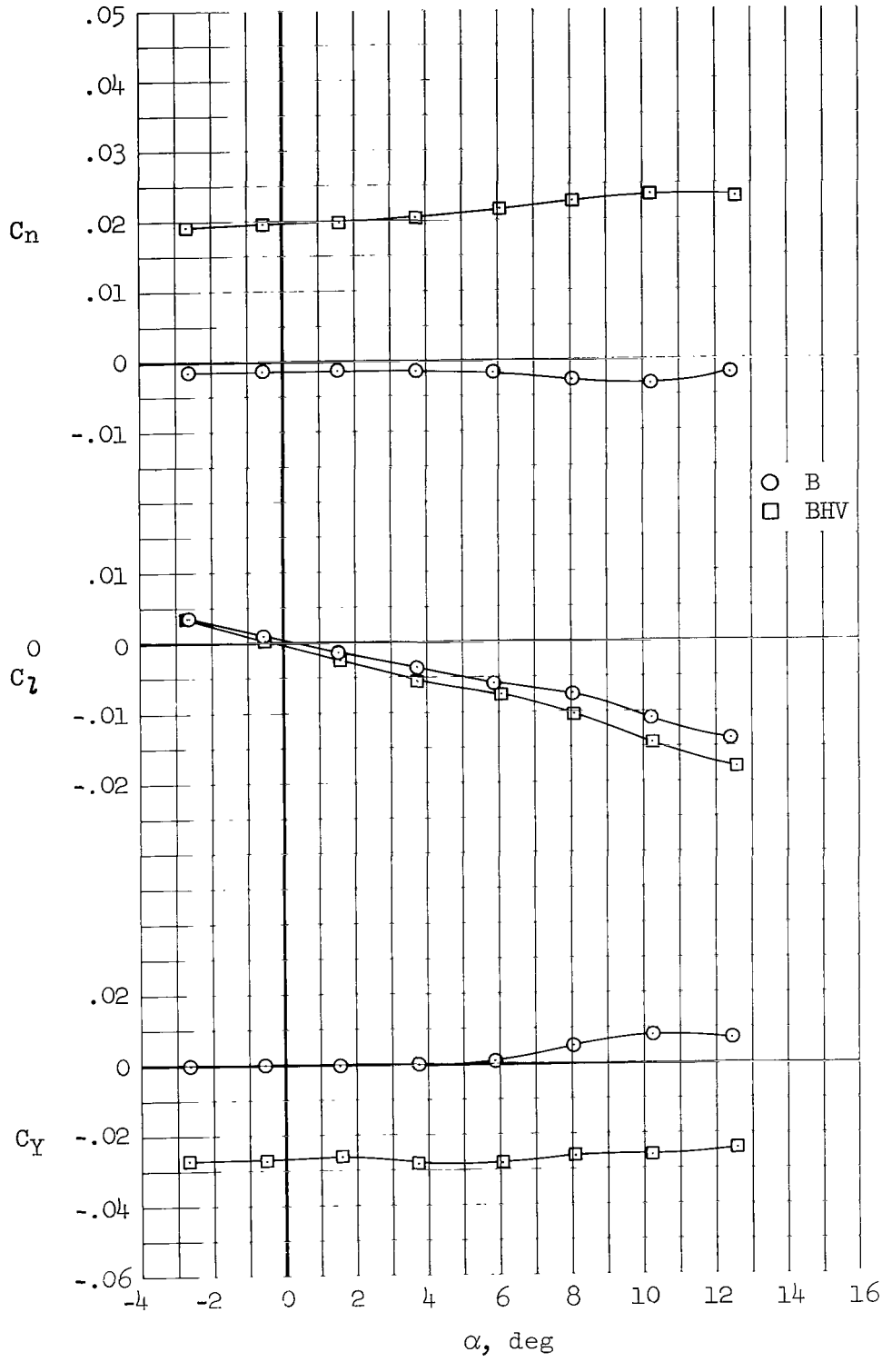

(a) M = 0.65

Figure 7.- Effect of addition of components on the lateral-directional aerodynamic characteristics in pitch, β = 4.0°.

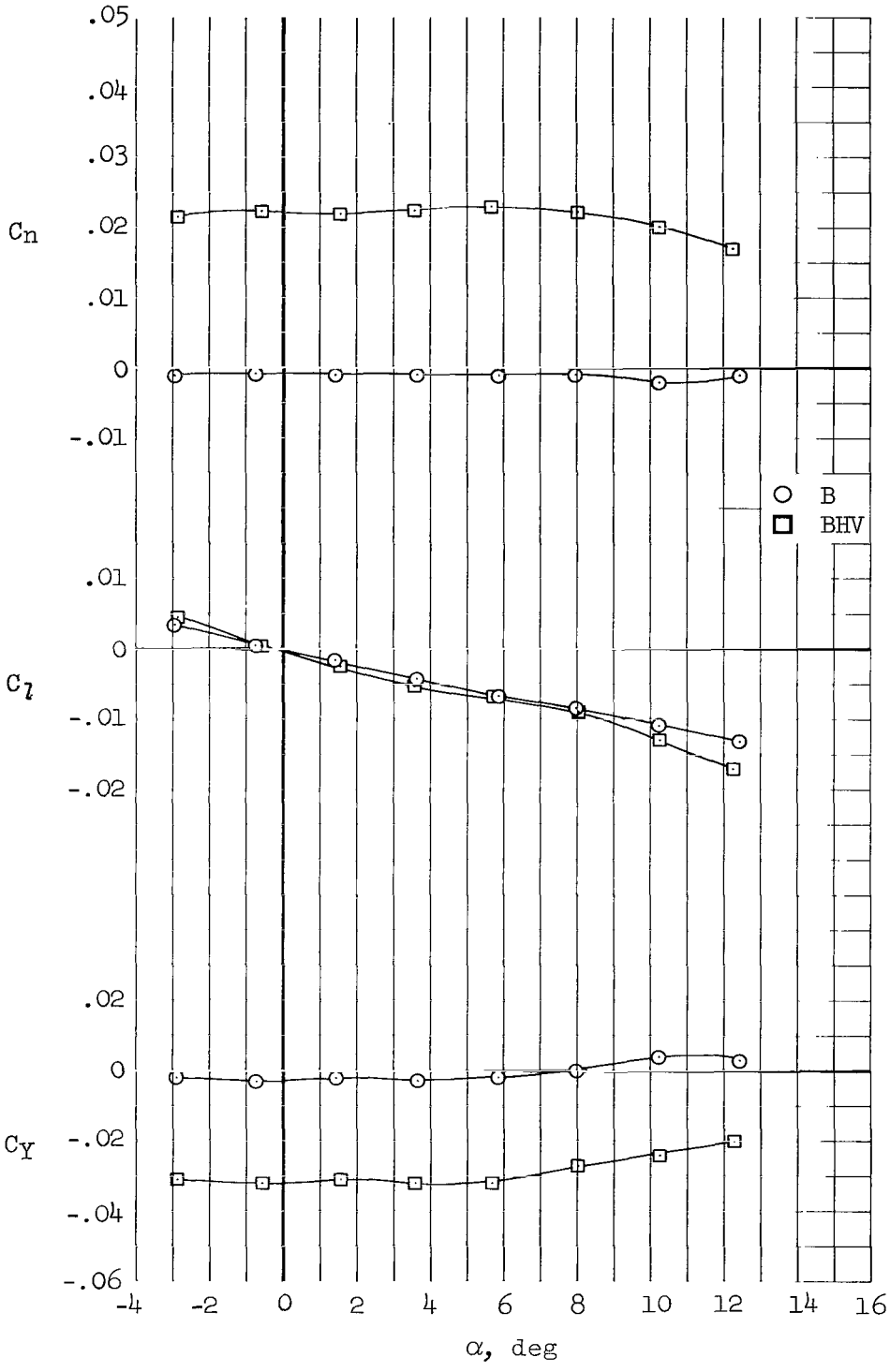

(b) M = 0.90

Figure 7.- Continued.

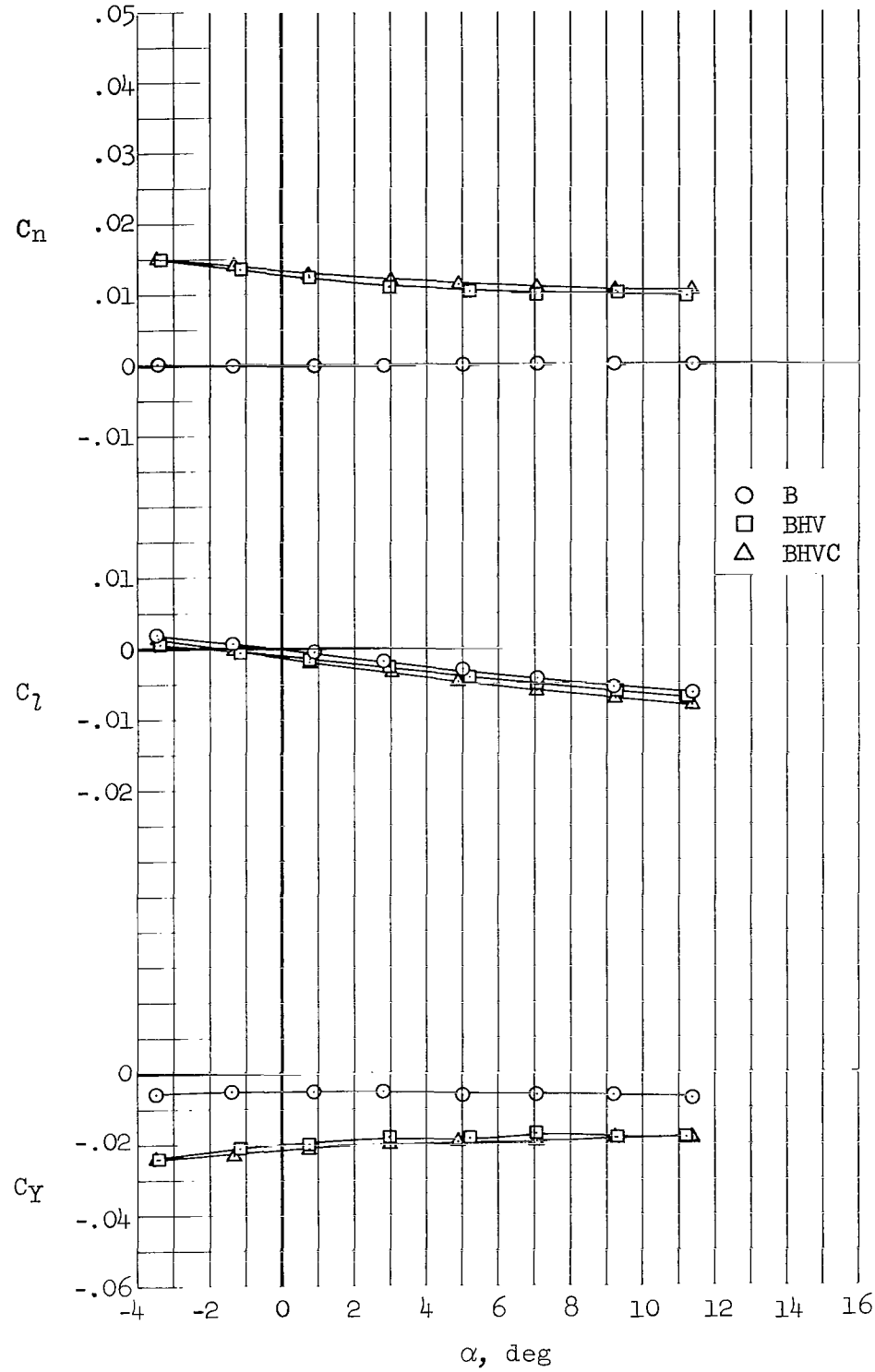

(c) M = 2.00

Figure 7.- Continued.

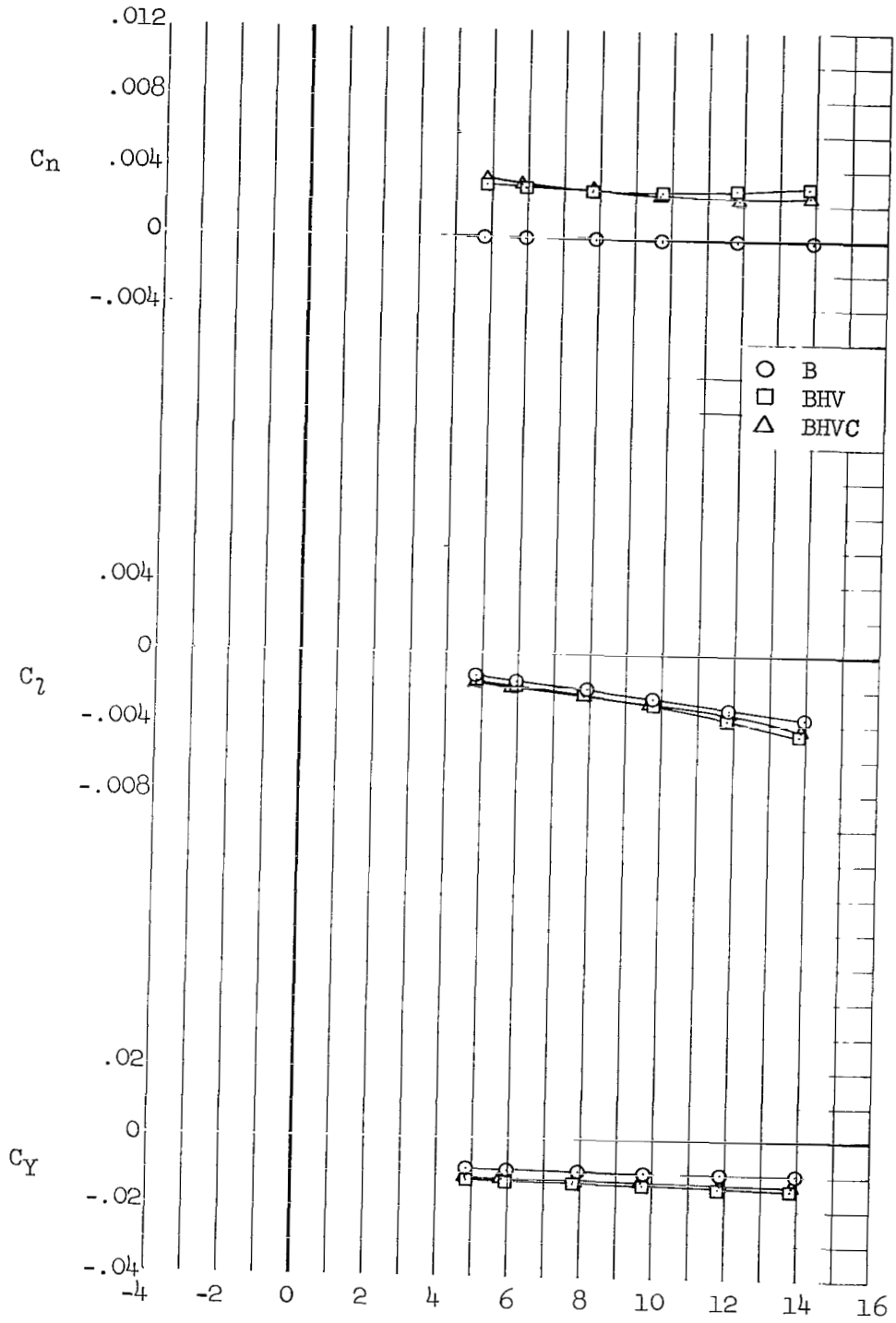

(d) M = 7.38

Figure 7.- Concluded.

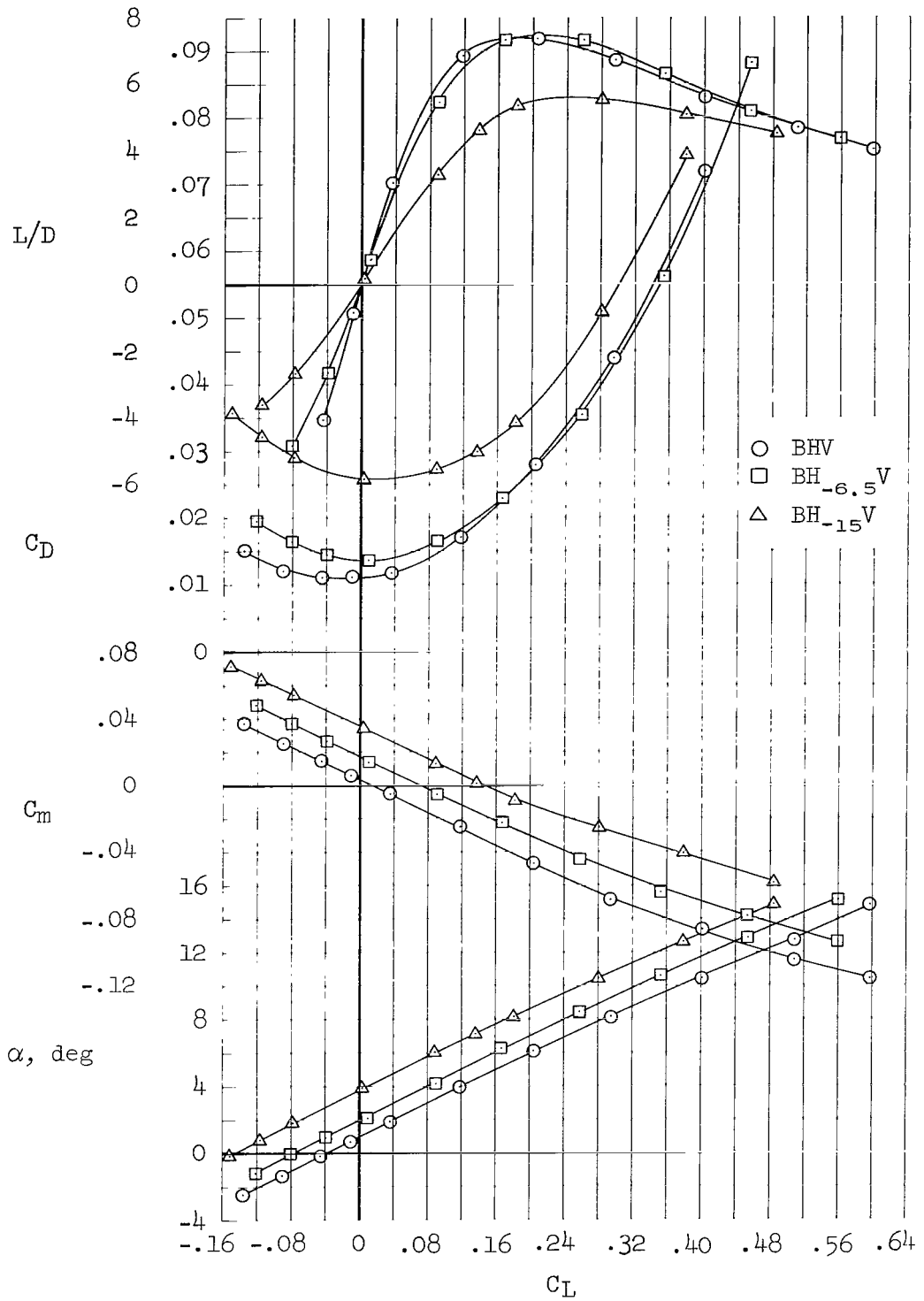

(a) M = 0.65

Figure 8.- Effect of horizontal-tail deflections on the longitudinal aerodynamic characteristics; canard off; β = 0°.

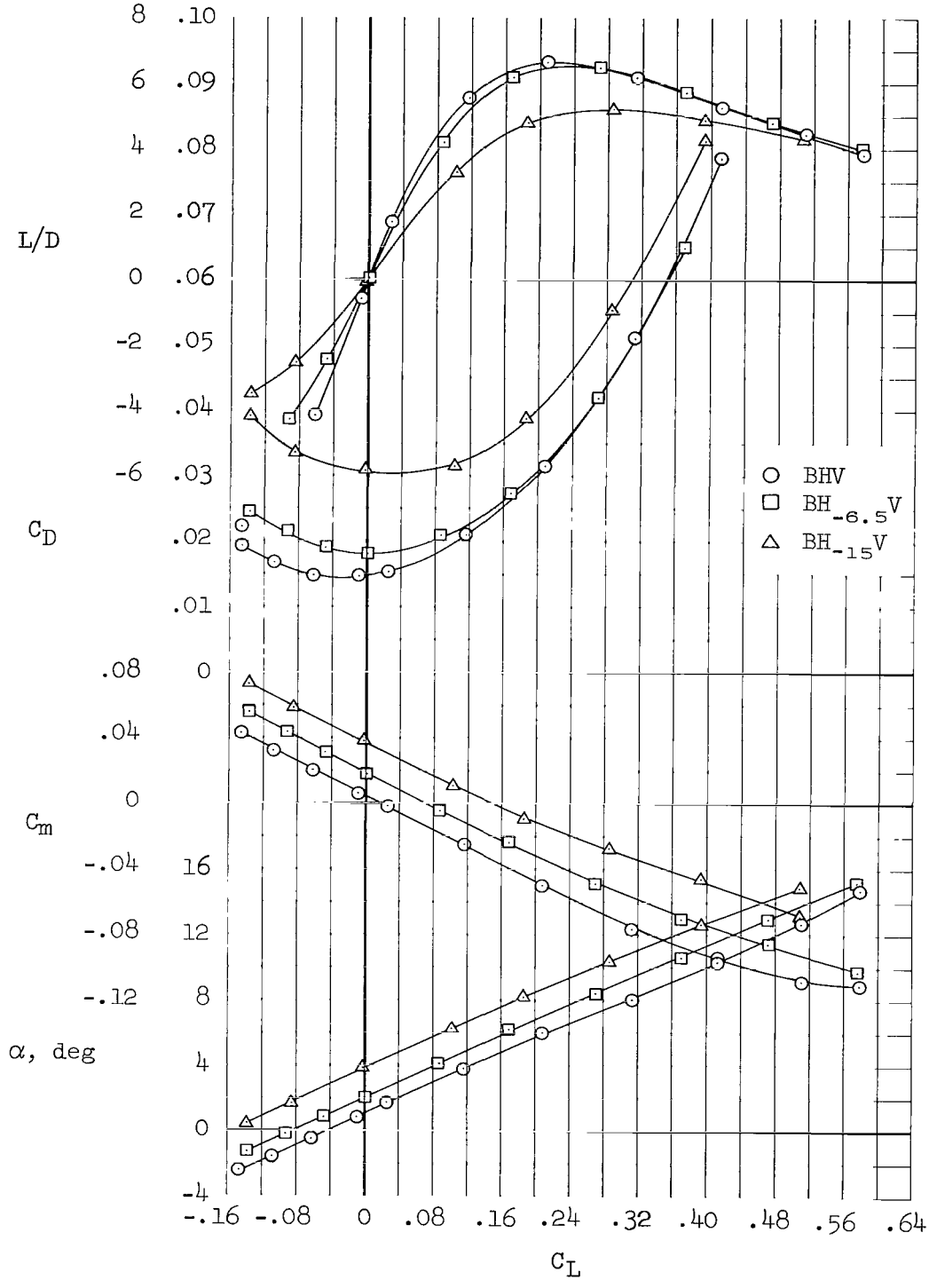

(b) M = 0.80

Figure 8.- Continued.

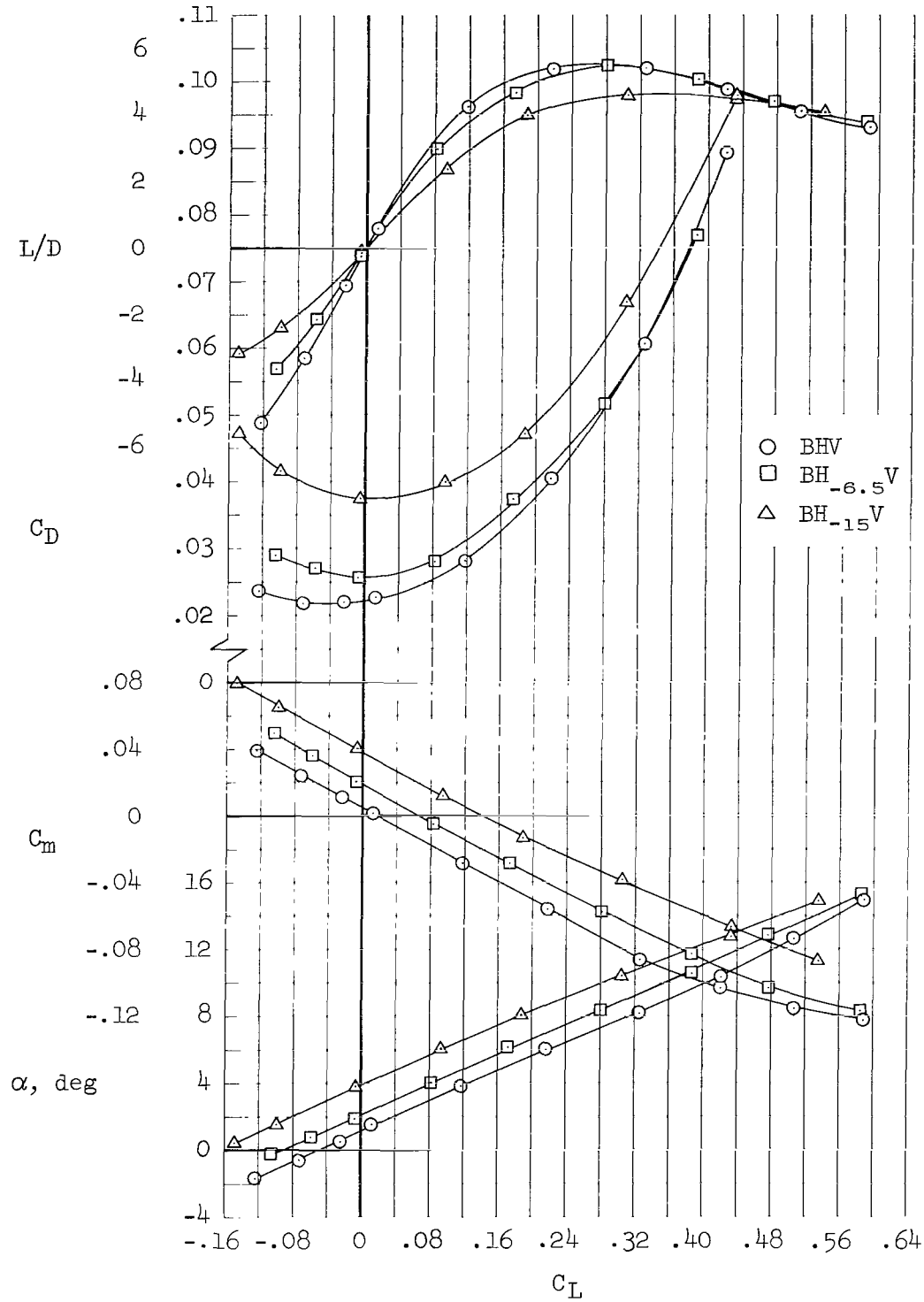

(c) M = 0.90

Figure 8.- Continued.

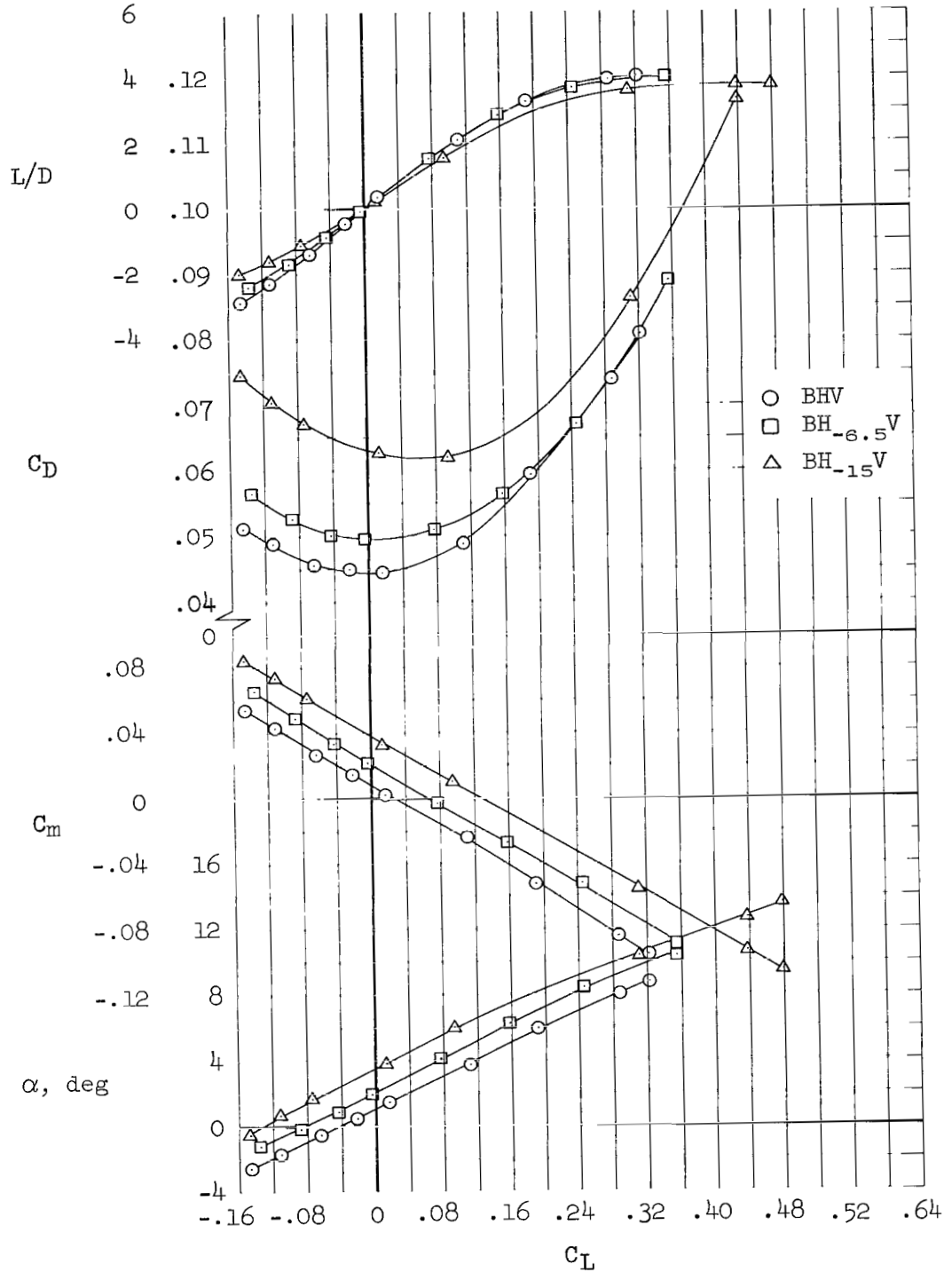

(d) M = 1.10

Figure 8.- Continued.

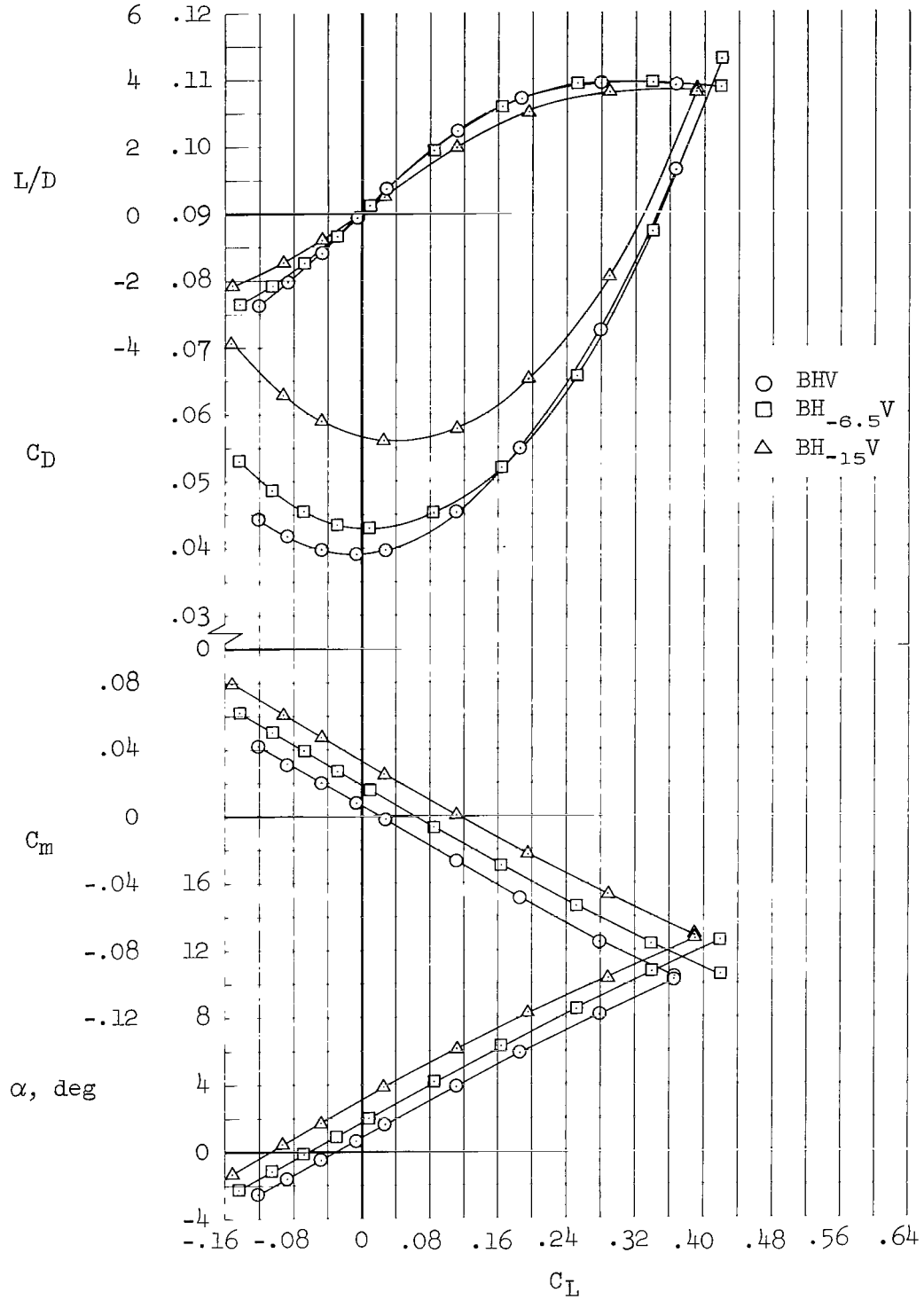

(e) M = 1.30

Figure 8.- Continued.

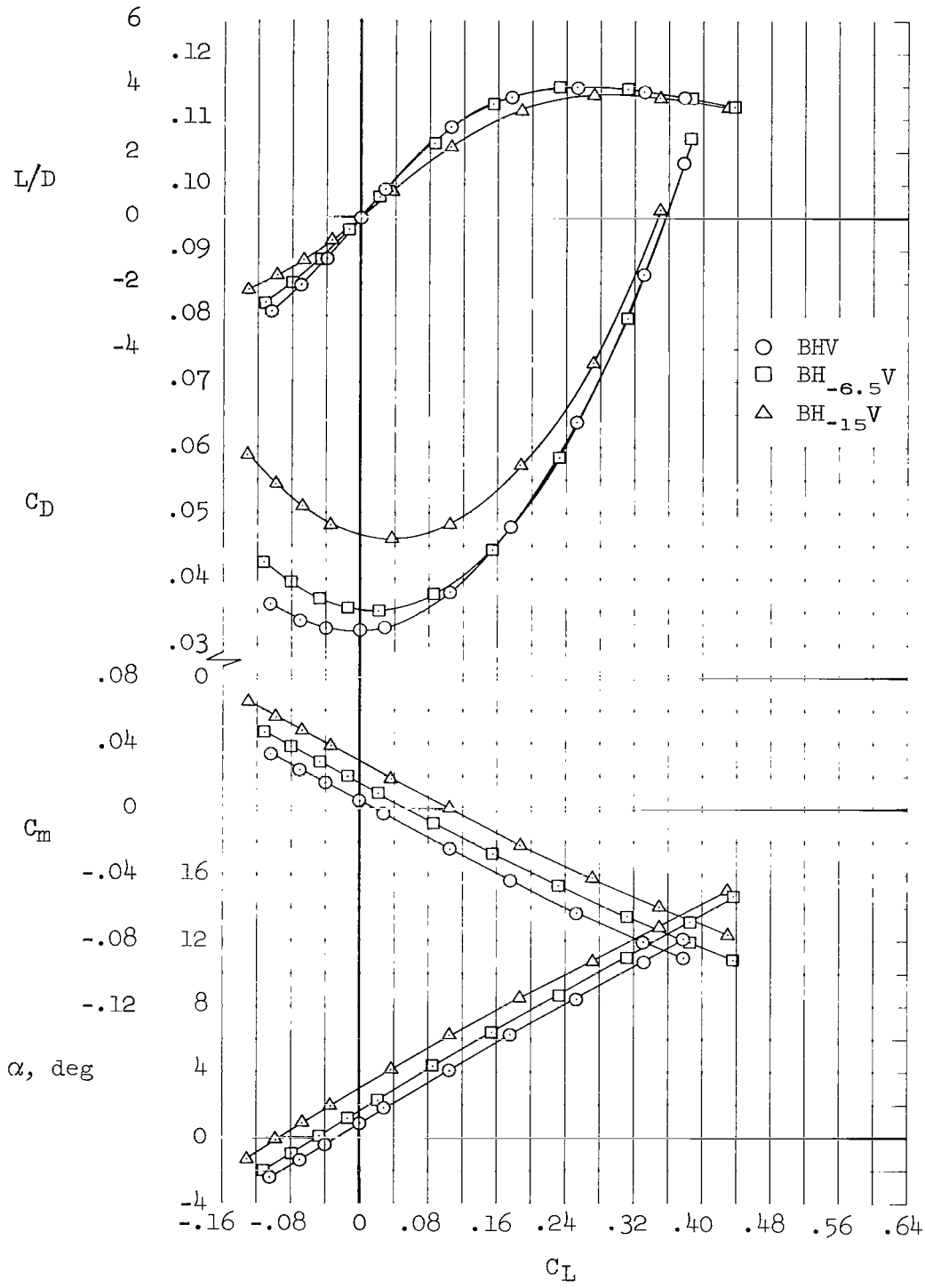

(f) M = 1.60

Figure 8.- Continued.

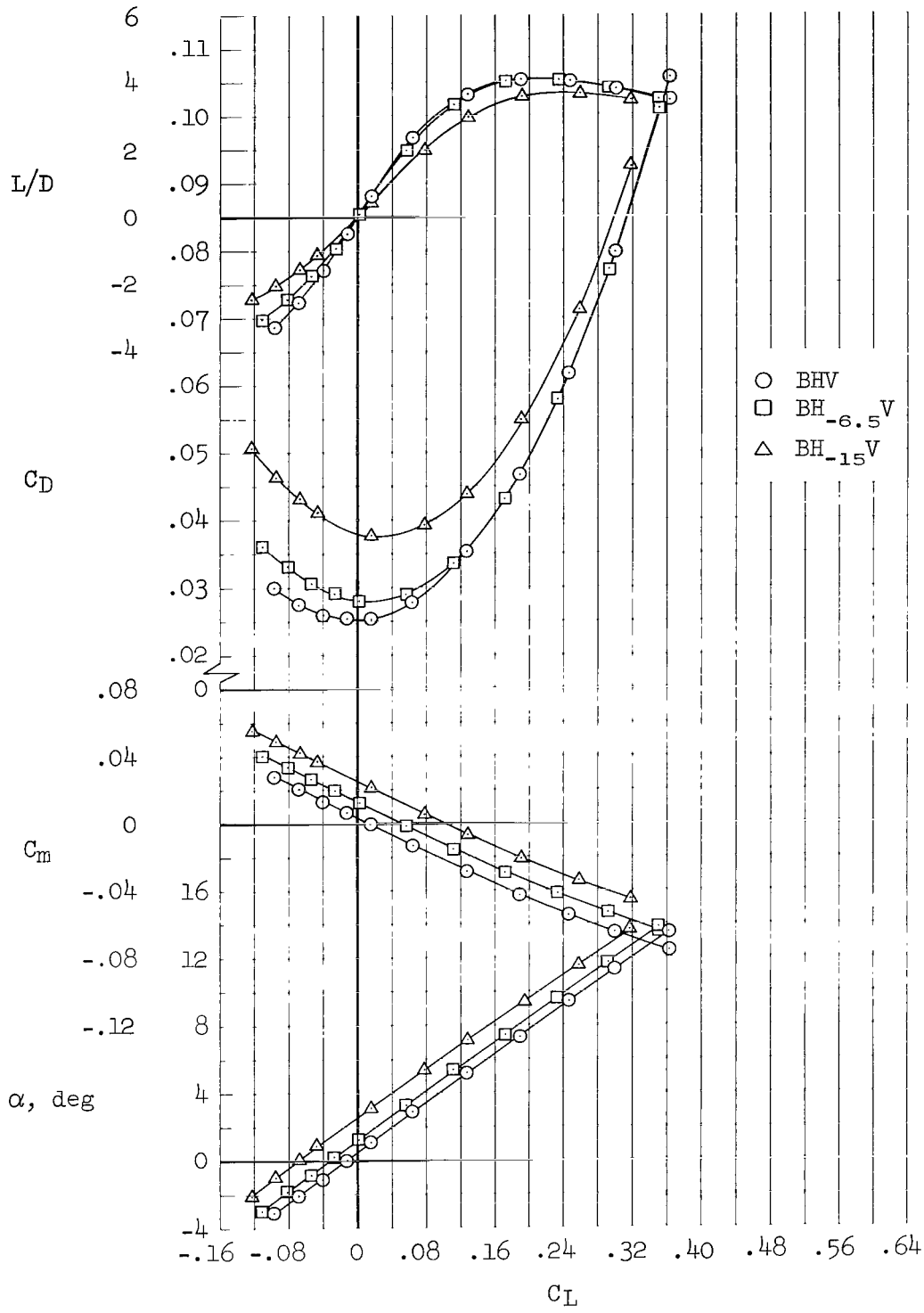

(g) M = 2.00

Figure 8.- Continued.

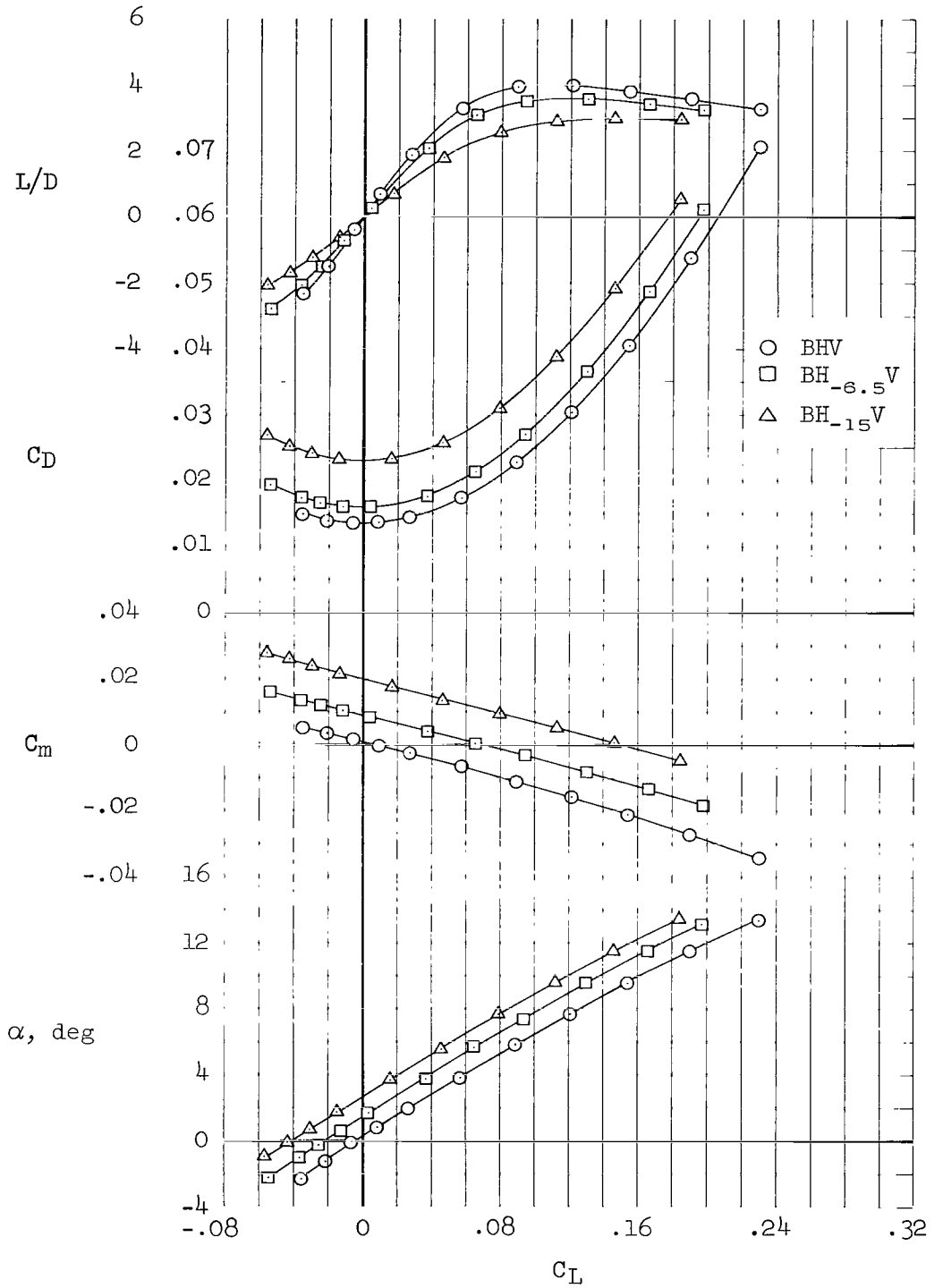

(h) M = 5.37

Figure 8.- Continued.

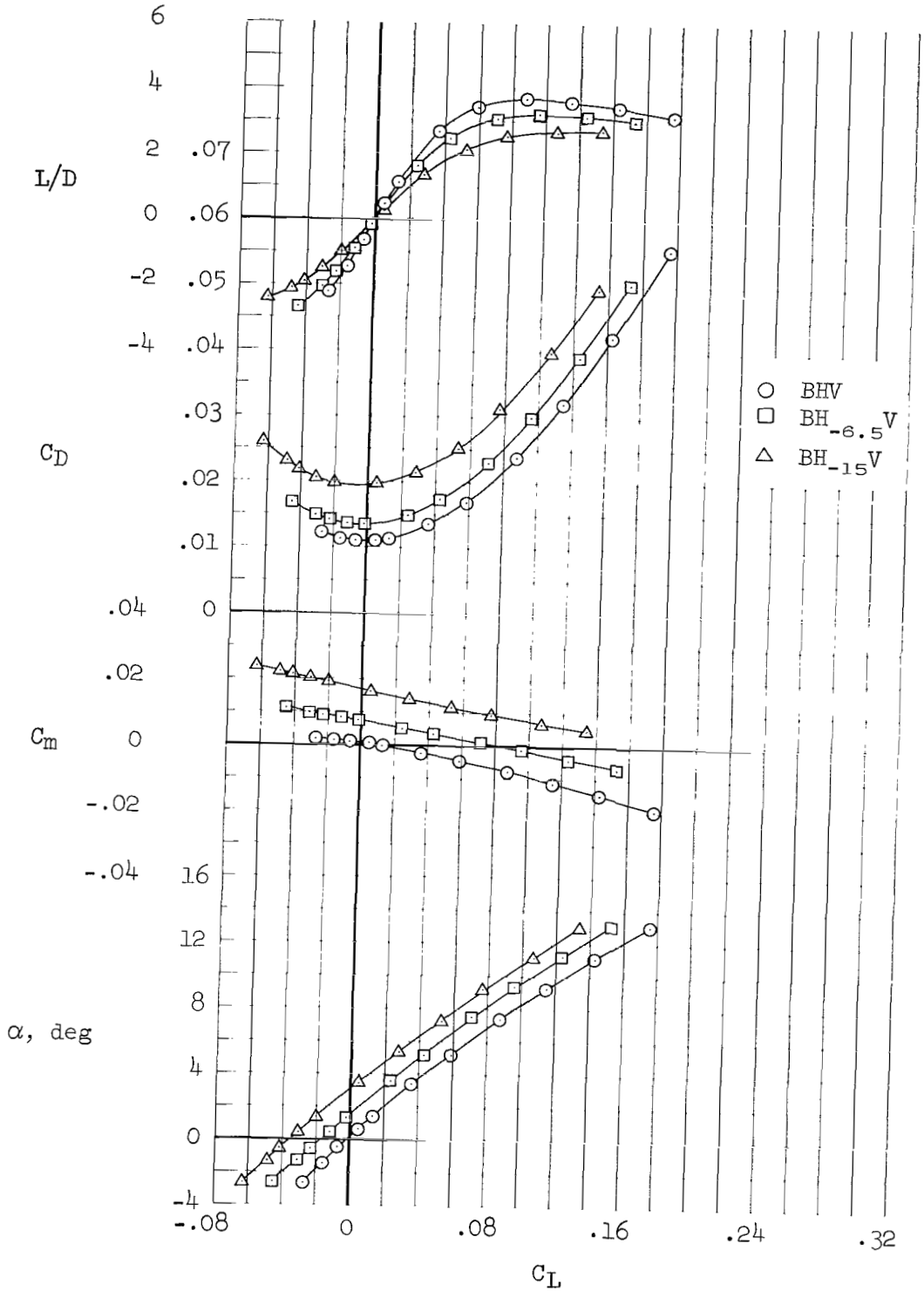

(i) M = 7.38

Figure 8.- Continued.

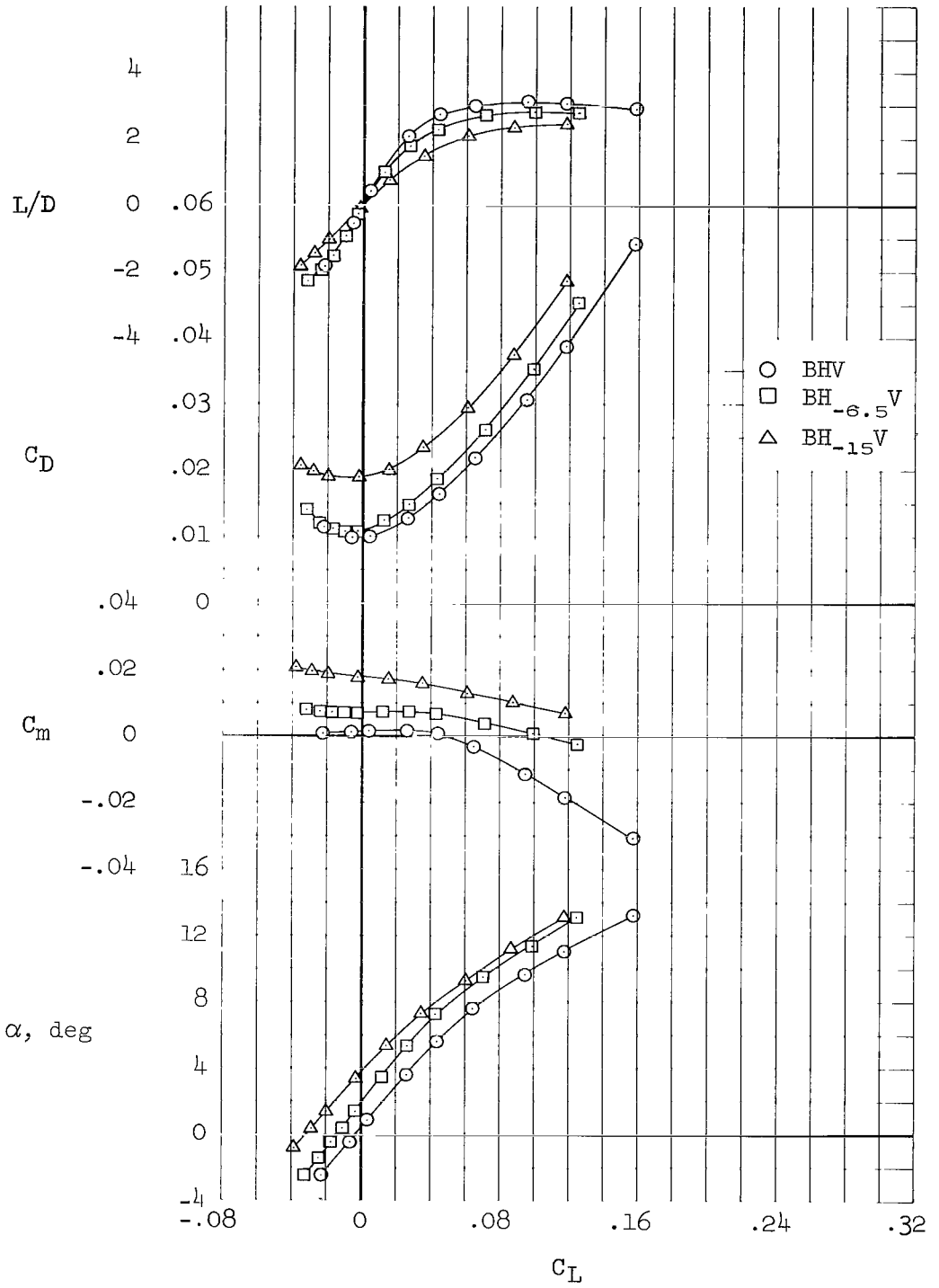

(j) M = 10.6

Figure 8.- Concluded.

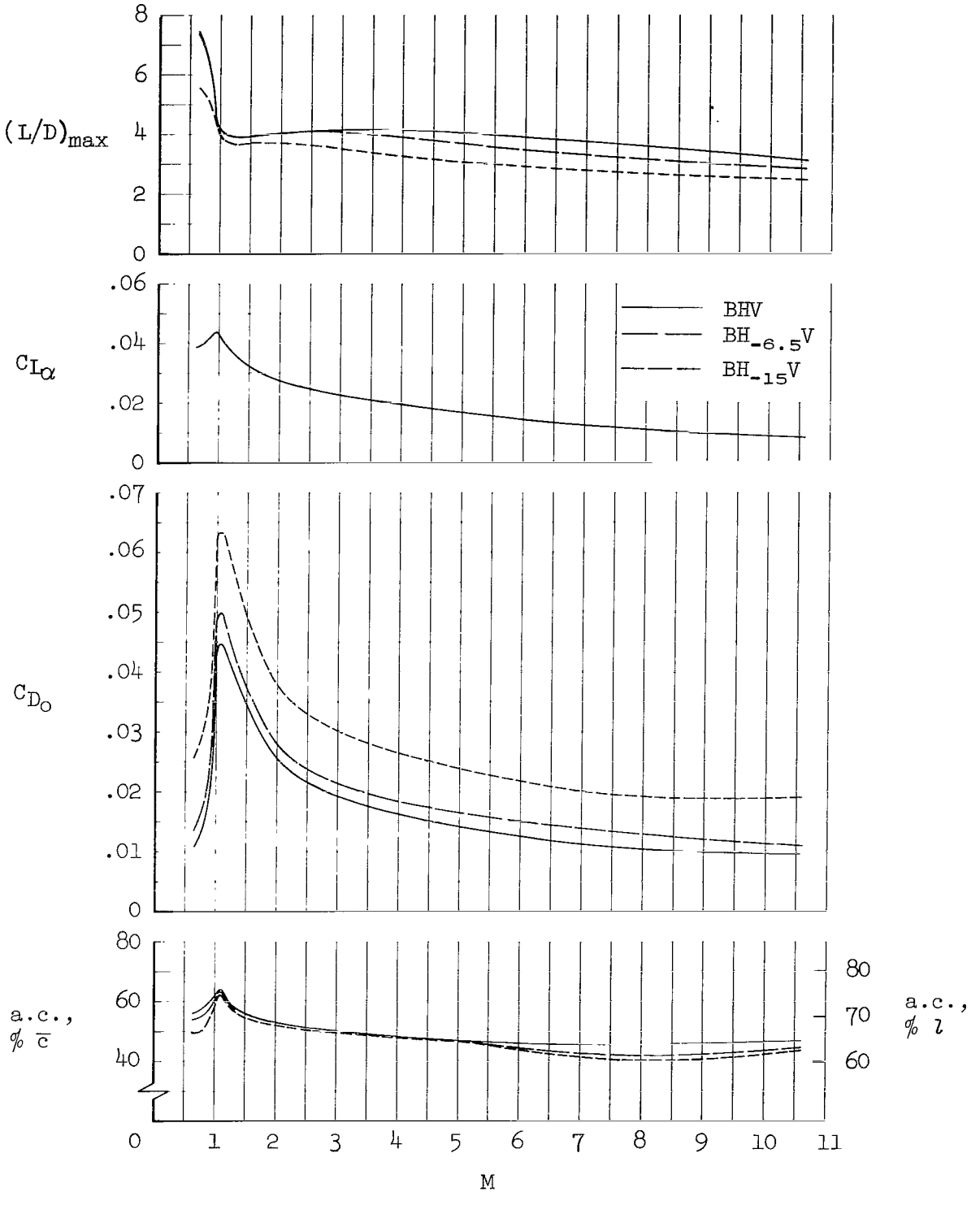

Figure 9.- Variation with Mach number of the effect of horizontal-tail deflections on the longitudinal aerodynamic characteristics; canard off; $\beta = 0°$.

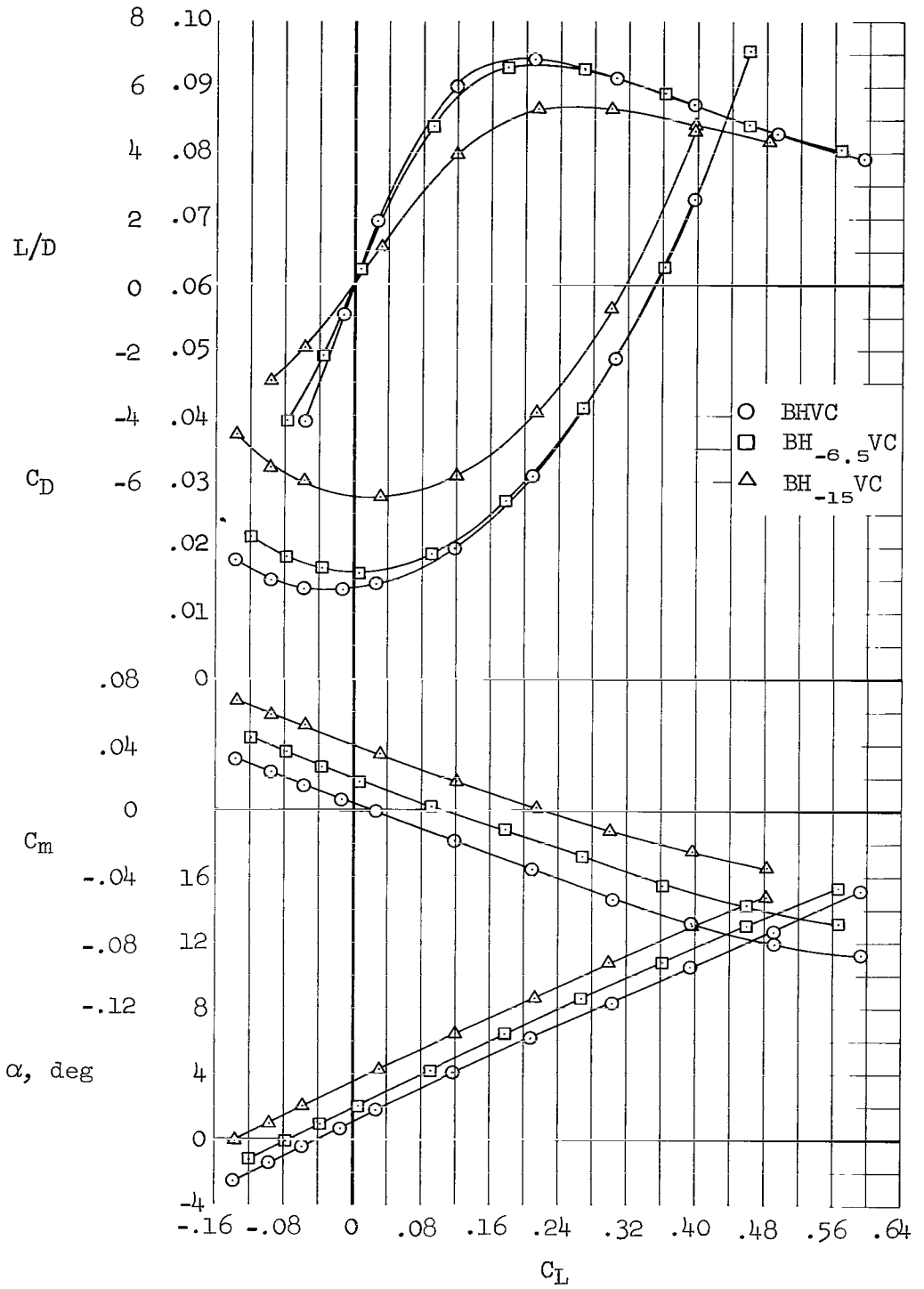

(a) M = 0.65

Figure 10.- Effect of horizontal-tail deflections on the longitudinal aerodynamic characteristics; canard on, β = 0°.

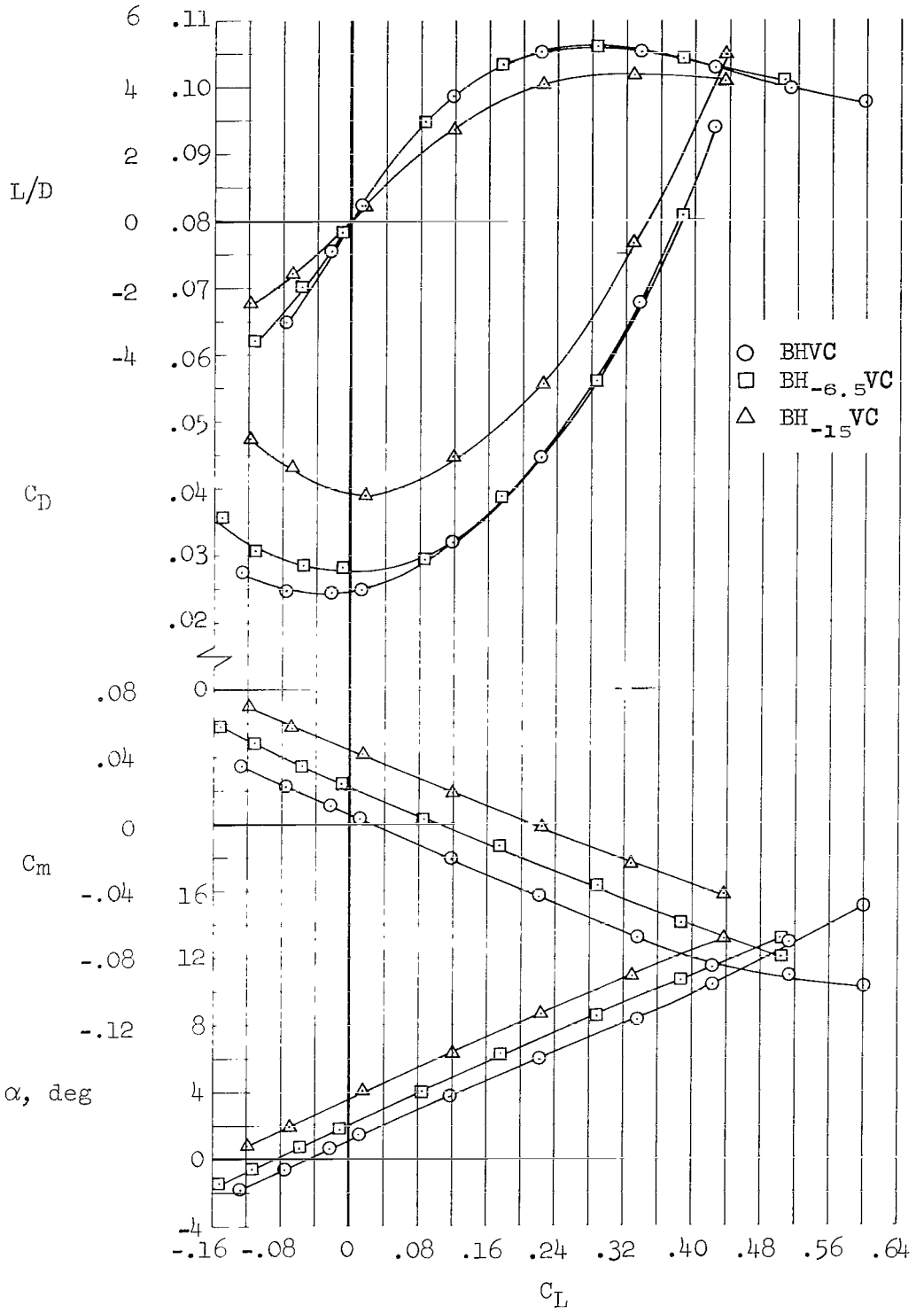

(b) M = 0.90

Figure 10.- Continued.

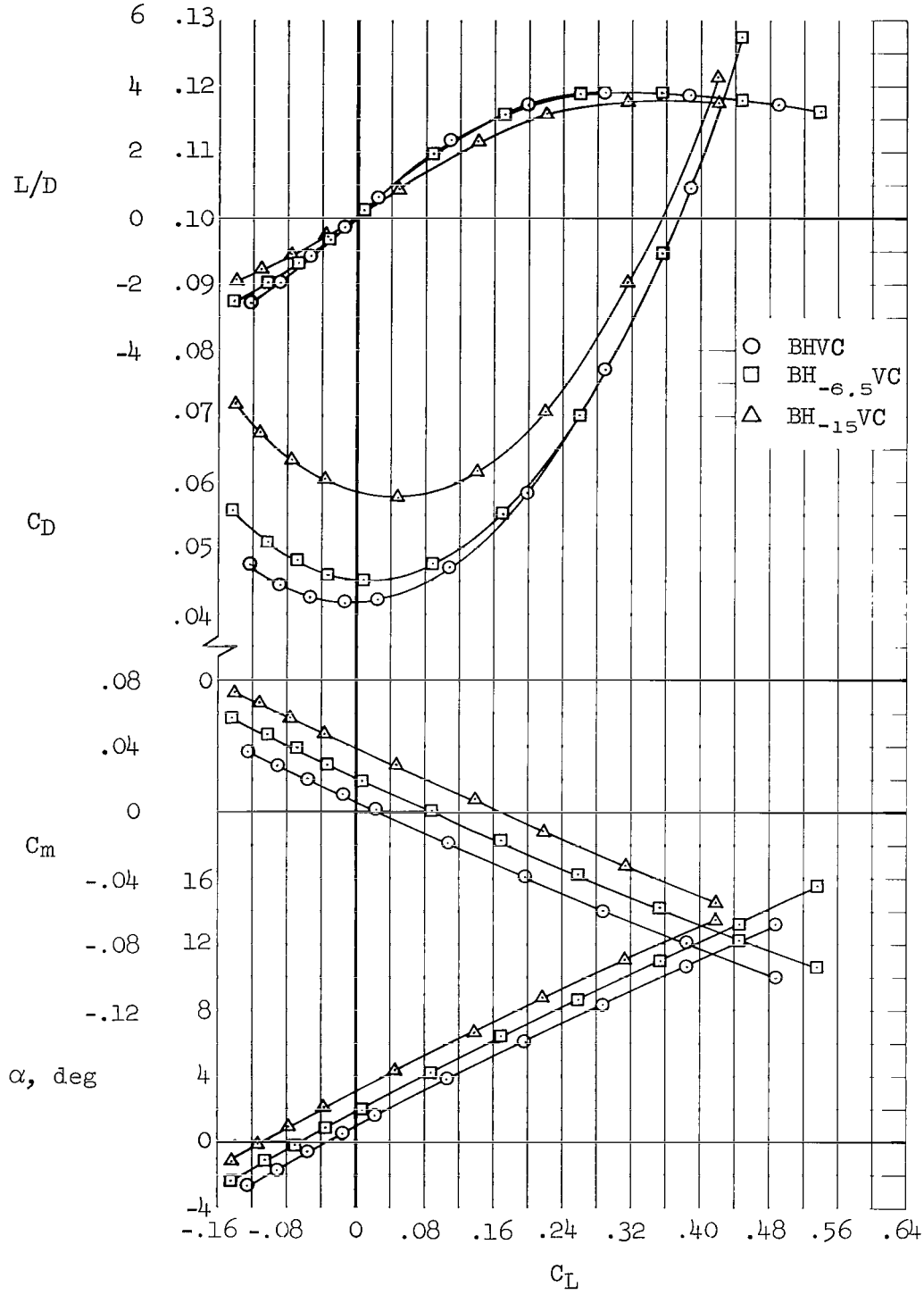

(c) M = 1.30

Figure 10.- Continued.

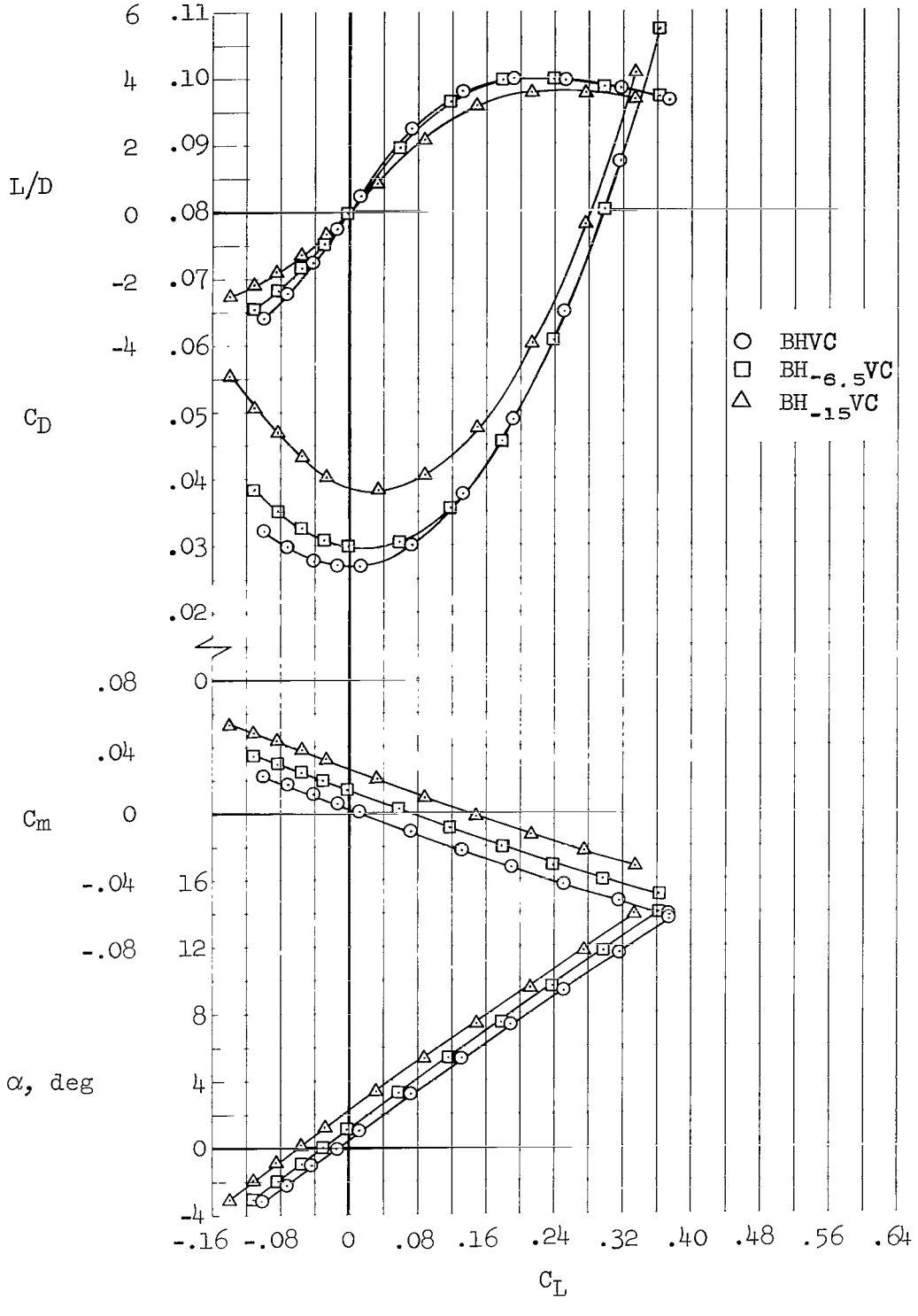

(d) M = 2.00

Figure 10.- Continued.

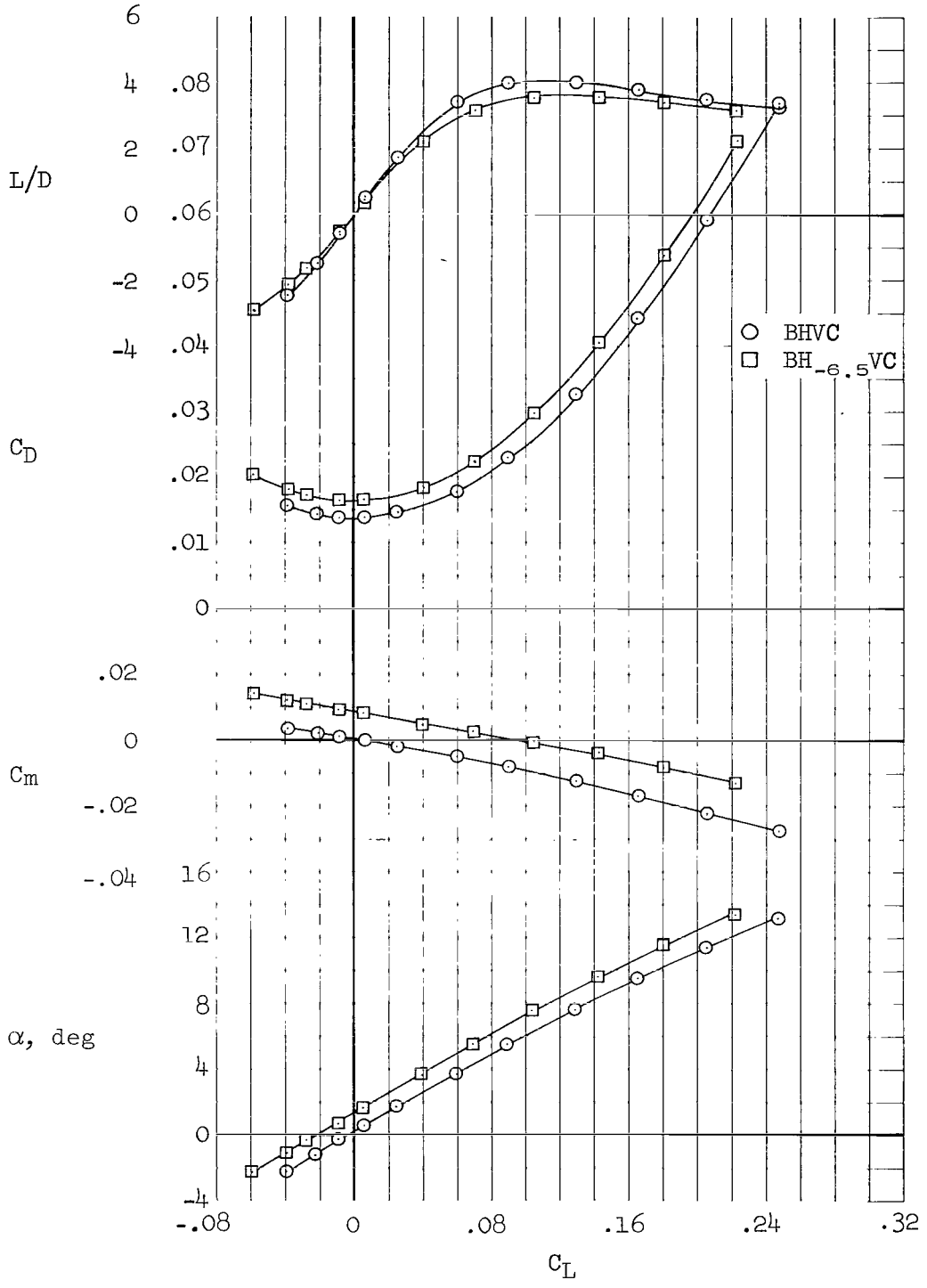

(e) M = 5.37

Figure 10.- Continued.

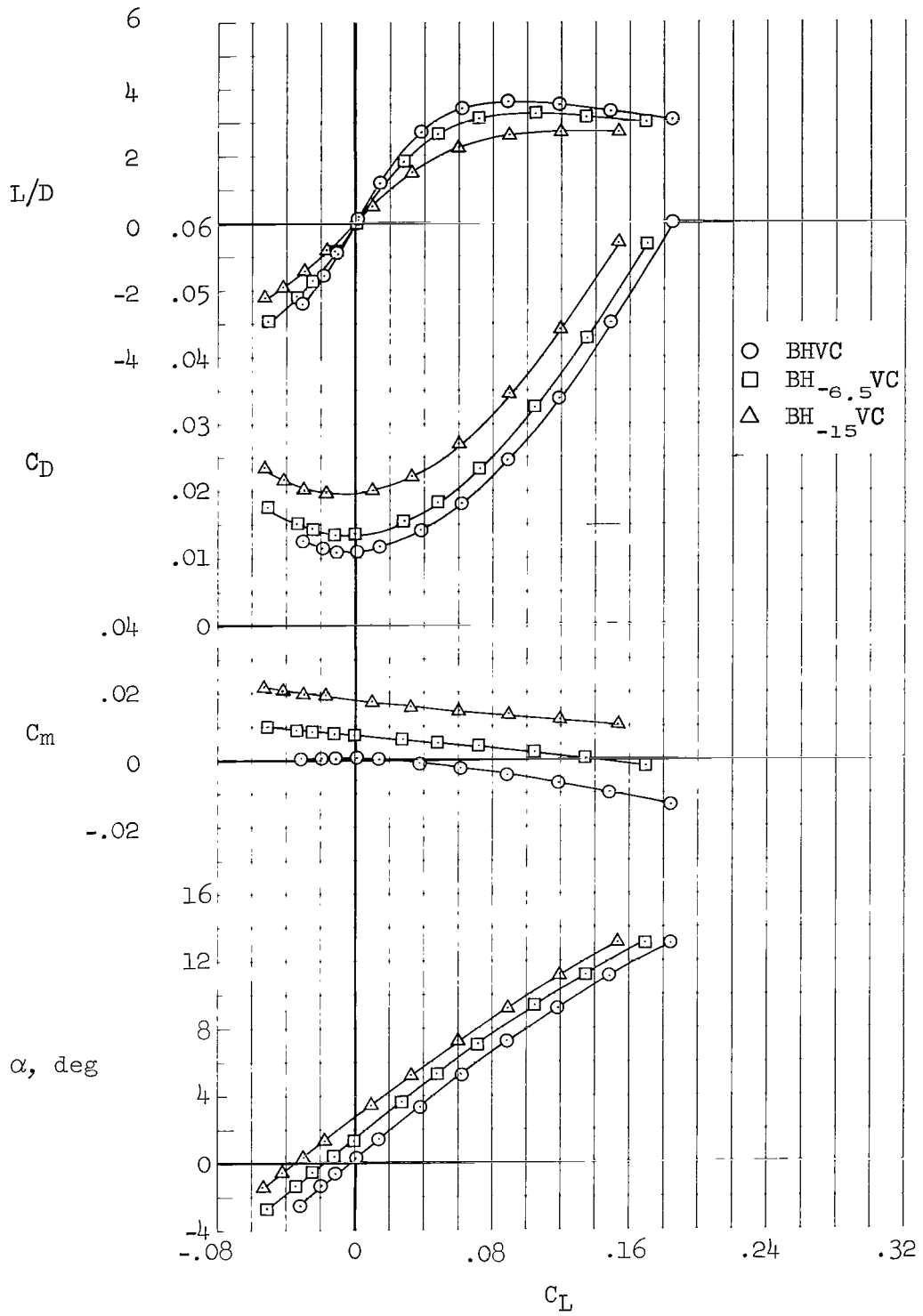

(f) M = 7.38

Figure 10.- Continued.

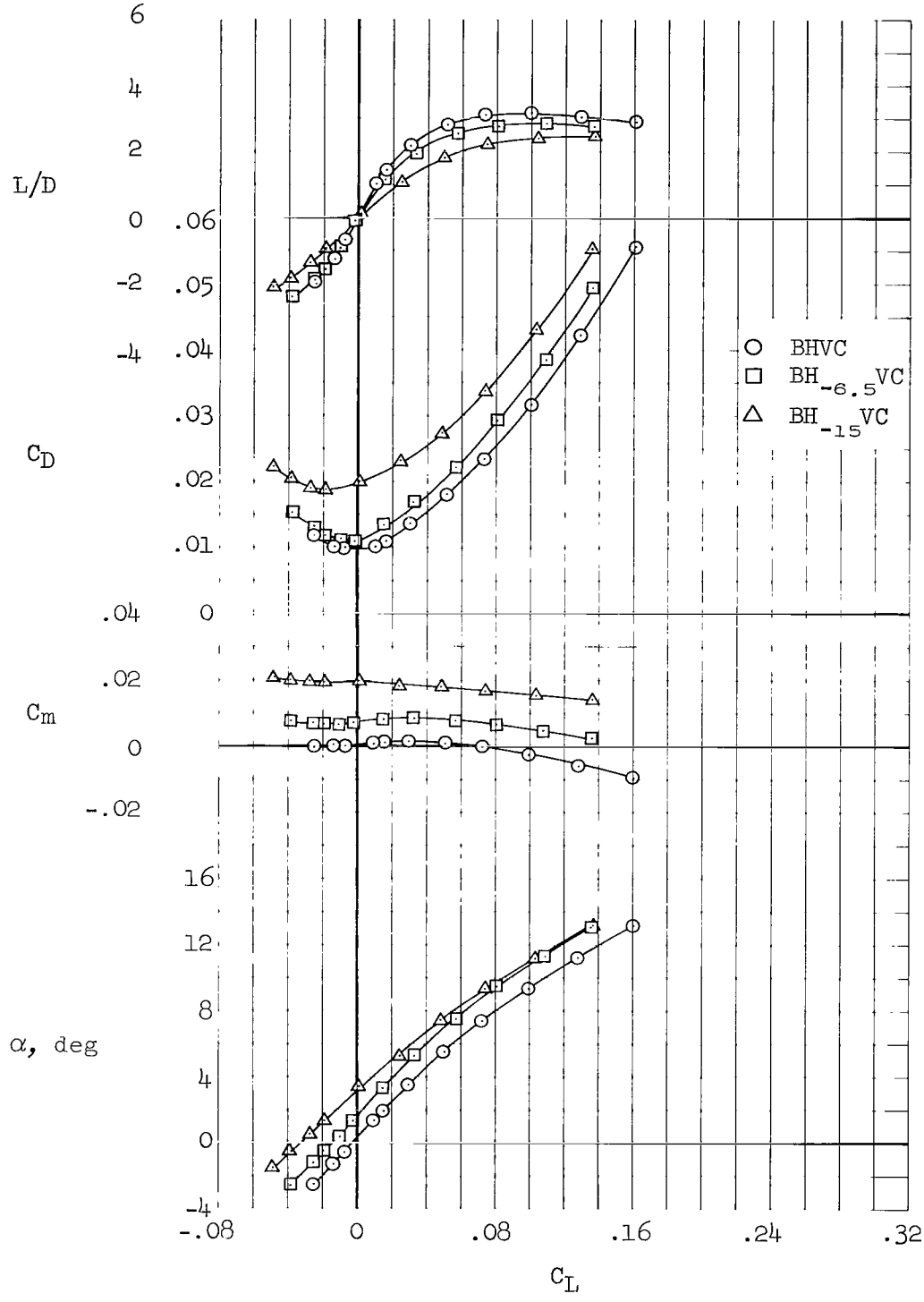

(g) M = 10.6

Figure 10.- Concluded.

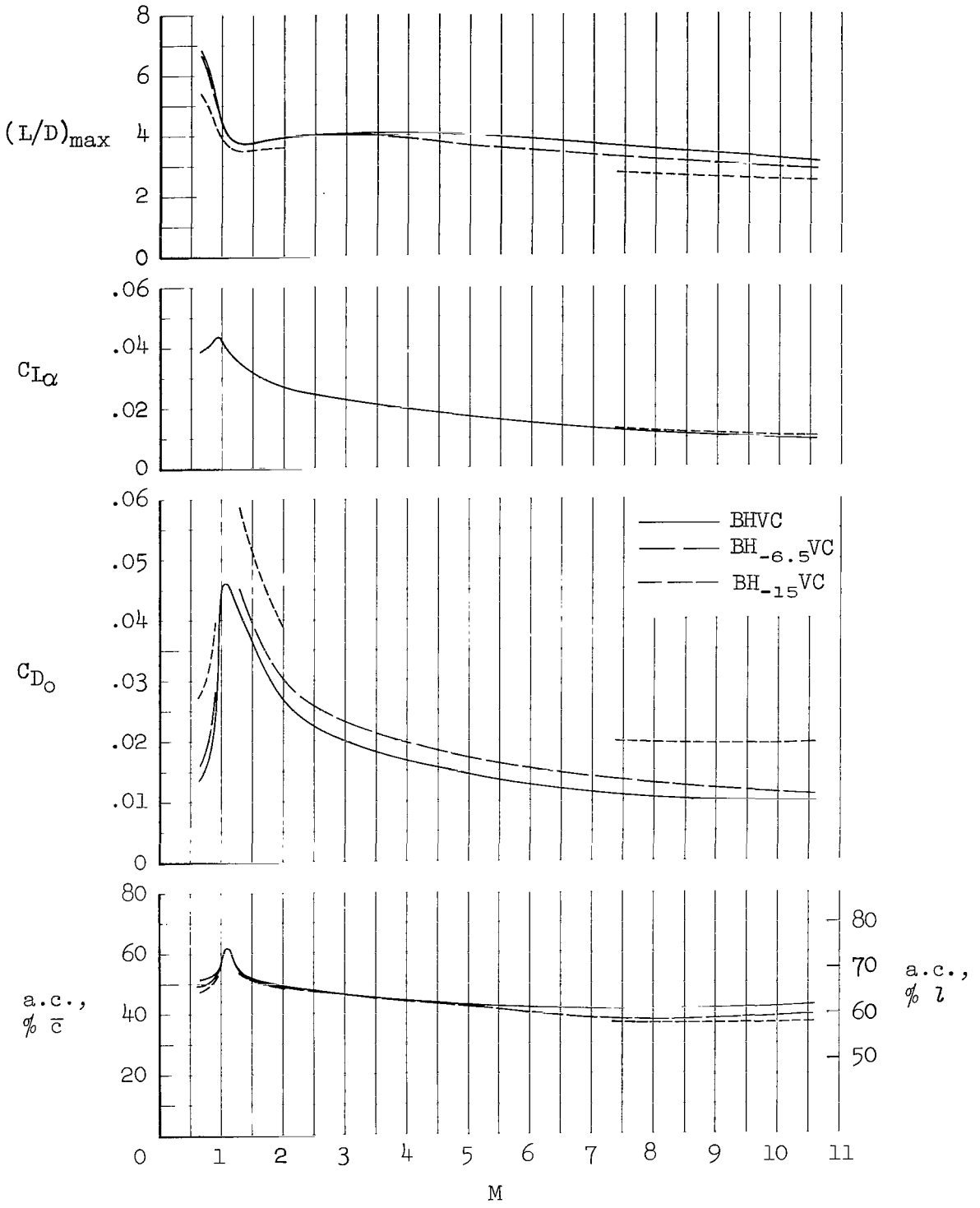

Figure 11.- Variation with Mach number of the effect of horizontal-tail deflections on the longitudinal aerodynamic characteristics; canard on; $\beta = 0°$.

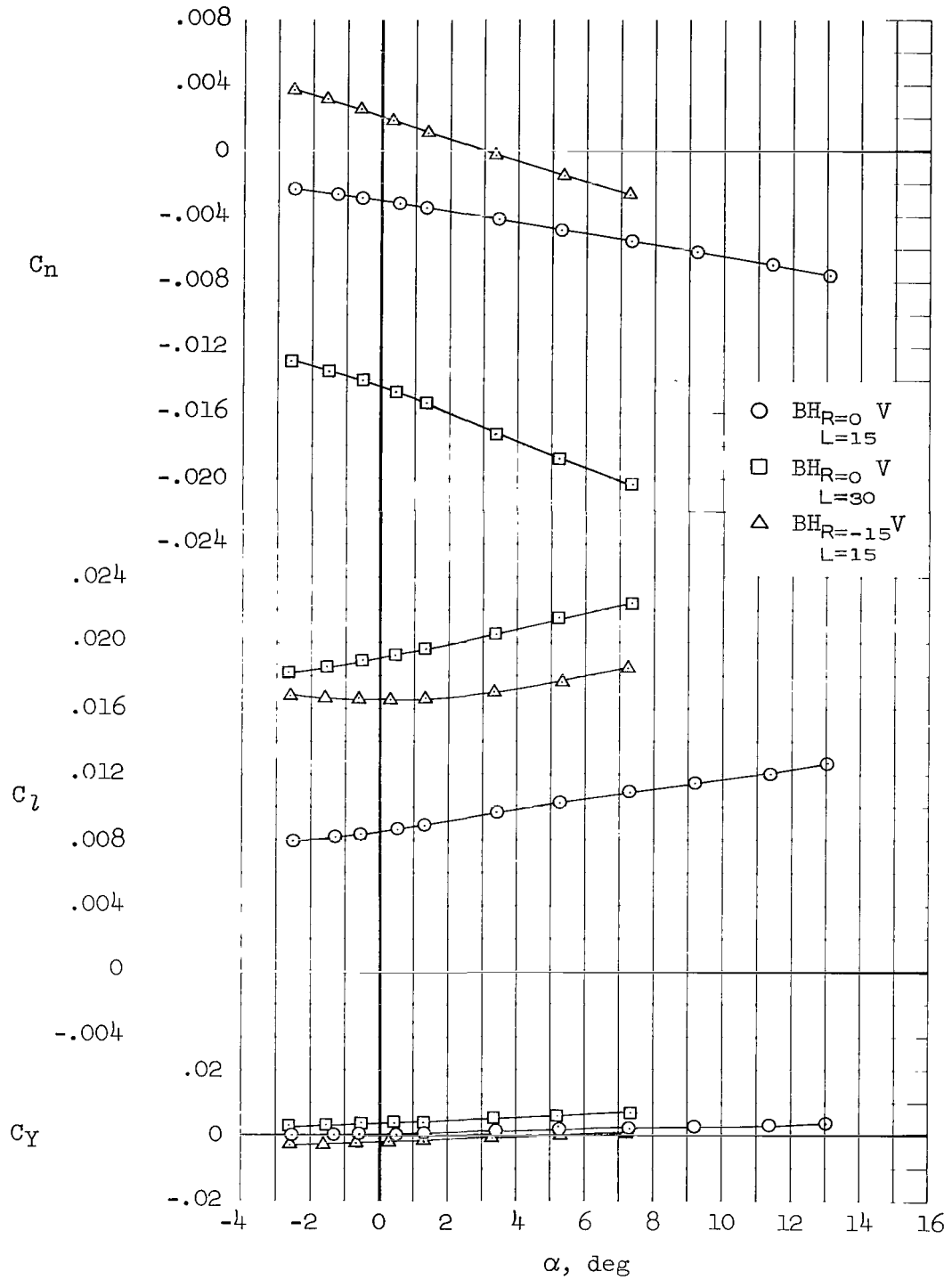

(a) M = 7.38

Figure 12.- Effect of differential horizontal tail deflections on the lateral-directional aerodynamic characteristics in pitch; β = 0°.

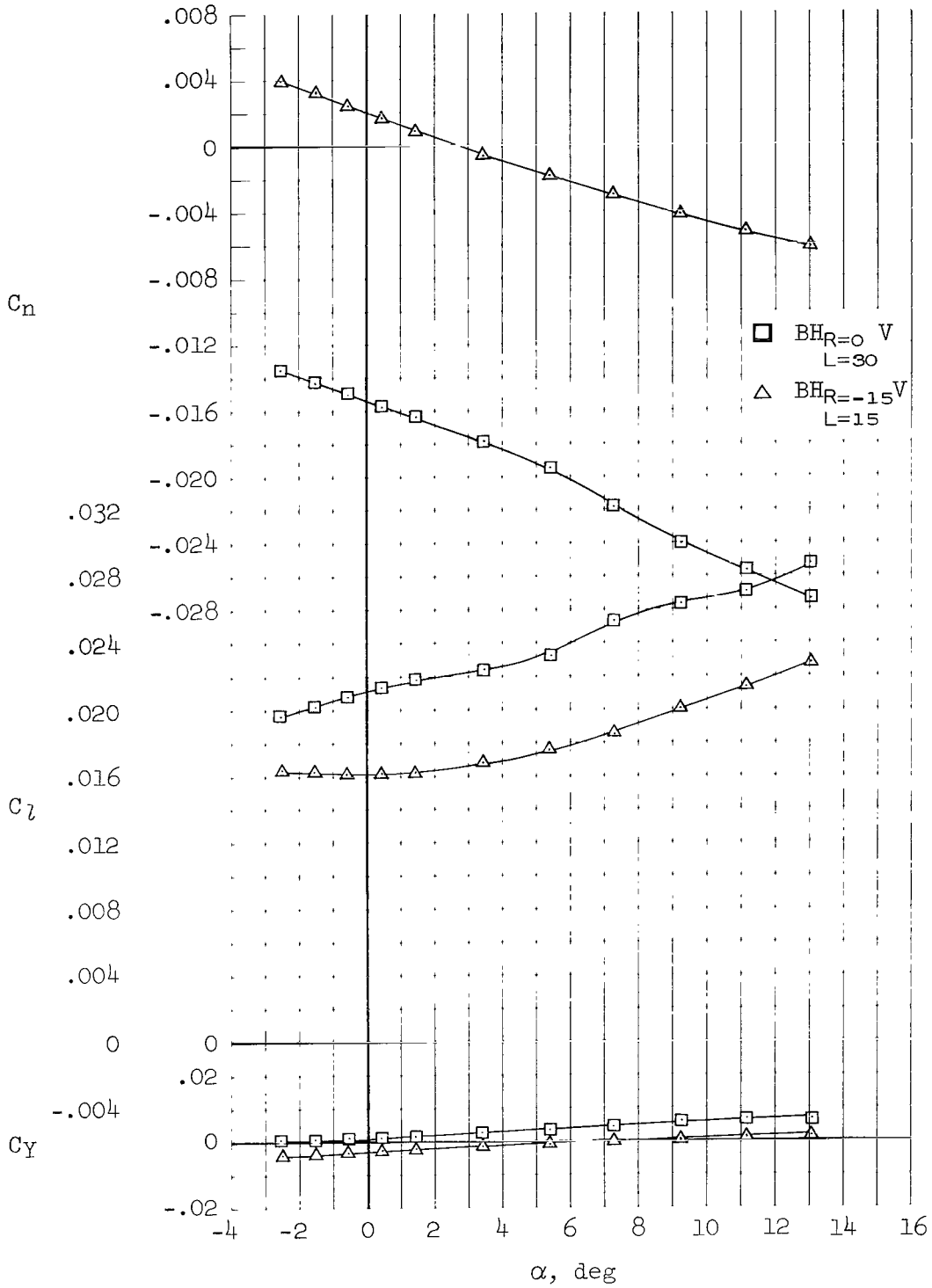

(b) M = 10.6

Figure 12.- Concluded.

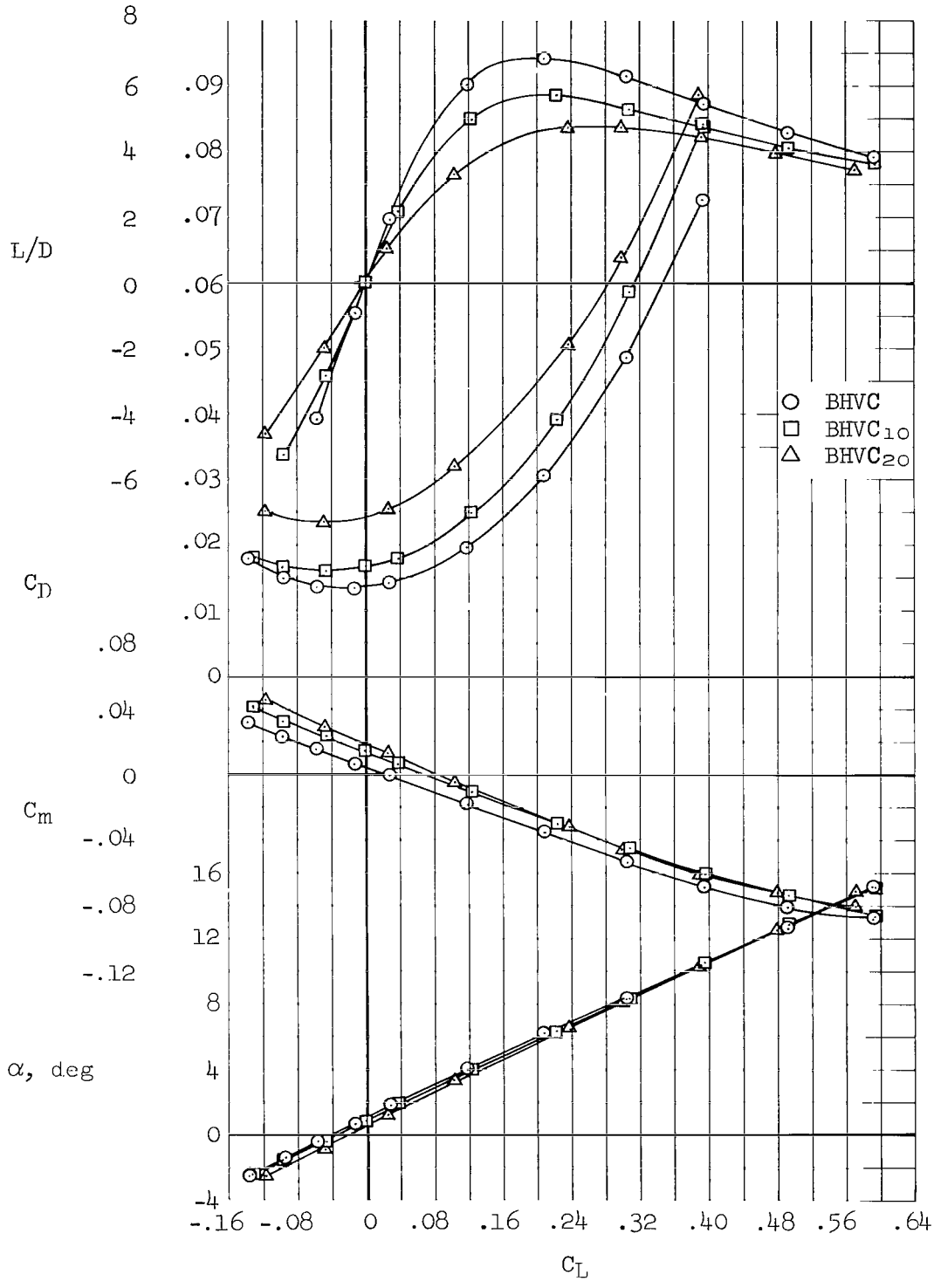

(a) M = 0.65

Figure 13.- Effect of canard deflections on the longitudinal aerodynamic characteristics; β = 0°.

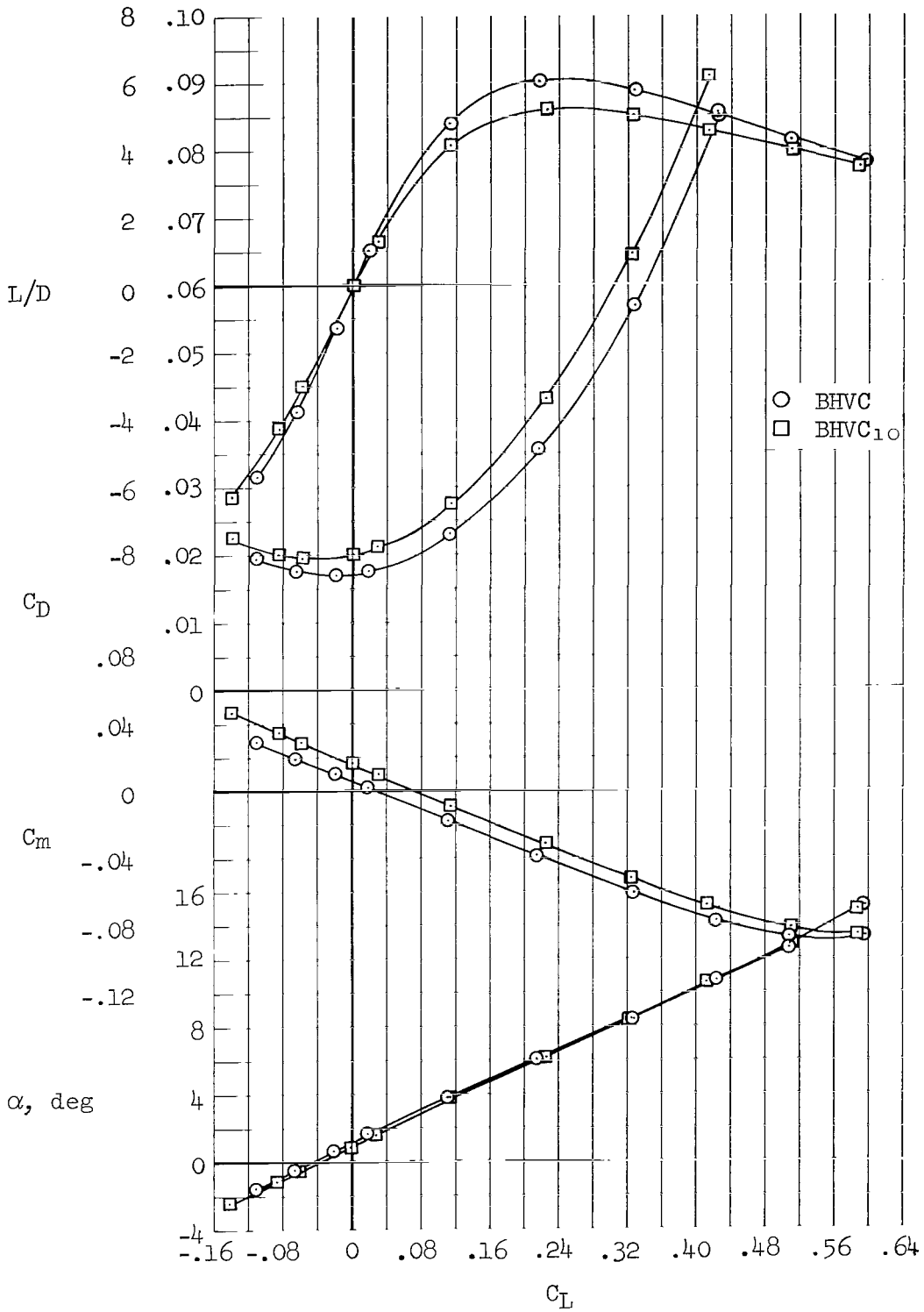

(b) M = 0.80

Figure 13.- Continued.

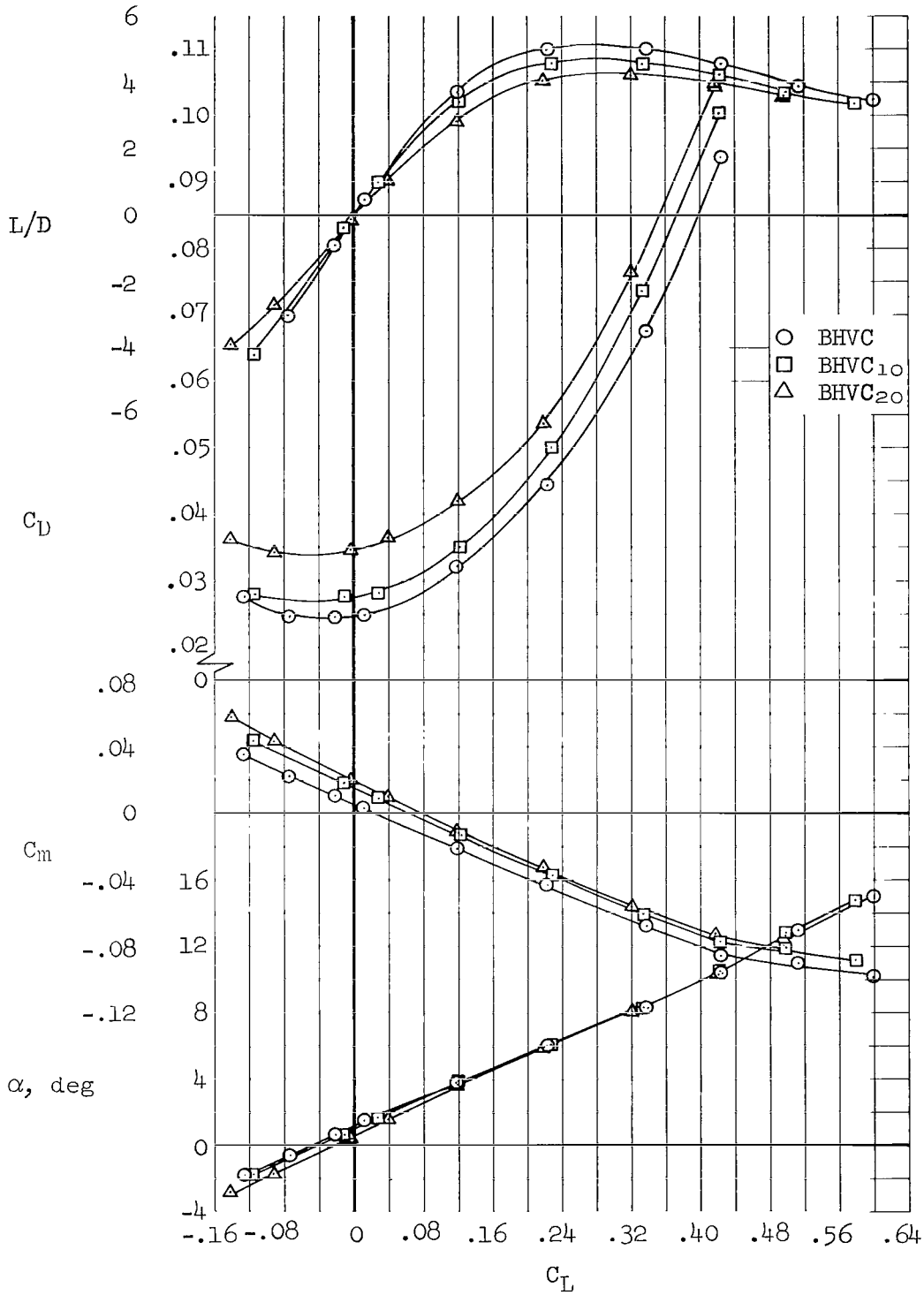

(c) M = 0.90

Figure 13.- Continued.

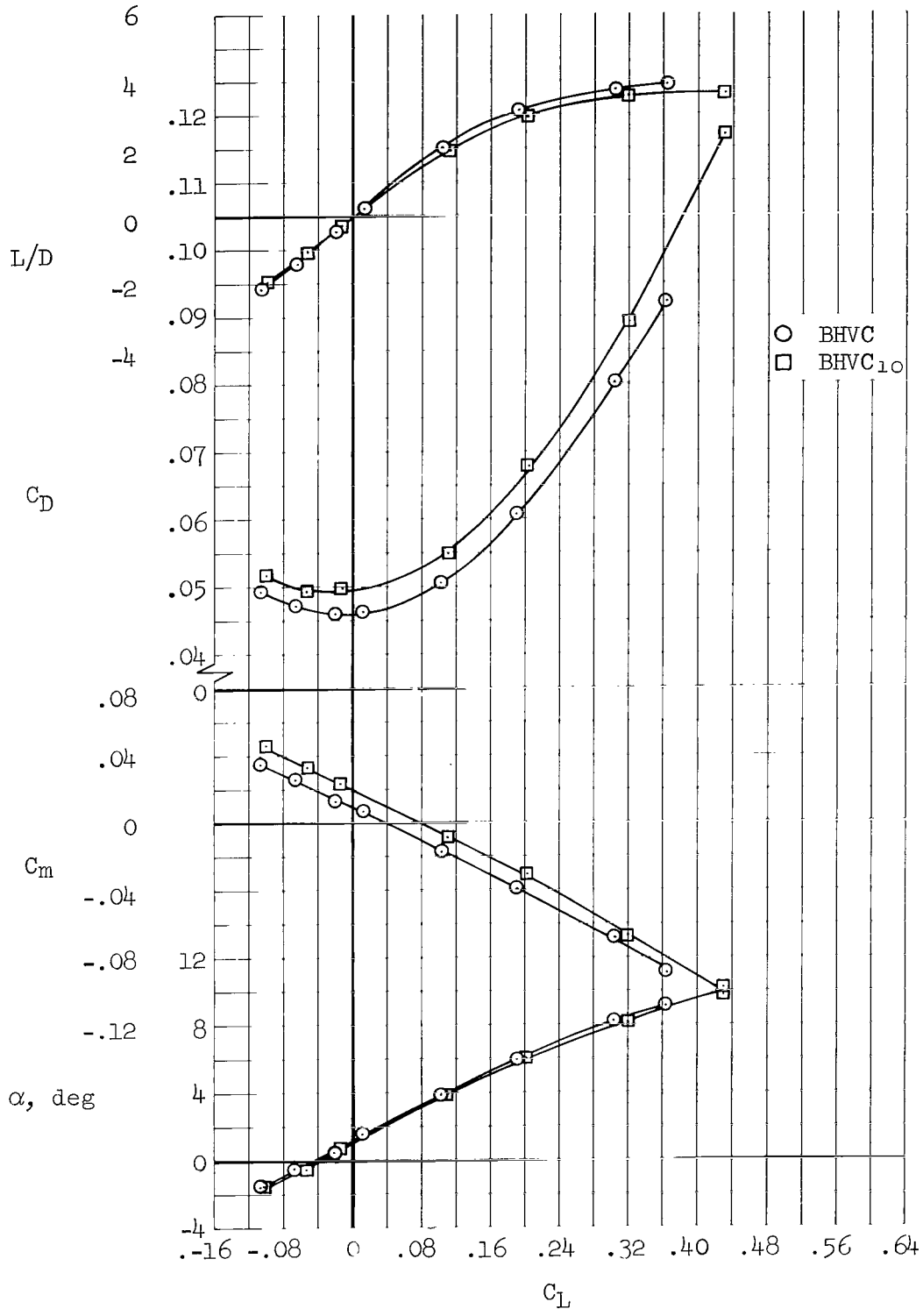

(d) M = 1.10

Figure 13.- Continued.

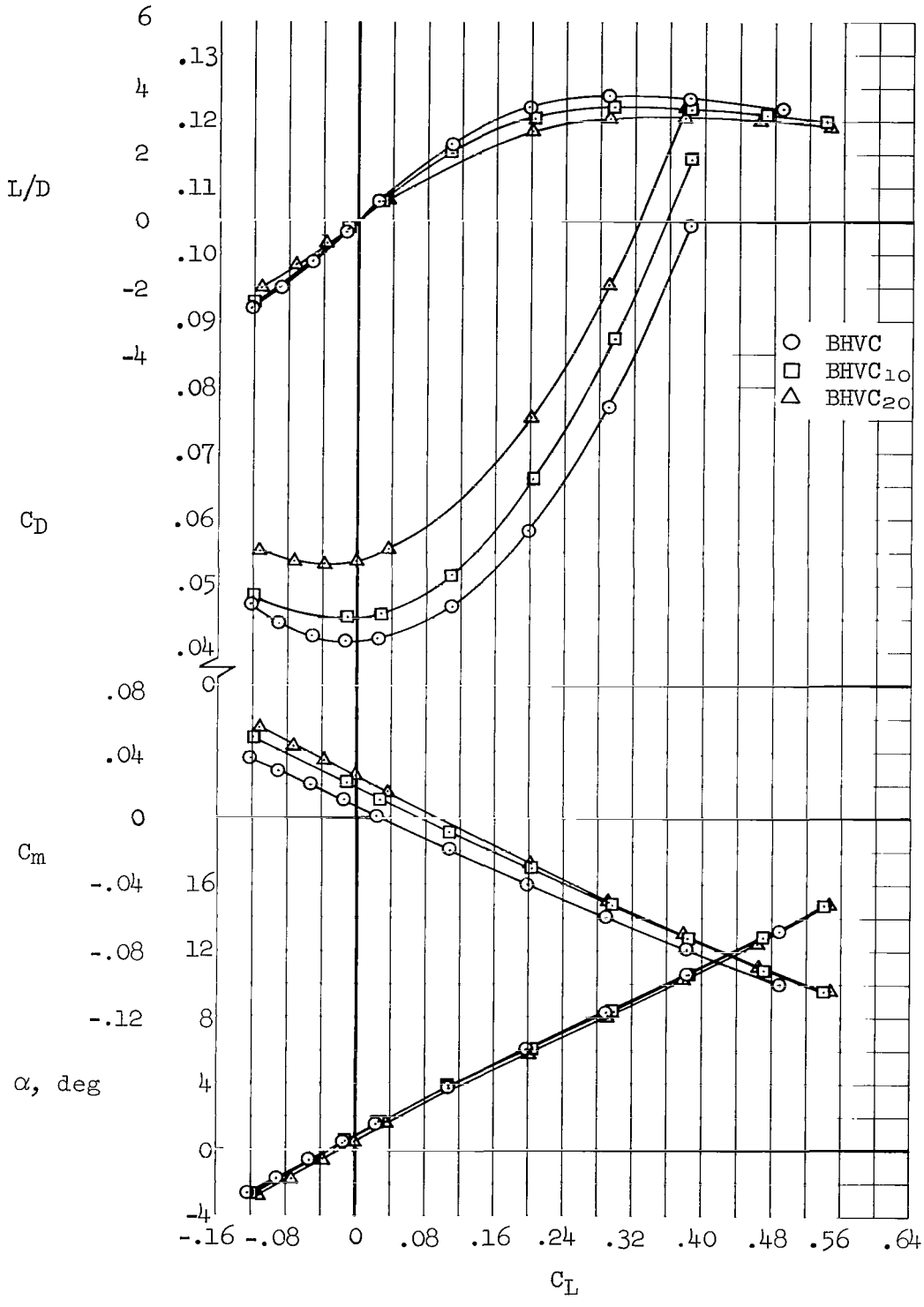

(e) M = 1.30

Figure 13.- Continued.

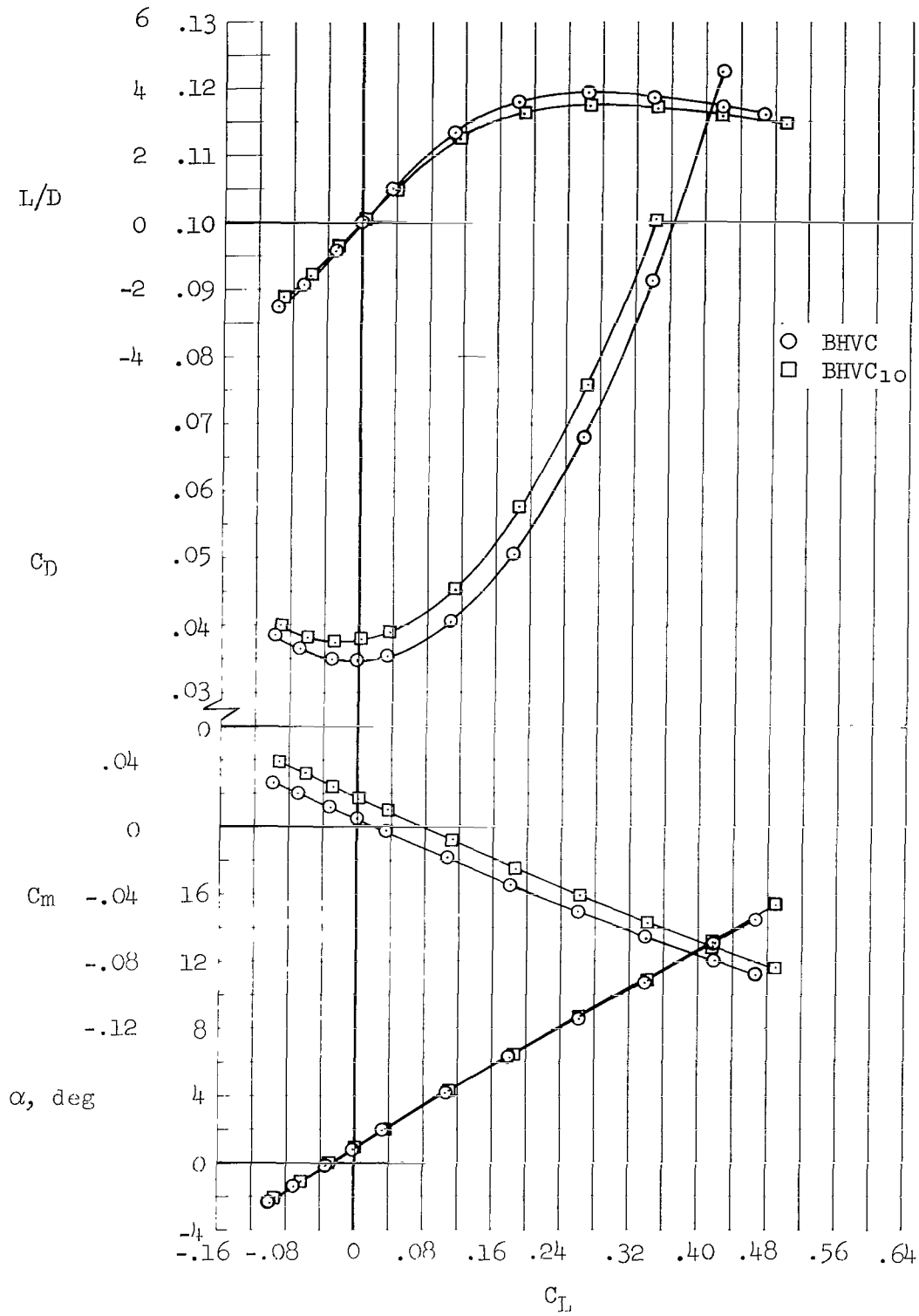

(f) M = 1.60

Figure 13.- Continued.

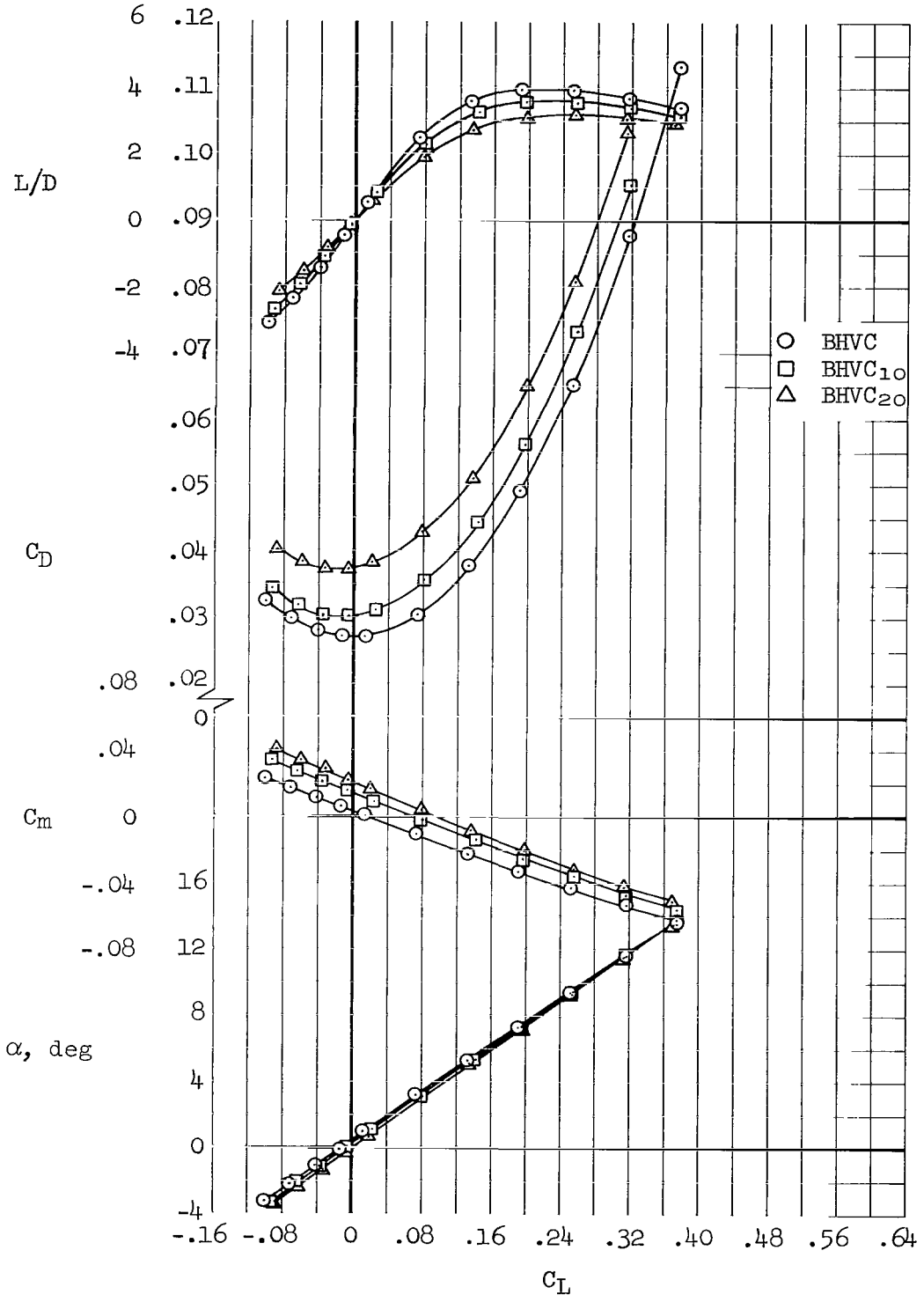

(g) M = 2.00

Figure 13.- Continued.

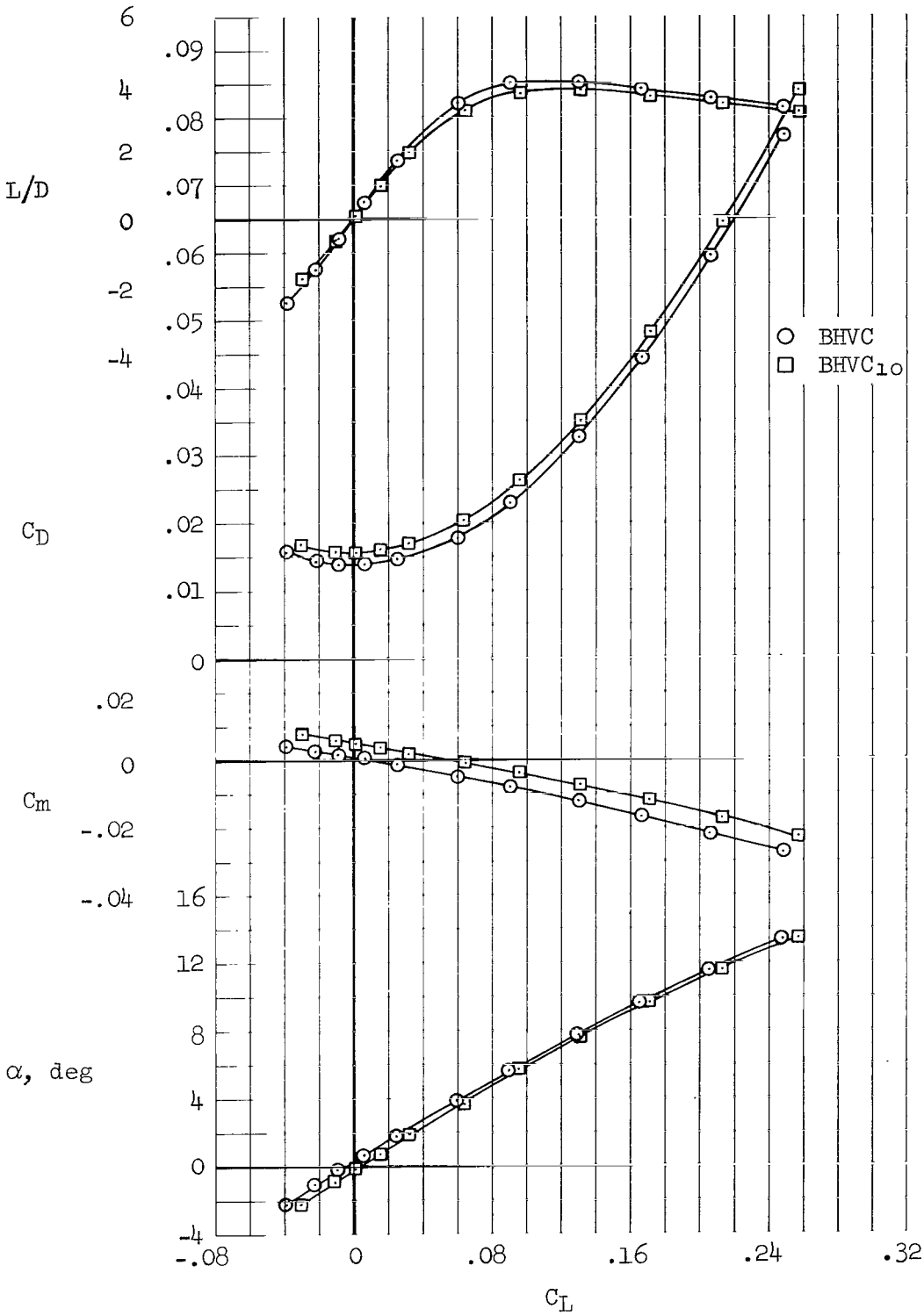

(h) M = 5.37

Figure 13.- Continued.

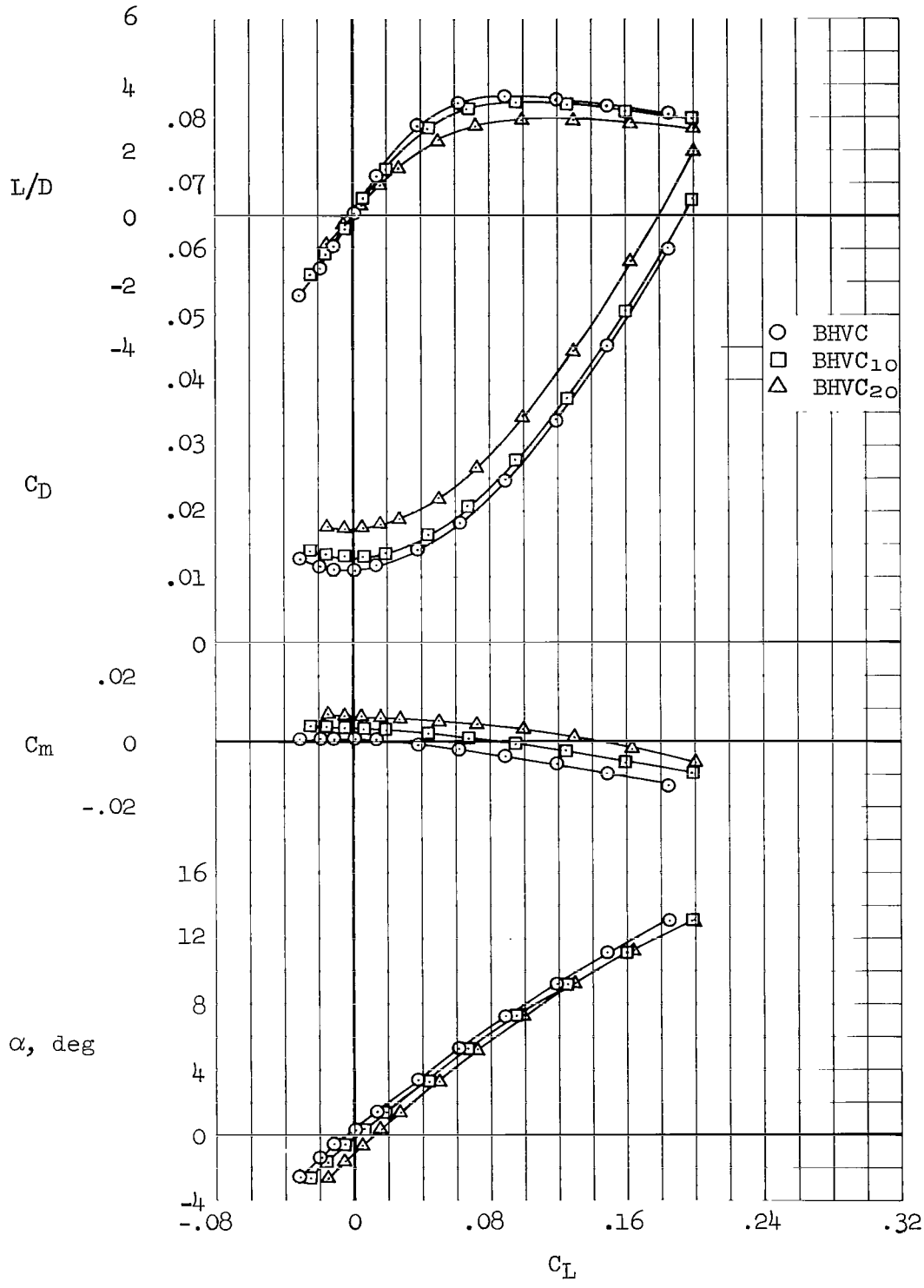

(i) M = 7.36

Figure 13.- Continued.

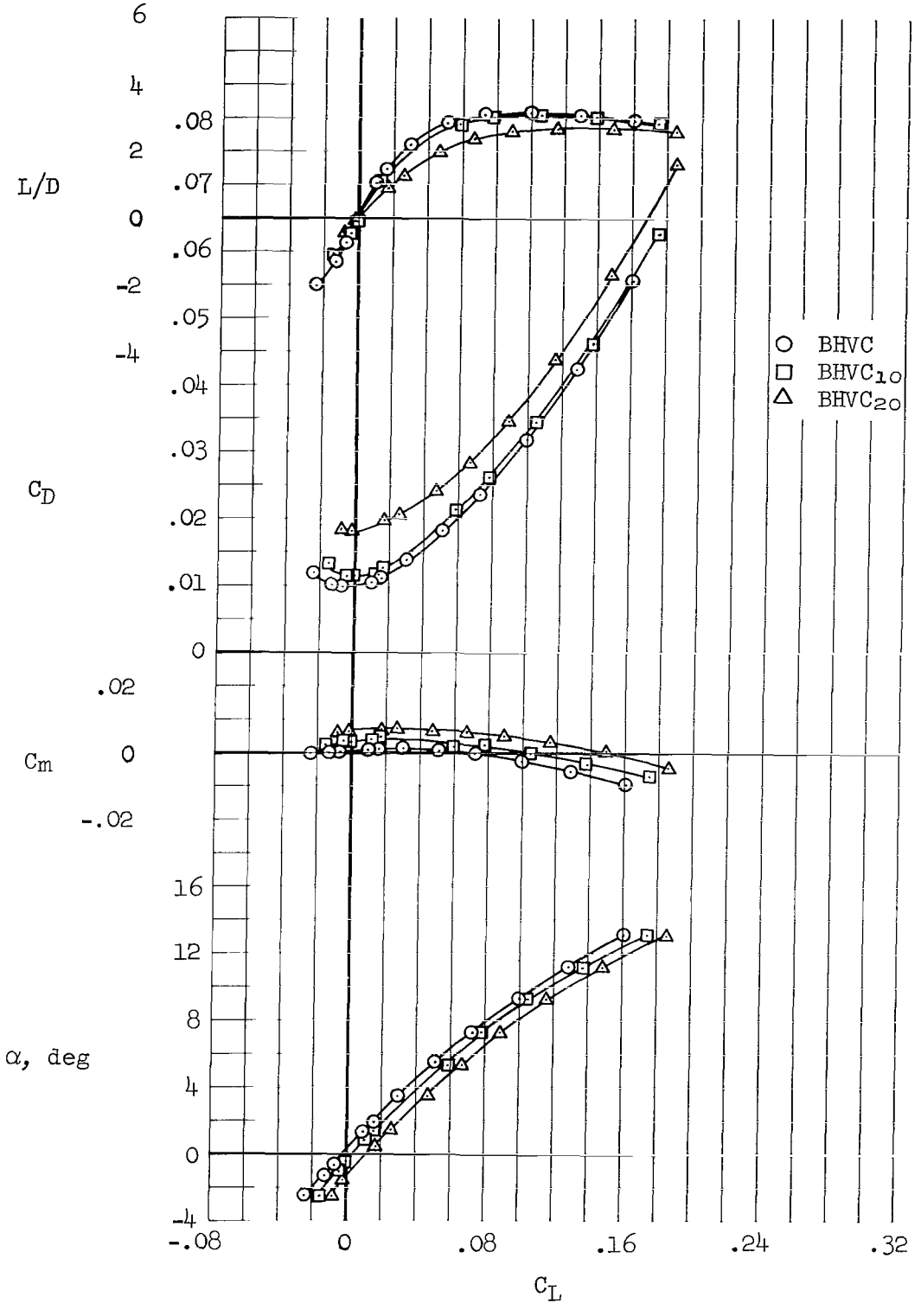

(j) M = 10.6

Figure 13.- Concluded.

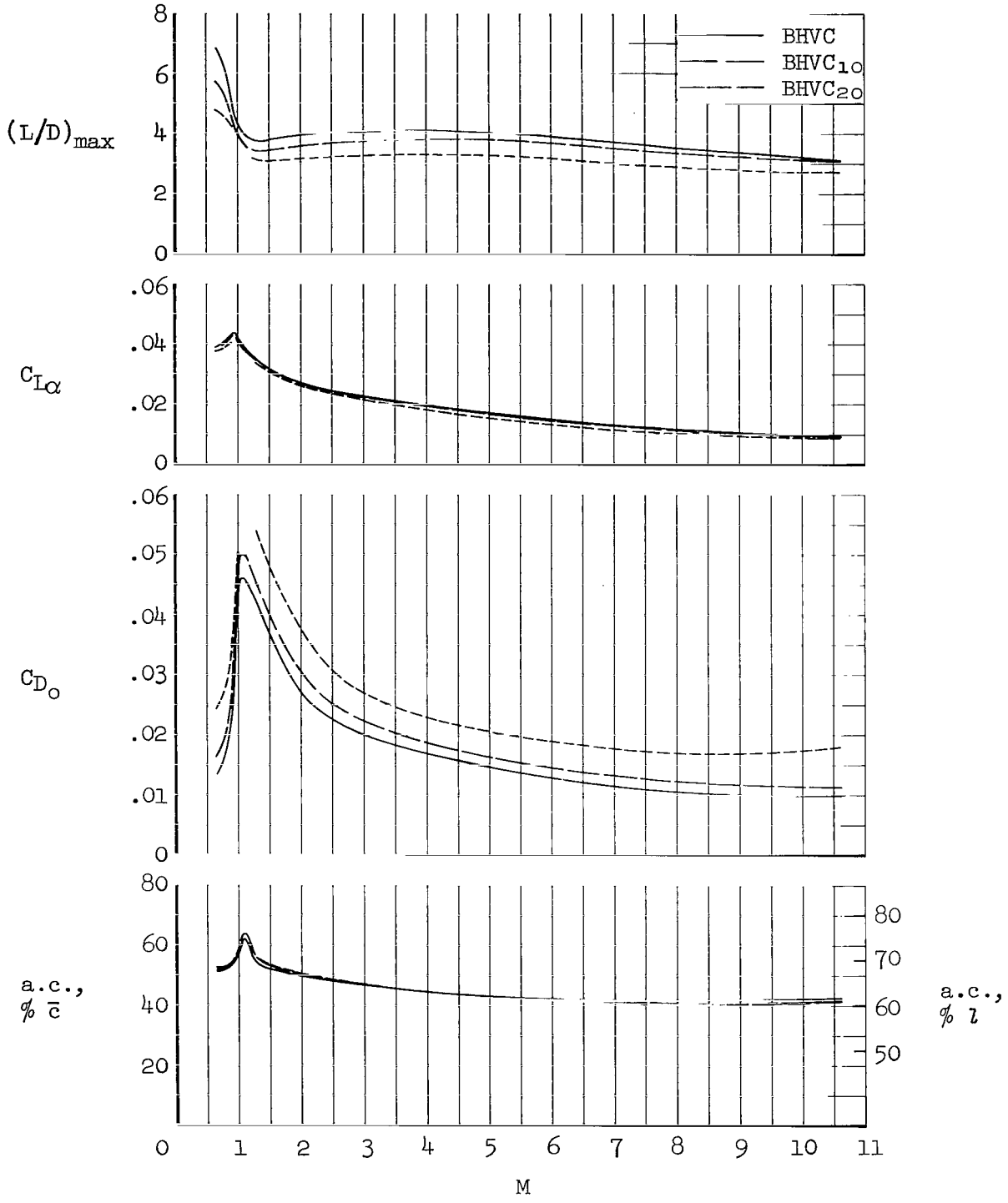

Figure 14.- Variation with Mach number of the effect of canard deflection on the longitudinal aerodynamic characteristics; $\beta = 0°$.

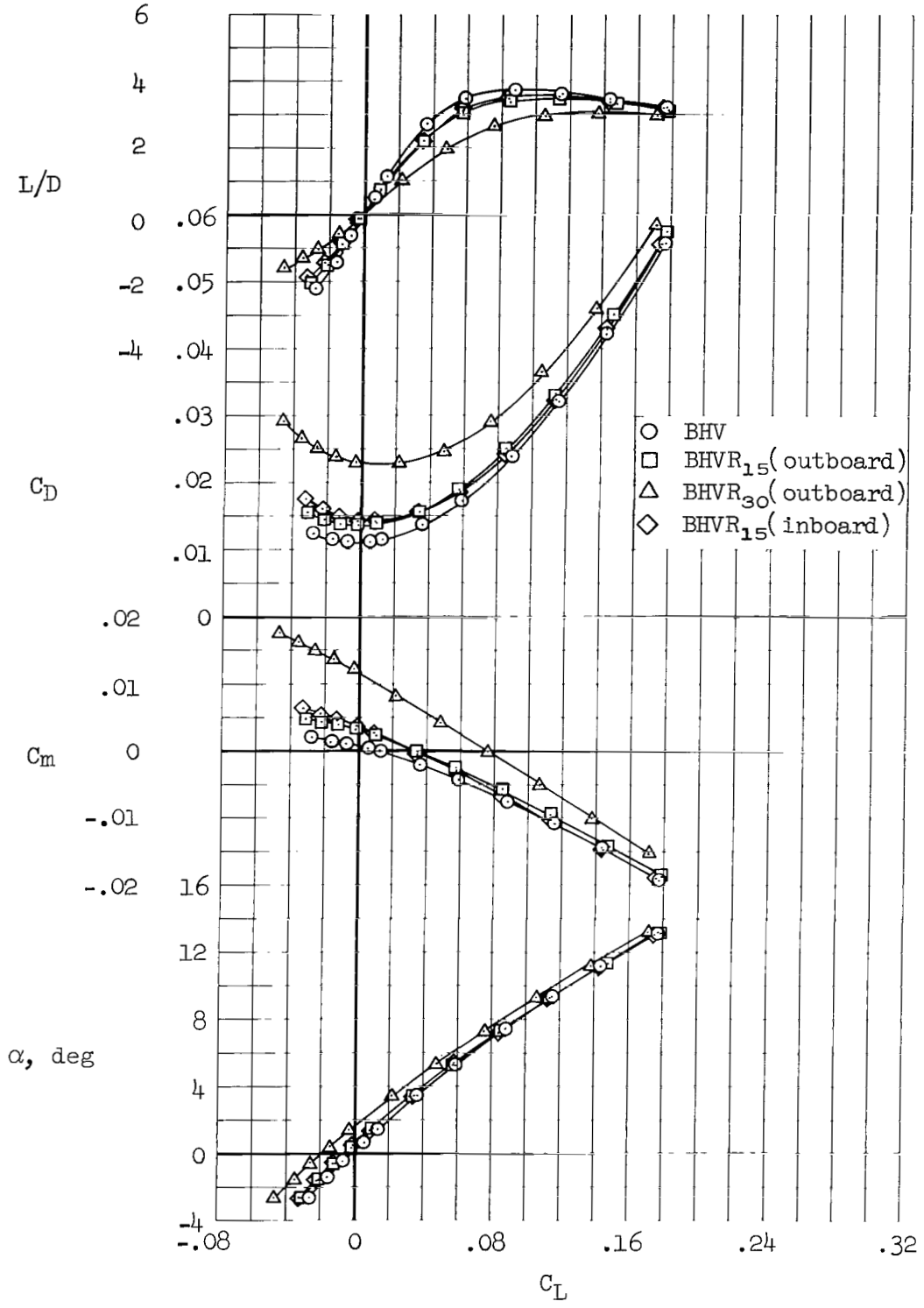

(a) M = 7.38

Figure 15.- Effect of rudder flare on the longitudinal aerodynamic characteristics at hypersonic speeds; β = 0°.

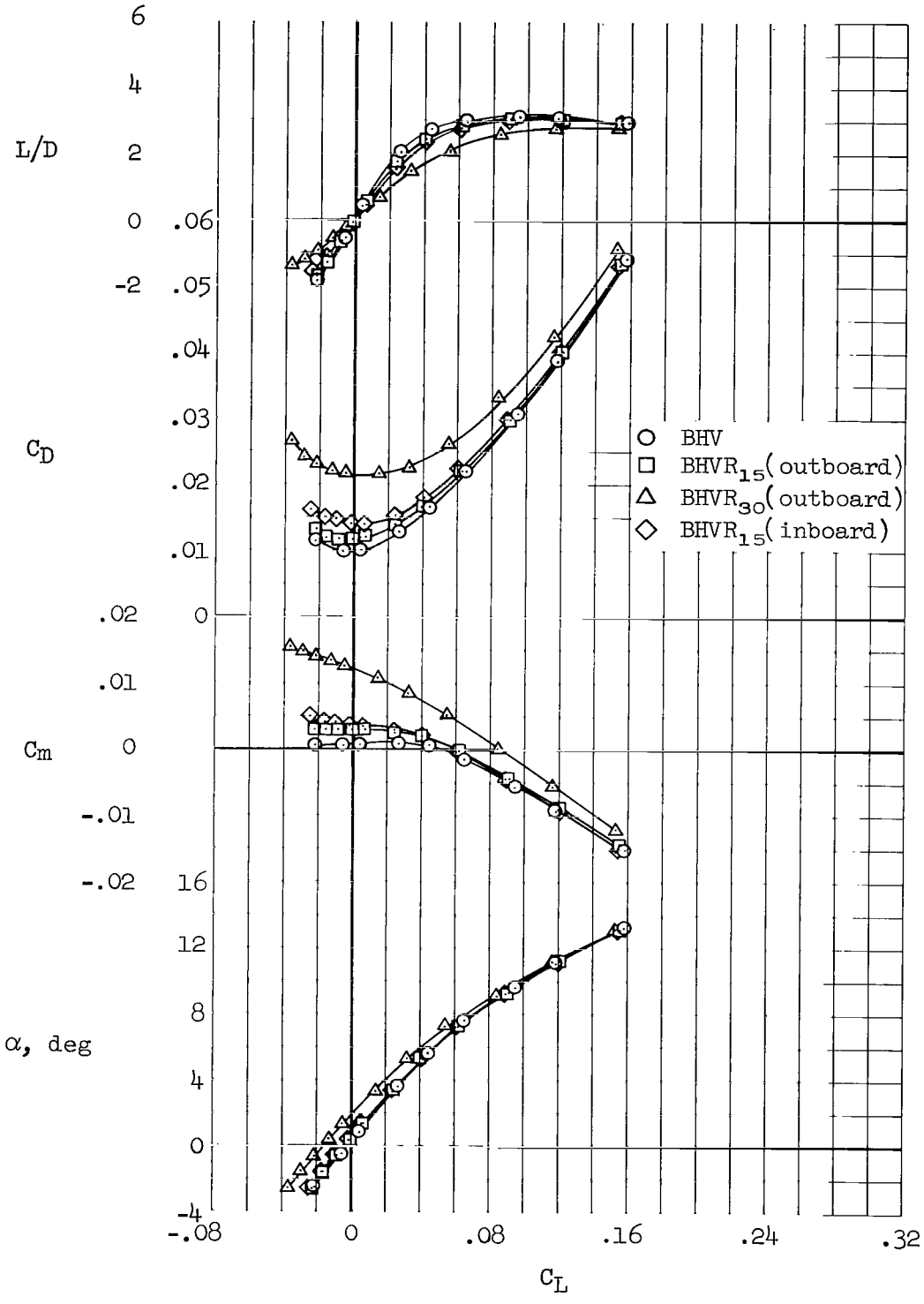

(b) M = 10.6

Figure 15.- Concluded.

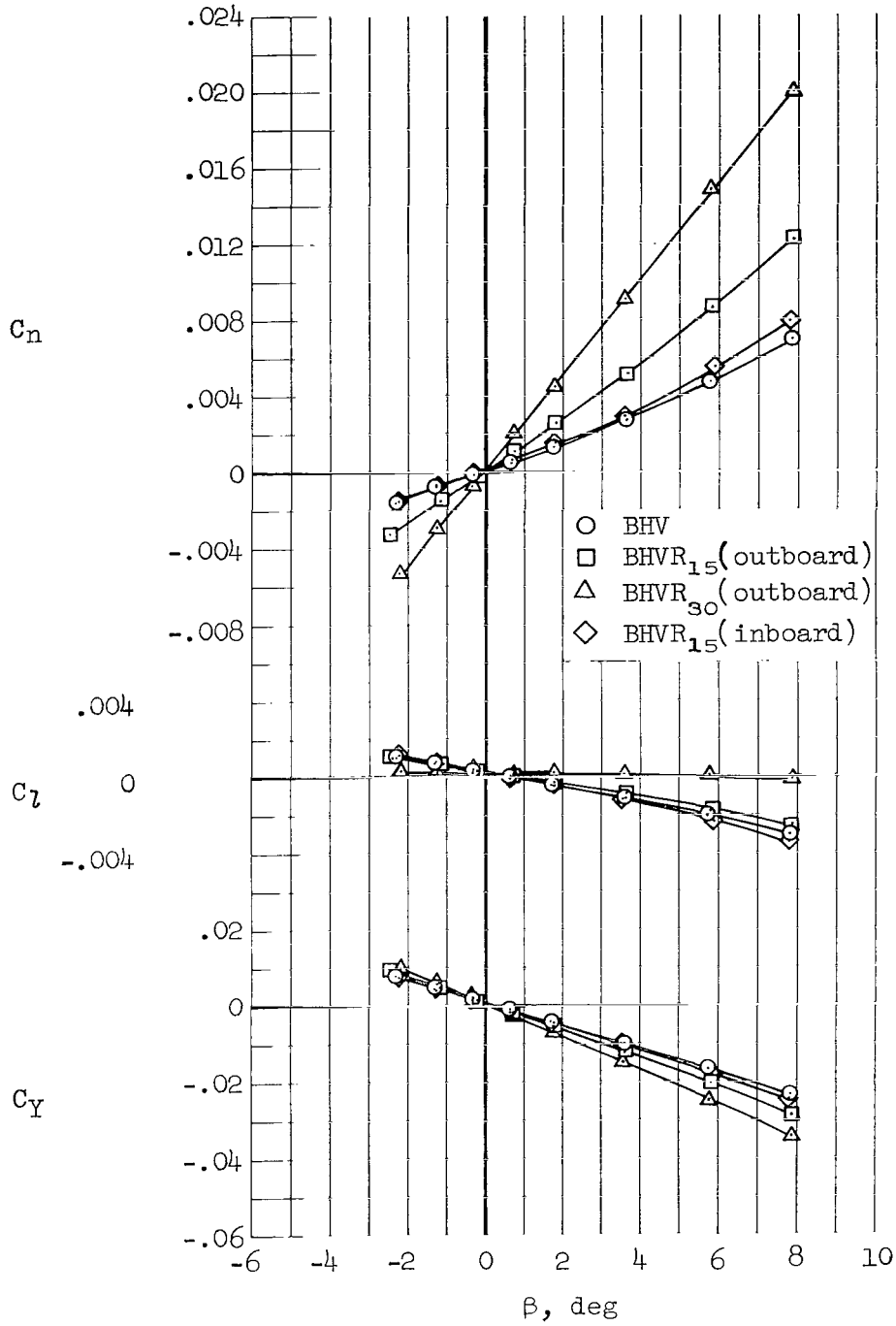

(a) M = 7.38; α = 4.8°

Figure 16.- Effect of rudder flare on the lateral-directional aerodynamic characteristics at hypersonic speeds.

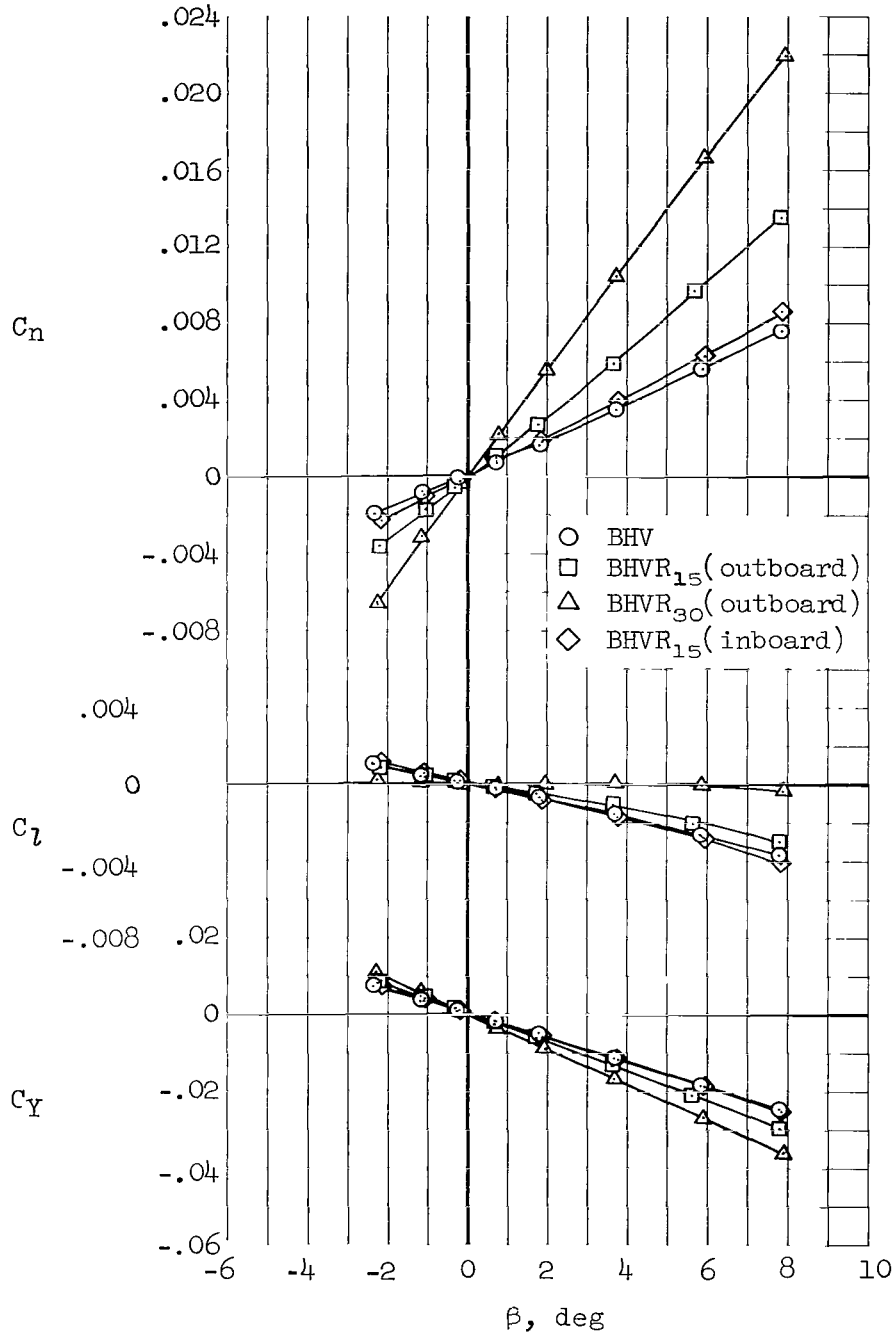

(b) M = 10.6; α = 4.7°

Figure 16.- Concluded.

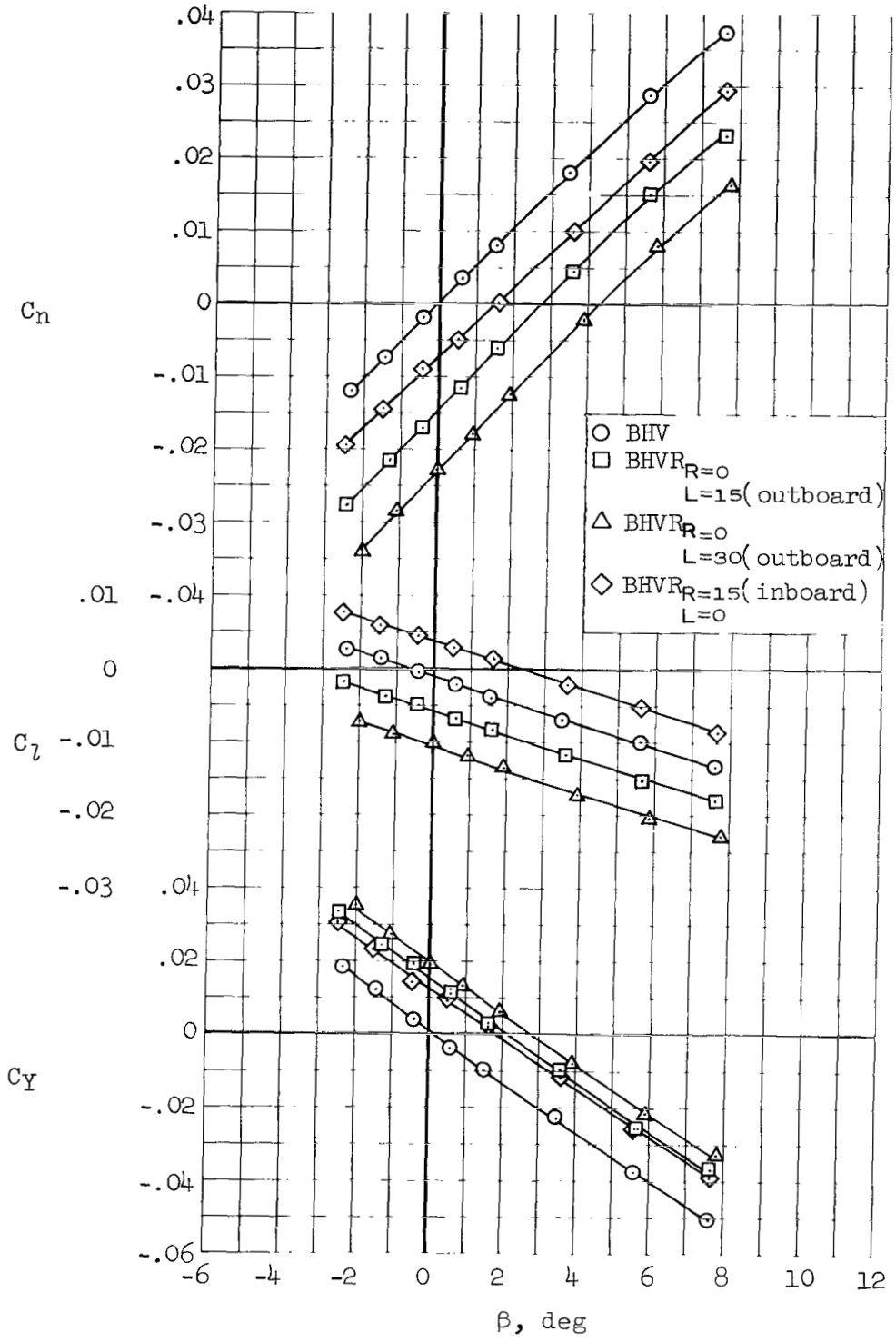

(a) M = 0.65; α = 5.3°

Figure 17.- Effect of individual rudder deflections on the lateral-directional aerodynamic characteristics in sideslip.

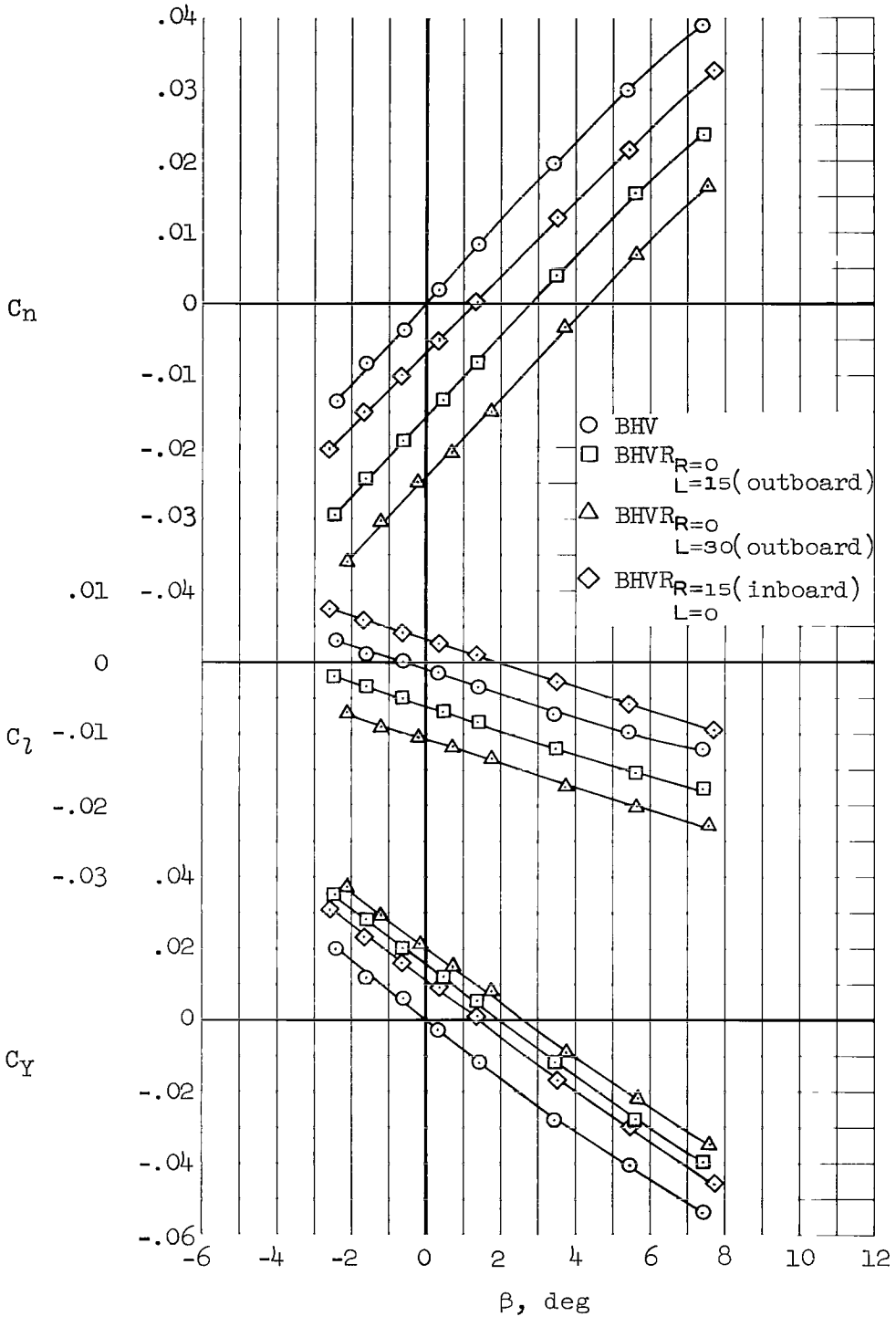

(b) M = 0.90; α = 5.3°

Figure 17.- Continued.

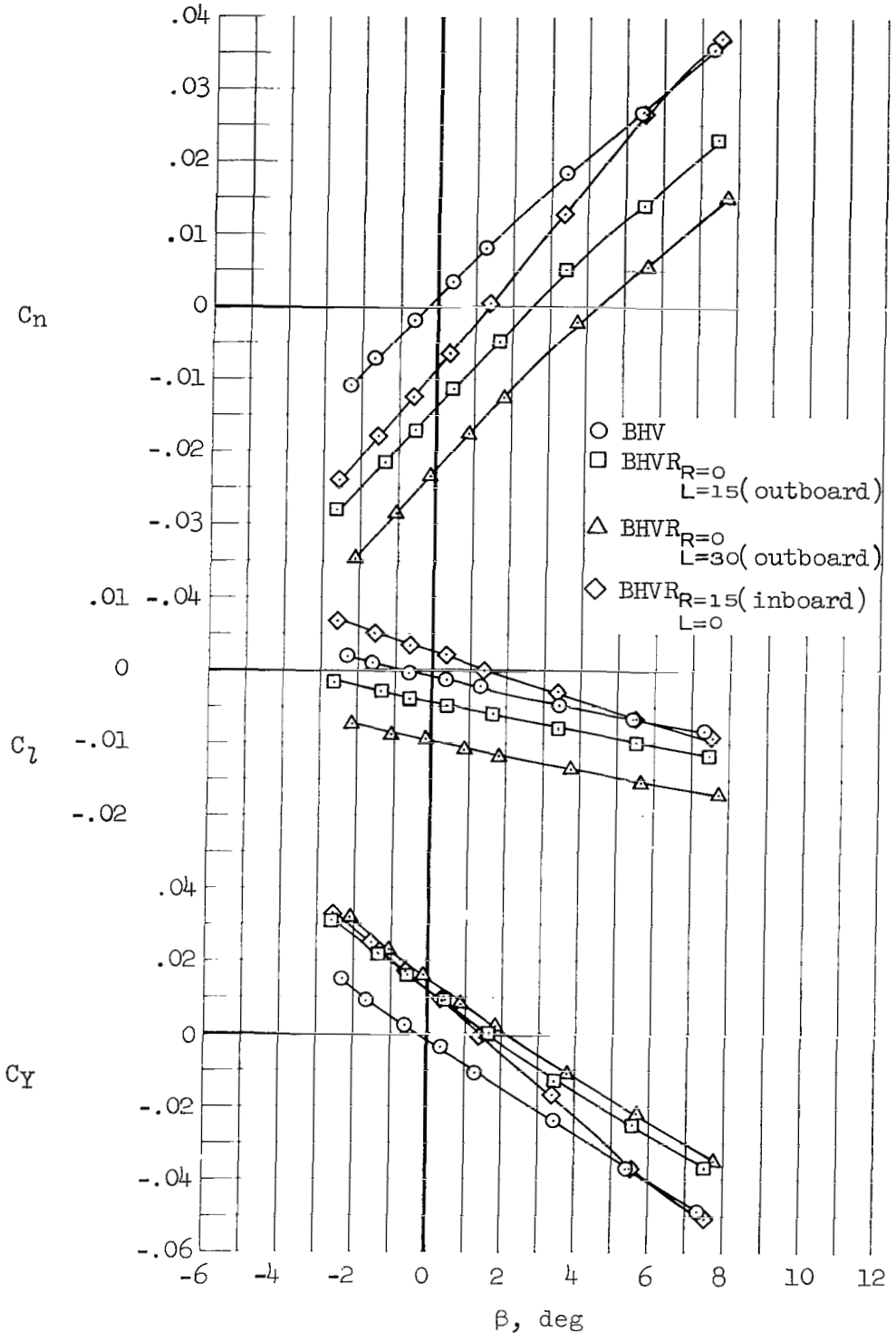

(c) M = 1.30; α = 5.4°

Figure 17.- Continued.

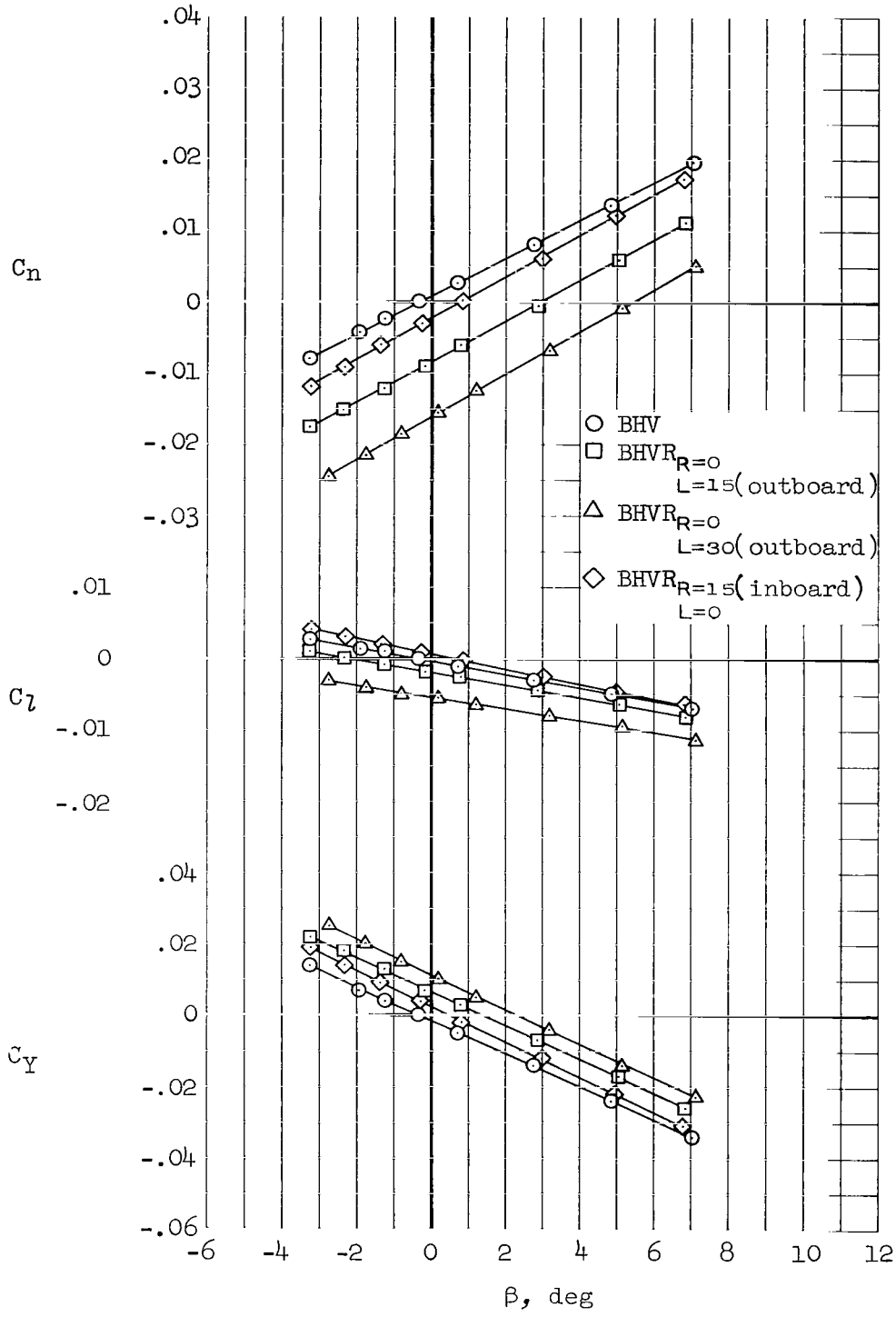

(d) M = 2.00; α = 5.2°

Figure 17.- Continued.

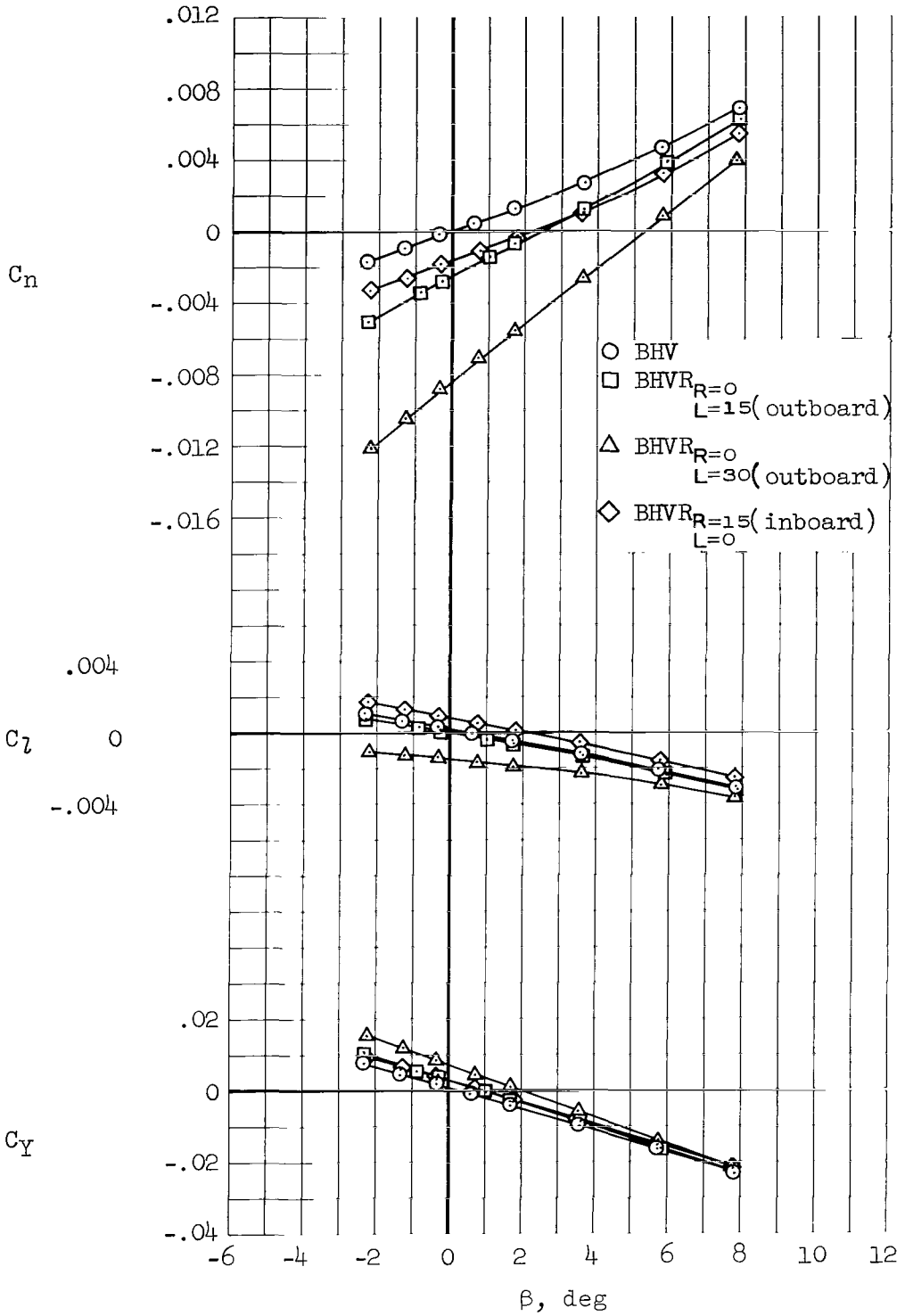

(e) M = 7.38; α = 4.8°

Figure 17.- Concluded.

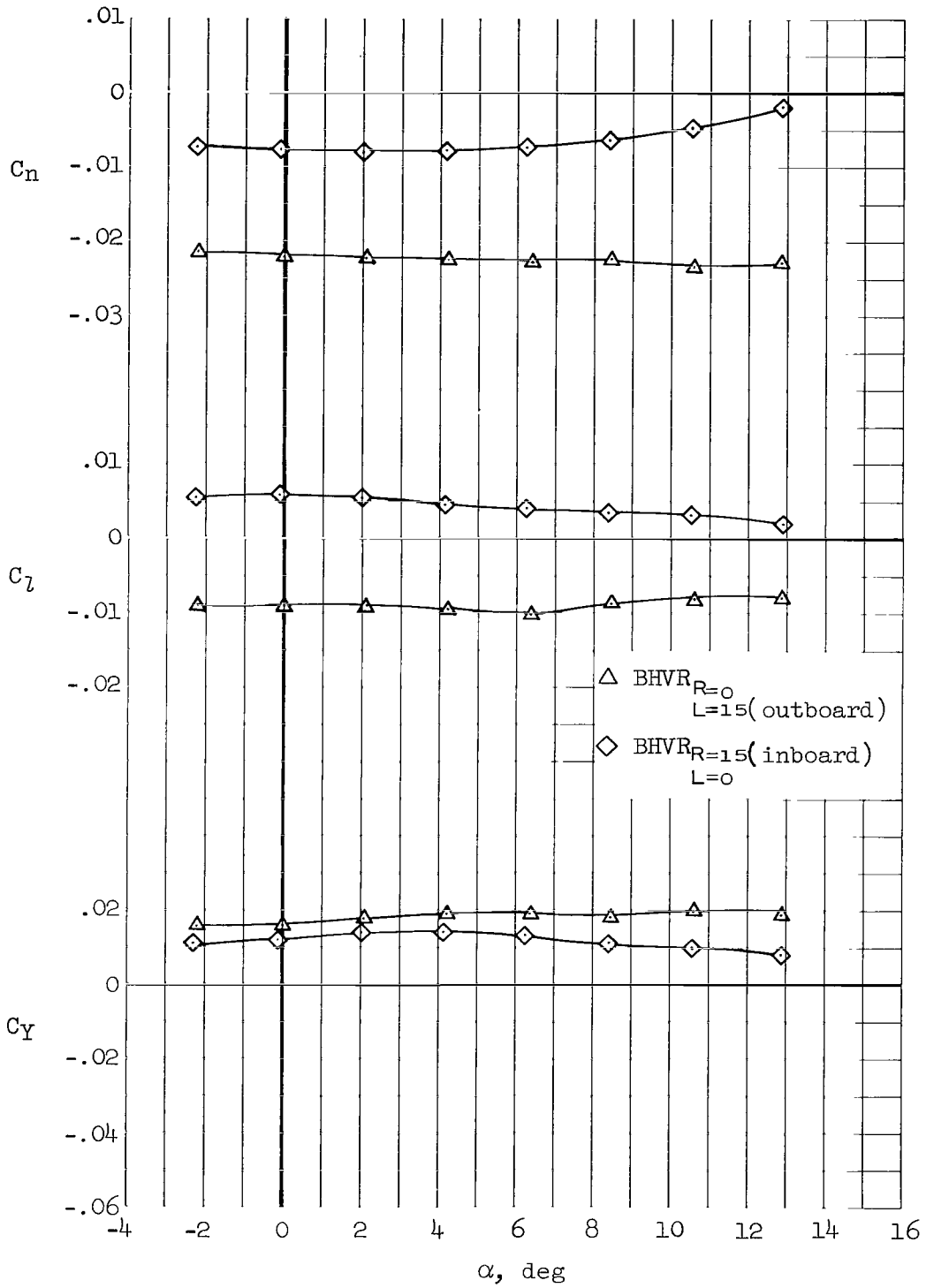

(a) M = 0.65

Figure 18.- Effect of individual rudder deflections on the lateral-directional aerodynamic characteristics in pitch; β = 0°.

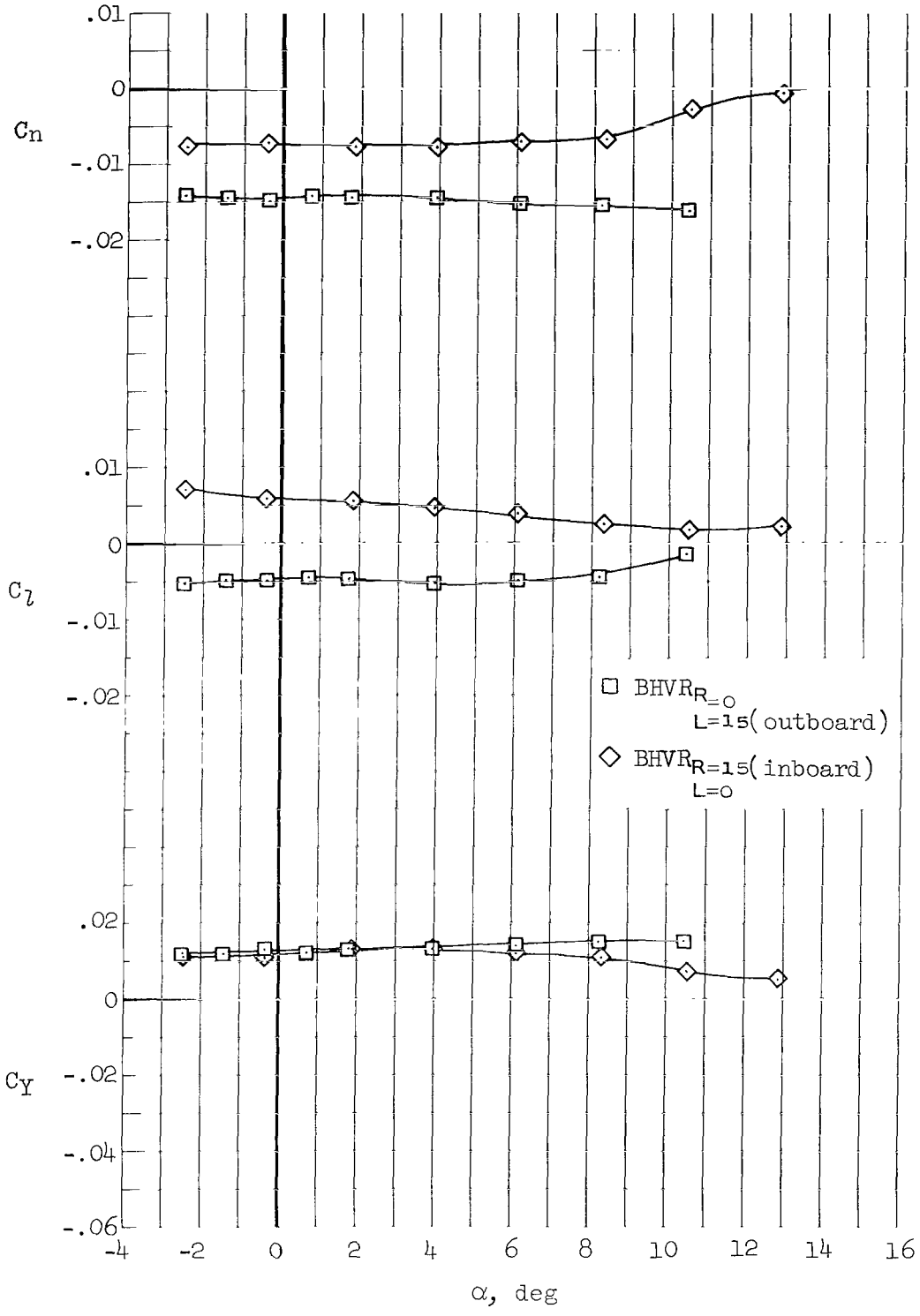

(b) M = 0.90

Figure 18.- Continued.

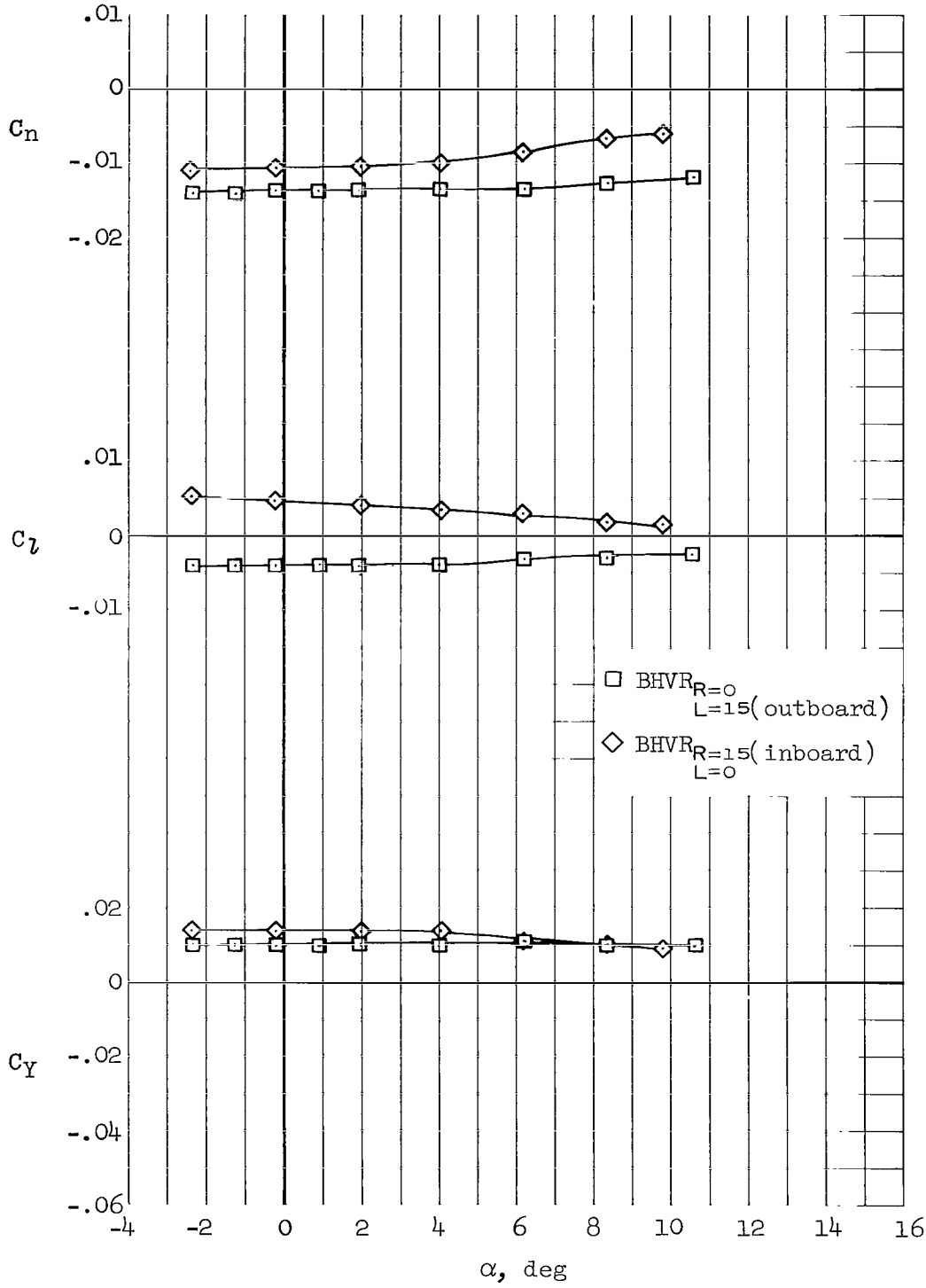

(c) M = 1.30

Figure 18.- Continued.

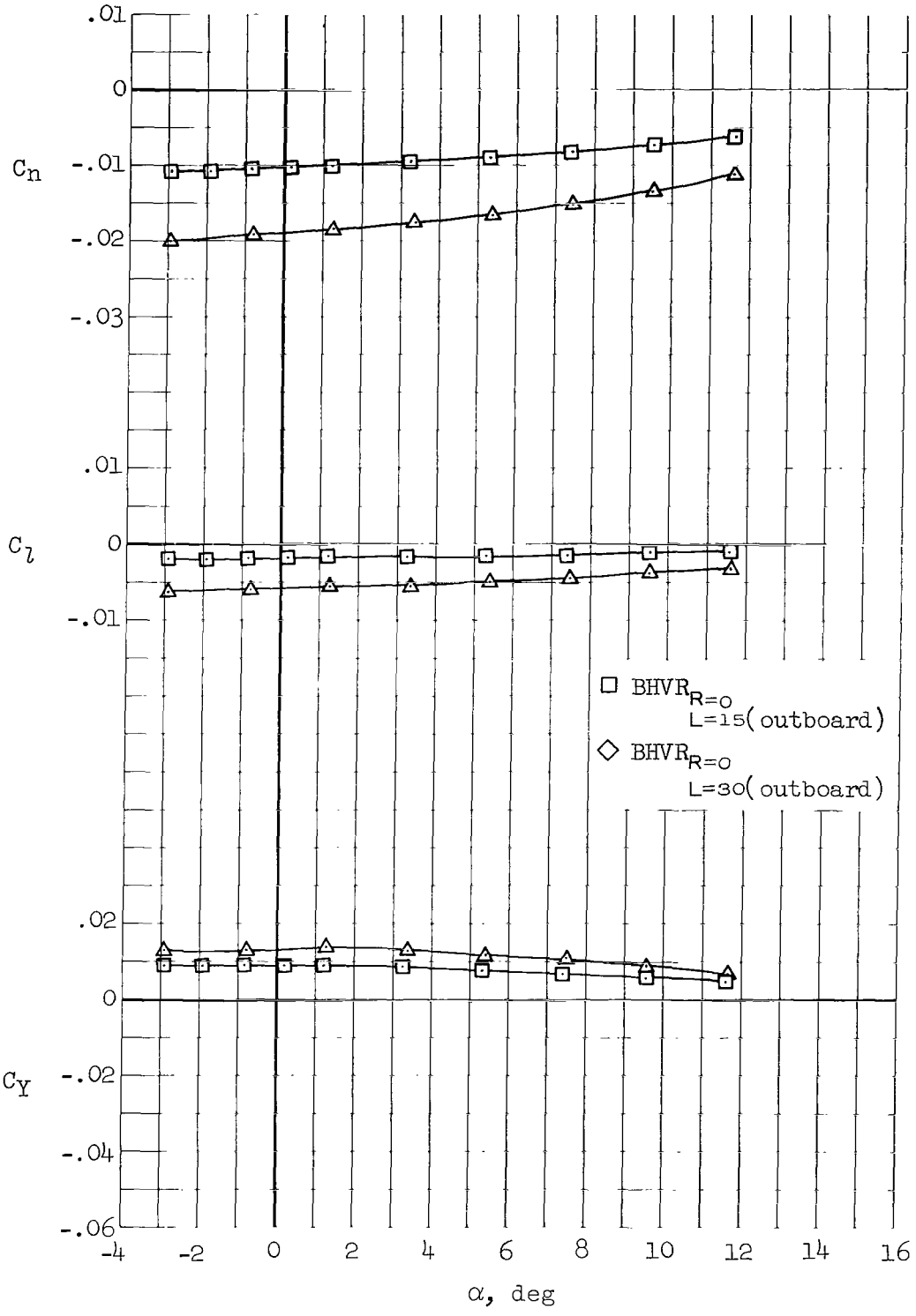

(d) M = 2.00

Figure 18.- Continued.

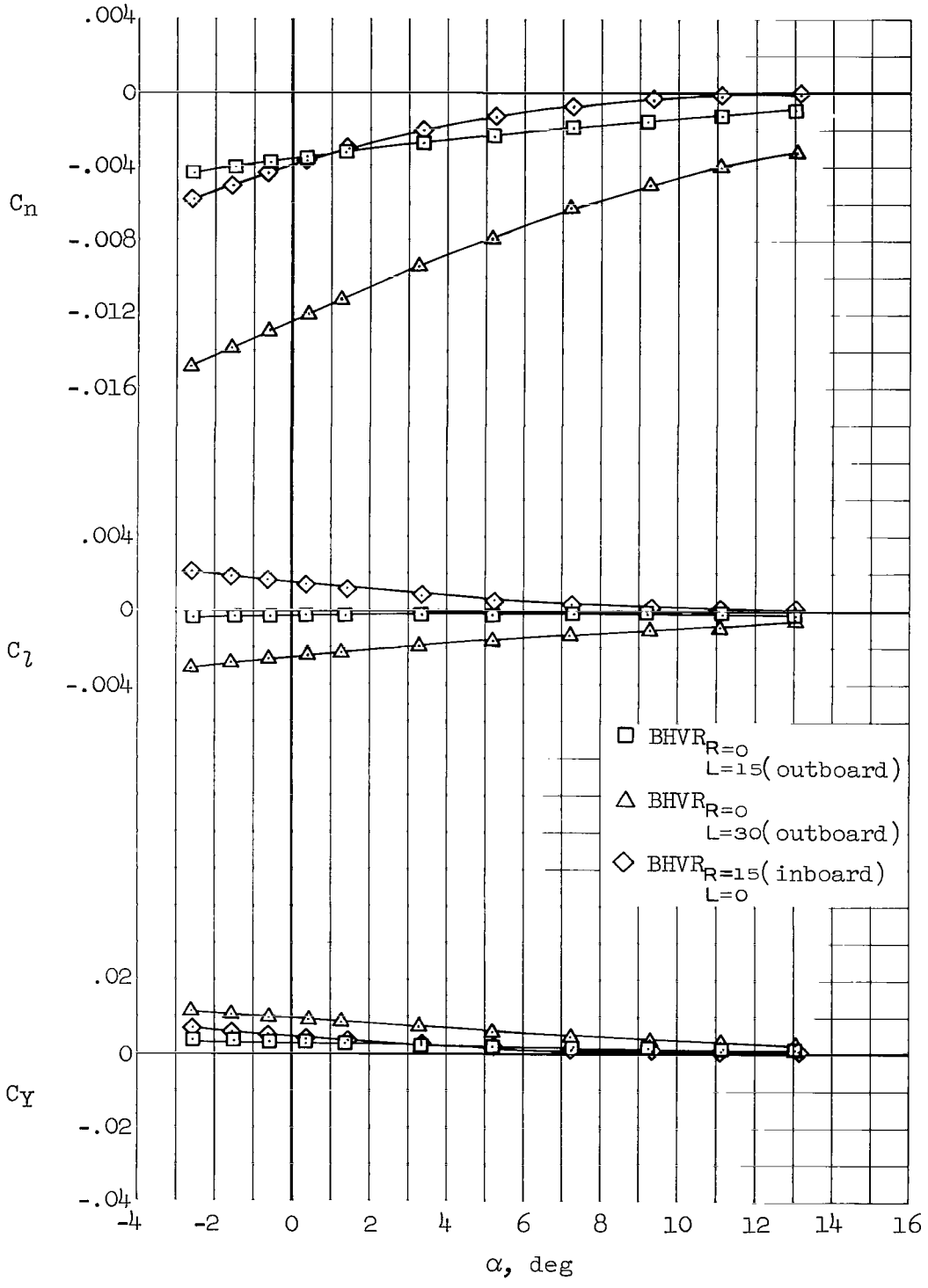

(e) M = 7.38

Figure 18.- Concluded.

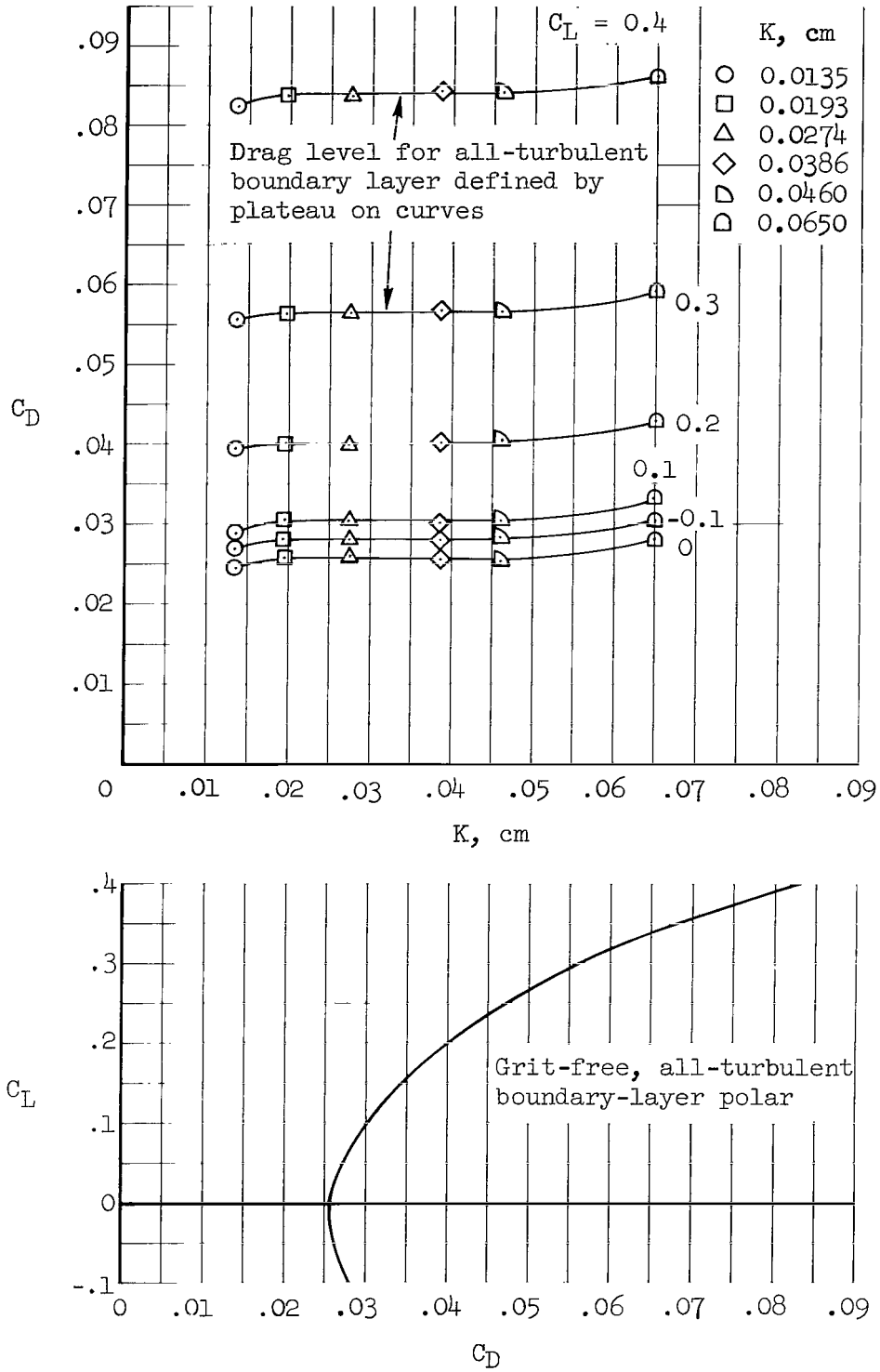

(a) M = 0.90

Figure 19.- Determination of the drag level for an all-turbulent boundary layer using variable size roughness; BHV configuration.

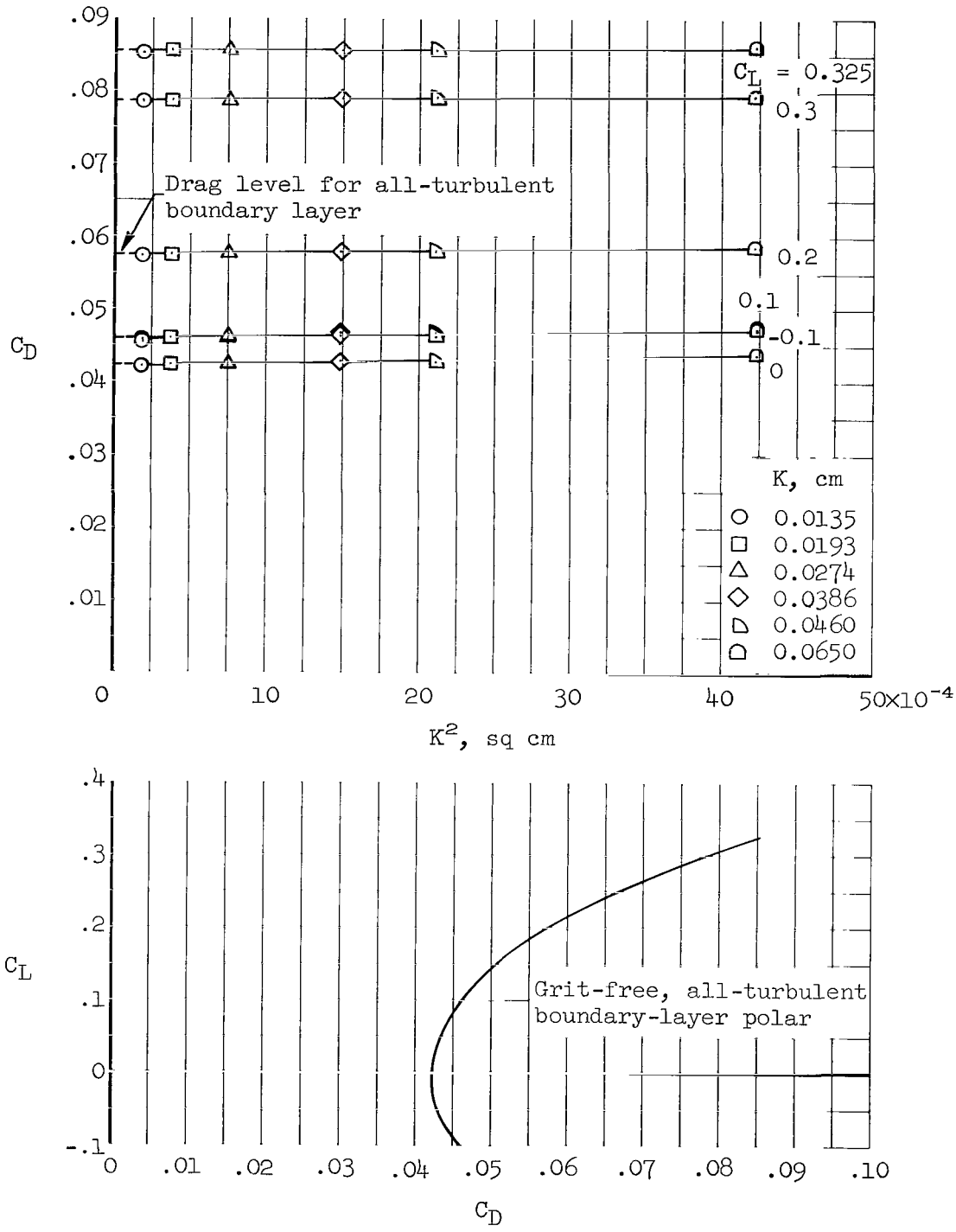

(b) M = 1.30

Figure 19.- Continued.

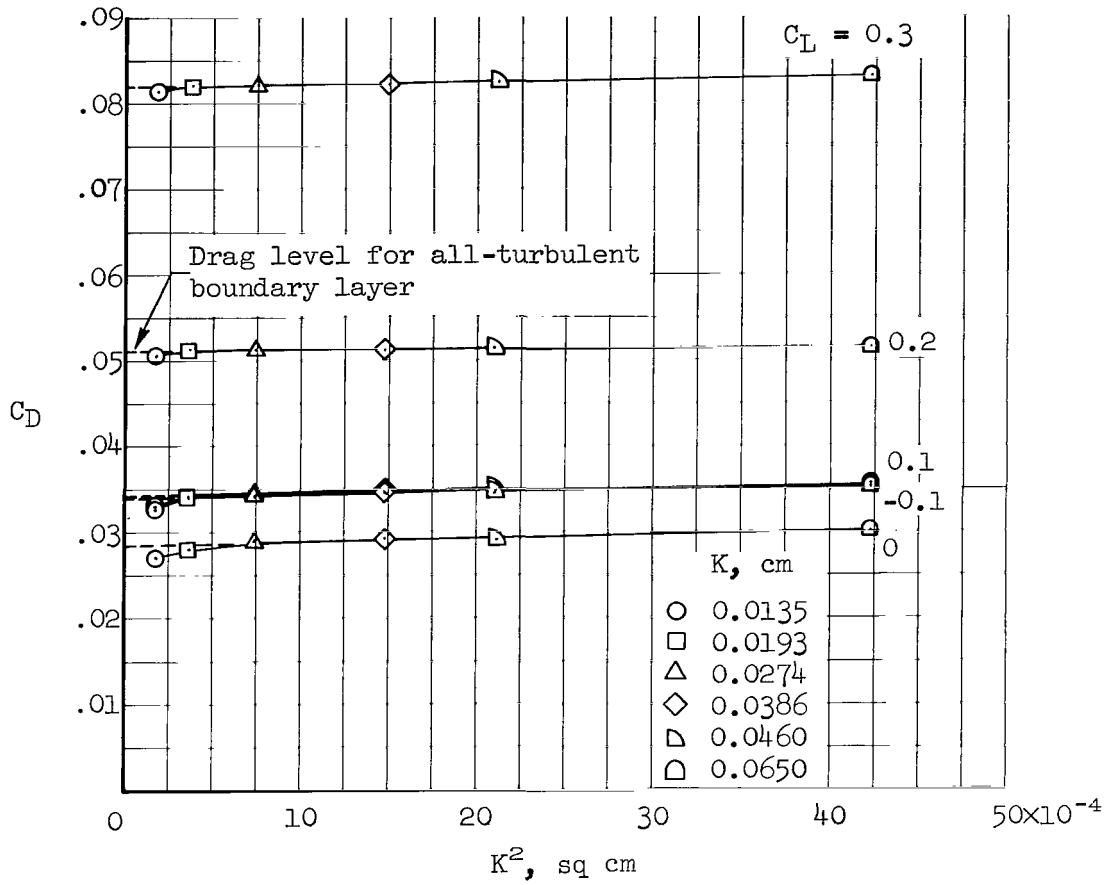

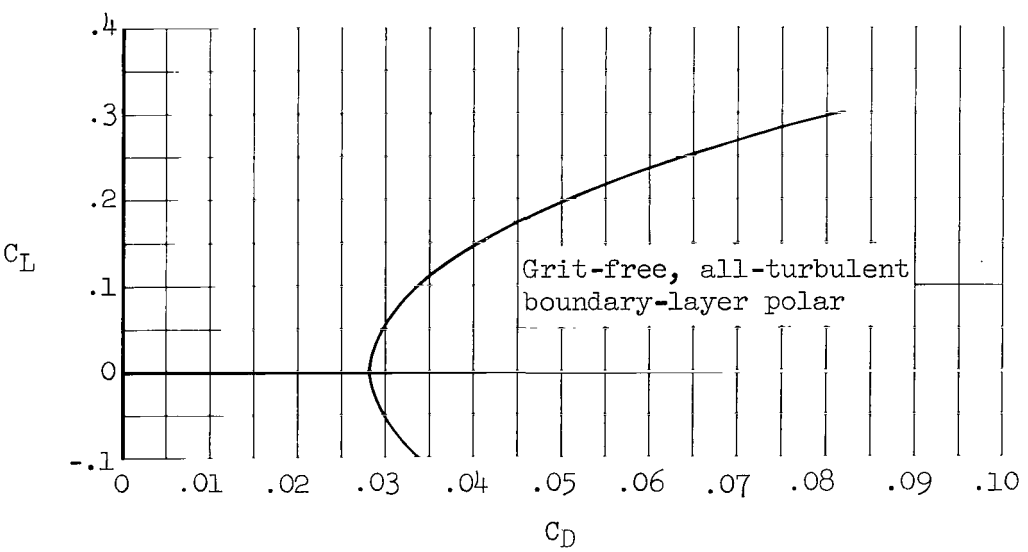

(c) M = 1.99

Figure 19.- Continued.

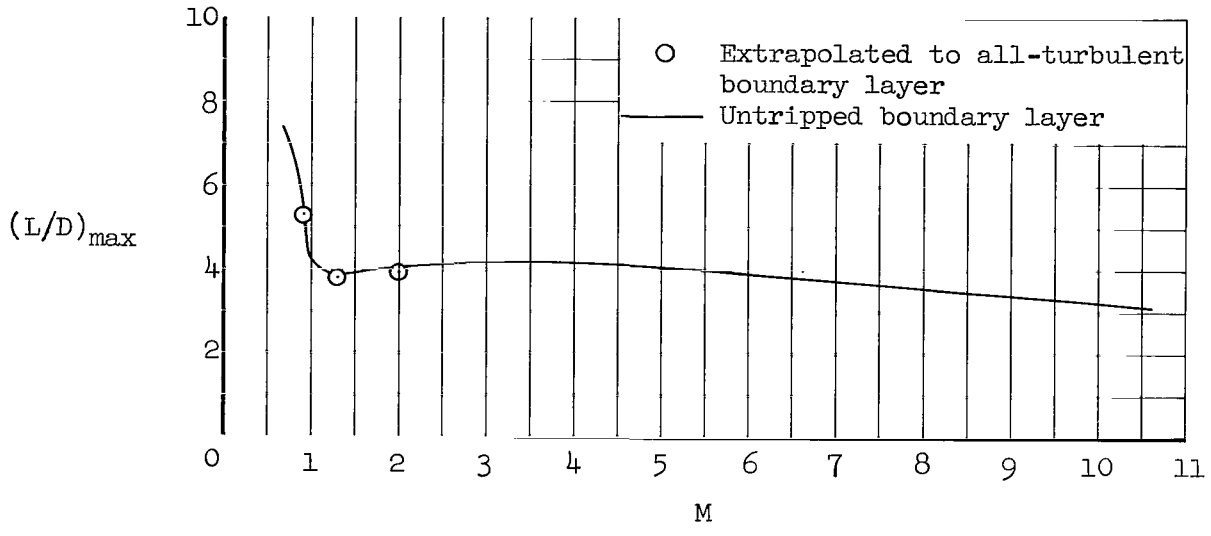

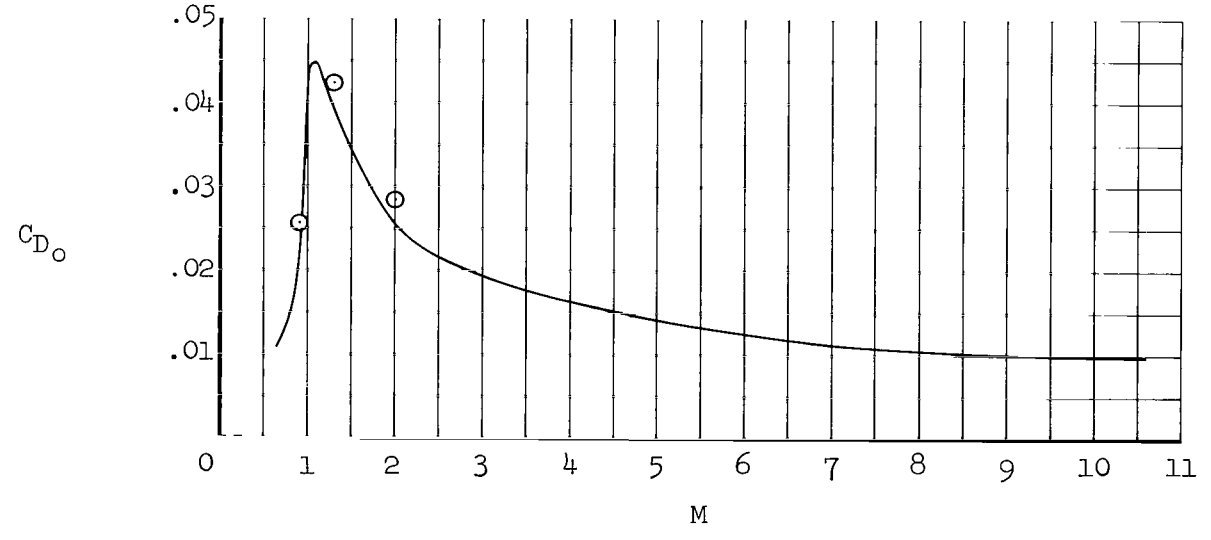

(d) Summary

Figure 19.- Concluded.

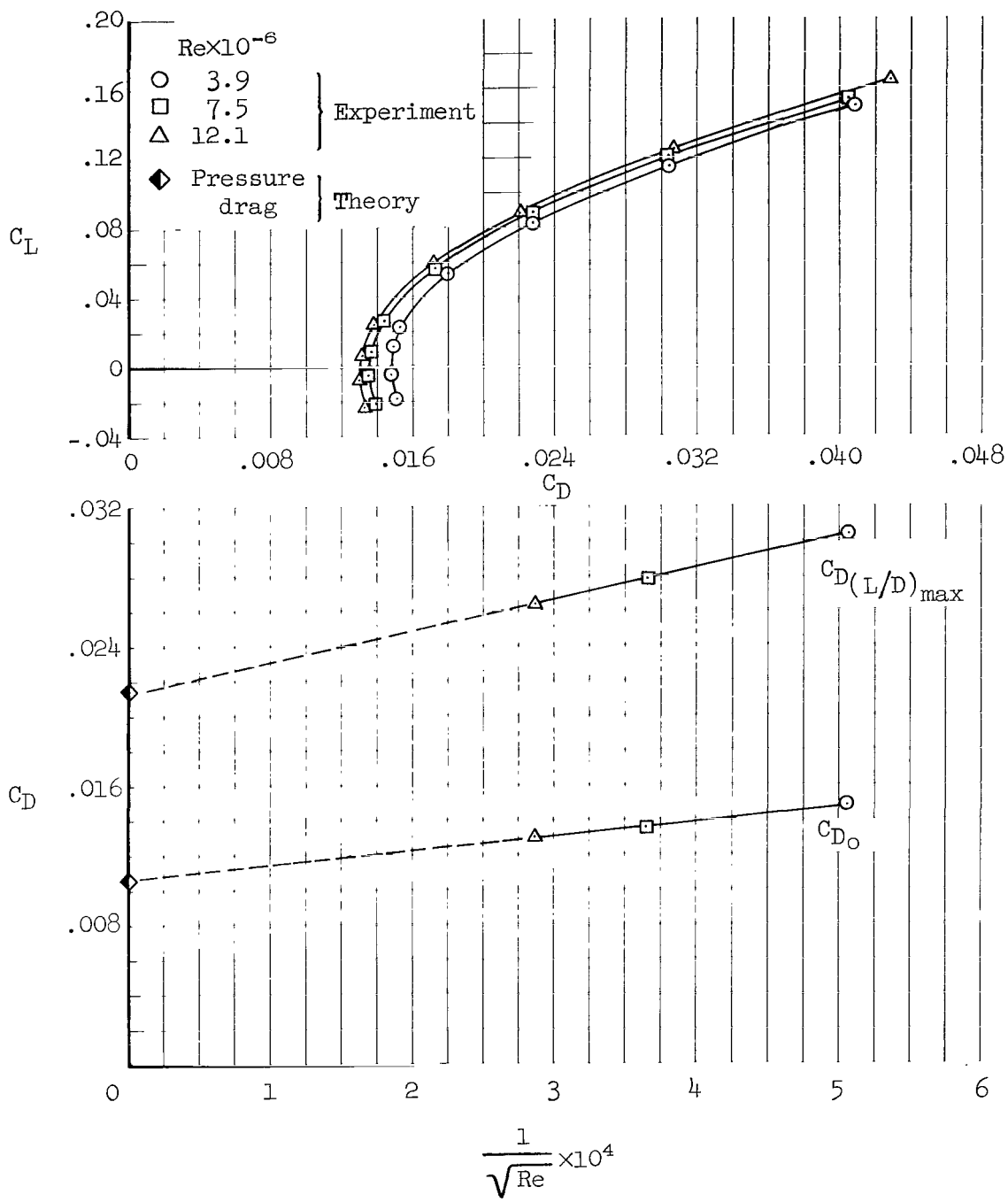

(a) M = 5.37

Figure 20.- Variation in unit Reynolds number; BHV configuration.

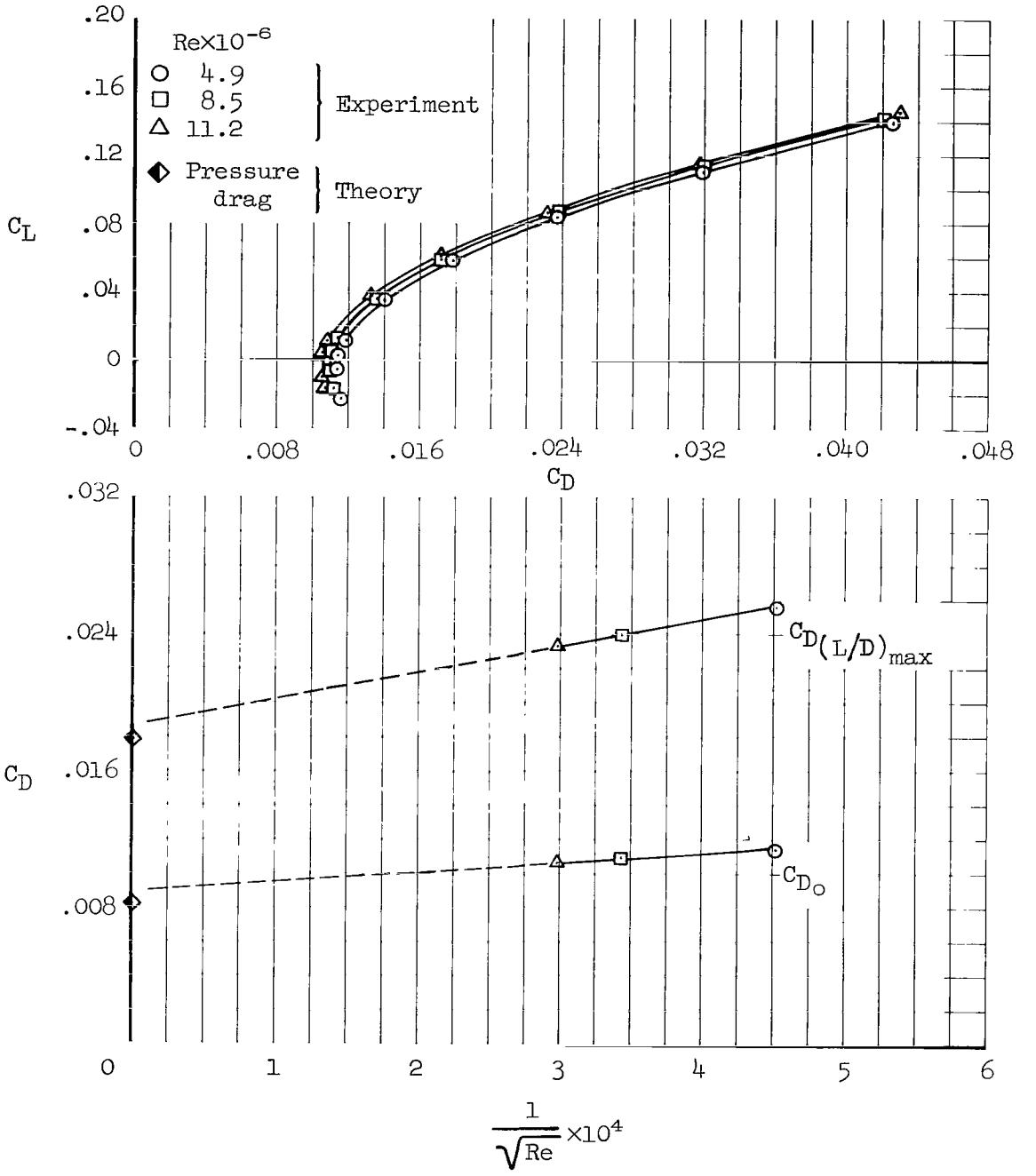

(b) M = 7.38

Figure 20.- Concluded.

NATIONAL AERONAUTICS AND SPACE ADMISTRATION
WASHINGTON, D.C. 20546

OFFICIAL BUSINESS
PENALTY FOR PRIVATE USE $300

FIRST CLASS MAIL

POSTAGE AND FEES PAID
NATIONAL AERONAUTICS AND
SPACE ADMINISTRATION

U.S.MAIL

022 001 C1 U 02 711029 S00903DS
DEPT OF THE AIR FORCE
AF WEAPONS LAB (AFSC)
TECH LIBRARY/WLOL/
ATTN: F LOU BOWMAN, CHIEF
KIRTLAND AFB NM 87117

POSTMASTER: If Undeliverable (Section 158 Postal Manual) Do Not Return

"The aeronautical and space activities of the United States shall be conducted so as to contribute . . . to the expansion of human knowledge of phenomena in the atmosphere and space. The Administration shall provide for the widest practicable and appropriate dissemination of information concerning its activities and the results thereof."

—NATIONAL AERONAUTICS AND SPACE ACT OF 1958

NASA SCIENTIFIC AND TECHNICAL PUBLICATIONS

TECHNICAL REPORTS: Scientific and technical information considered important, complete, and a lasting contribution to existing knowledge.

TECHNICAL NOTES: Information less broad in scope but nevertheless of importance as a contribution to existing knowledge.

TECHNICAL MEMORANDUMS: Information receiving limited distribution because of preliminary data, security classification, or other reasons.

CONTRACTOR REPORTS: Scientific and technical information generated under a NASA contract or grant and considered an important contribution to existing knowledge.

TECHNICAL TRANSLATIONS: Information published in a foreign language considered to merit NASA distribution in English.

SPECIAL PUBLICATIONS: Information derived from or of value to NASA activities. Publications include conference proceedings, monographs, data compilations, handbooks, sourcebooks, and special bibliographies.

TECHNOLOGY UTILIZATION PUBLICATIONS: Information on technology used by NASA that may be of particular interest in commercial and other non-aerospace applications. Publications include Tech Briefs, Technology Utilization Reports and Technology Surveys.

Details on the availability of these publications may be obtained from:

SCIENTIFIC AND TECHNICAL INFORMATION OFFICE

NATIONAL AERONAUTICS AND SPACE ADMINISTRATION

Washington, D.C. 20546